



Possibilities of Using Metallic Interlayers during Diffusion Welding of Ti and Steel AISI 316L

Diplomová práce

Studijní program: N2301 – Mechanical Engineering
Studijní obor: 2301T048 – Engineering Technology and Materials
Autor práce: **Krunalkumar Patel, B.Eng.**
Vedoucí práce: doc. Ing. Jaromír Moravec, Ph.D.





TECHNICAL UNIVERSITY OF LIBEREC
Faculty of Mechanical Engineering ■

Possibilities of Using Metallic Interlayers during Diffusion Welding of Ti and Steel AISI 316L

Master thesis

Study programme: N2301 – Mechanical Engineering
Study branch: 2301T048 – Engineering Technology and Materials
Author: **Krunalkumar Patel, B.Eng.**
Supervisor: doc. Ing. Jaromír Moravec, Ph.D.



DIPLOMA THESIS ASSIGNMENT

(PROJECT, ART WORK, ART PERFORMANCE)

First name and surname: **Krunalkumar Patel, B.Eng.**
Study program: **N2301 Mechanical Engineering**
Identification number: **S16000544**
Specialization: **Engineering Technology and Materiales**
Topic name: **Possibilities of Using Metallic Interlayers during Diffusion Welding of Ti and Steel AISI 316L**
Assigning department: **Department of Engineering Technology**

R u l e s f o r e l a b o r a t i o n :

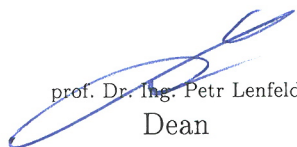
1. To get acquainted with the principles and fundamentals of the diffusion welding.
2. To carry out literature review concerning the principle of diffusion and possibilities of diffusion welding.
3. To carry out literature review concerning utilization of the interlayers at diffusion welding.
4. To get acquainted with material properties of steel AISI 316L and Titan Grade 2.
5. To become familiar with possibilities and operation of thermos-mechanical simulator Gleeble 3500.
6. To propose and perform experimental program for diffusion welding with chosen types of interlayers.
7. To evaluate experiments and make conclusions.

Scope of graphic works: **tables, graphs**
Scope of work report
(scope of dissertation): **approx. 50 p**
Form of dissertation elaboration: **printed/electronical**
List of specialized literature:

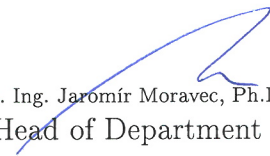
- [1] **Kazakov, N.F. 1985. *Diffusion Bonding of Materials*. Moscow : Mashinostroenie Publishers, 1985. 0-08-032550-5.**
[2] **Kearns, W. H. 1980. *Welding Handbook: Resistance and Solid-State Welding and Other Joining Processes* . United Kindom : American Welding Society, 1980. ISBN 978-1-349-04961-5.**
[3] **Gleeble User Training 2012, Gleeble systems and application, DSI: 120419.**
[4] **AWS Welding Handbook: *Welding Science and Technology*. 9th Ed., Vol.1, 2001.**

Tutor for dissertation: **doc. Ing. Jaromír Moravec, Ph.D.**
Department of Engineering Technology

Date of dissertation assignment: **31 October 2017**
Date of dissertation submission: **31 January 2019**


prof. Dr. Ing. Petr Lenfeld
Dean




doc. Ing. Jaromír Moravec, Ph.D.
Head of Department

Liberec, dated: 1 November 2017

Declaration:

I hereby certify that I have been informed the Act 121/2000, the Copyright Act of the Czech Republic, namely §60 – Schoolwork; applies to my master thesis in full scope.

I acknowledge that the Technical University of Liberec (TUL) does not infringe my copyrights by using my master thesis for TUL's internal purposes.

I am aware of my obligation to inform TUL on having used or licensed to use my master thesis; in such a case TUL may require compensation of costs spent on creating the work at up to their actual amount.

I have written my master thesis myself using literature listed therein and consulting it with my thesis supervisor and my tutor.

Concurrently, I confirm that the printed version of my master thesis is coincident with an electric version, inserted into the IS STAG.

Date:

Signature:

Abstract:

Joining of different materials, which have different physical and mechanical characteristics, is always a challenging task. One method, by which very good results can be attained, is diffusion bonding. The main aim of writing this diploma thesis is to figure out the suitable metallic interlayer with negligible deformation and then achieve good ductility by adopting diffusion welding technology between titanium grade 2 and high-alloy austenitic AISI 316L steel. Fundamental theory of diffusion, its bonding mechanism, effect of distinct variables and real world examples were discussed in the theoretical part. Experiments were executed on Gleeble 3500 thermal-mechanical simulator machine. Weldments were subsequently evaluated in light of mechanical properties by carrying out micro-hardness test and also analyzed metallography by using scanning electron microscope (SEM) and optical microscope (OM).

Key words:

Diffusion bonding, Process variables, Gleeble 3500, Titanium Grade 2, AISI 316L Steel, Different interlayers.

Acknowledgement:

Foremost, I would like to express my sincere gratitude to almighty God who dwells inside all of us. I also would like to say special thanks to my beloved Guru who is always with me as a divine form and showers continuously his blessing on me. I am even quite far from him but his divine word gives me strength in every stage of my life. Without his divine grace, it would not be possible for me to accomplish this diploma work.

Next, I would like to express my deep and sincere gratitude to my supervisor, who is also a head of my department, doc. Ing. Jaromir Moravec, Ph.D. He also gave his continuous endeavours and guidance during my research. I must thank to all those who have helped me in different manner. I think, I am not able to accomplish this whole work without them. During study period, I learnt a lot thing especially in metals, for which I owe to them.

In addition to, I feel proud to have such a wonderful family who always love and look after me very well. They give me moral and financial support as well.

Last but not least, I would like to thank my dearer and nearer friends who are always ready for help and also give their guidance to me. How could I forget them...!!!

This diploma thesis was written at the Technical University of Liberec as part of the Student Grant Contest "SGS 21122" with the support of the Specific University Research Grant, as provided by the Ministry of Education, Youth and Sports of the Czech Republic in the year 2018.

List of Contents:

1. Introduction	16
2. Theoretical part	17
2.1. Physical principal of diffusion	17
2.1.1. Diffusion mechanisms	17
2.2. Mechanism of bonding	19
2.3. Principle and technological parameters of diffusion welding	21
2.3.1. Main technological parameters.....	21
2.3.2. Influence of metallurgical factors	24
2.3.3. Impact of surface cleanliness and roughness	25
2.4. Diffusion welding with interlayer	27
2.5 Advantages, disadvantages and applications of diffusion welding	28
2.6. Types of diffusion bonding furnaces	29
2.6.1. Device separation according to vacuum	30
2.6.2 Basic types of heat sources and methods of heating.....	31
2.7 Research focus on diffusion welding with the use of interlayers	32
3. Gleeble simulator machine for diffusion welding.....	36
3.1. Gleeble 3500 Thermal-Mechanical Simulator.....	36
3.2. Basic components of the Gleeble system.....	37
3.3. Operation of Gleeble 3500	38
3.3.1. Gleeble thermal system.....	38
3.3.2 Gleeble mechanical system.....	39
3.3.3 Temperature gradient and high temperature jaws	40
4. Experimental part.....	43
4.1 Titanium Grade 2	43
4.2 Steel AISI 316L (X2CrNiMo17-12-2)	44
4.3 Feasible interlayers for experiments.....	46
5. Diffusion welding of Titanium Grade 2 to AISI 316L Steel	47
5.1 Reason for using different interlayers	47
5.2 Sample preparation.....	48
5.3 Design and Implementation of the experiment	49
5.3.1 Realization of experiment.....	49
5.3.2 Diffusion bonding with Ni interlayer	51
5.3.3 Diffusion bonding with Ag interlayer	53
5.3.4 Diffusion bonding with Cu interlayer	59
5.3.5 Diffusion bonding with Ag-Cu multi-interlayers	64

6. Conclusion 67

7. References 69

8. Appendix..... 73

List of Figures:

Figure 1 Vacancy mechanism	18
Figure 2 Interstitial mechanism	18
Figure 3 Direct exchange mechanism	19
Figure 4 Ring mechanism	19
Figure 5 Stages of joint formation.....	20
Figure 6 Effect of roughness on the strength of weld joints.....	25
Figure 7 Strength of joints in steel 45 as a function of surface preparation for bonding.....	26
Figure 8 Joint strength of steel 45 as a function of chemical treatment of the mating surfaces	26
Figure 9 Scheme of diffusion welding with interlayer	27
Figure 10 Diffusion bonding furnace	30
Figure 11 Gleeble 3500 Thermal-Mechanical Simulator	36
Figure 12 Arrangement of the Gleeble system.....	37
Figure 13 Four thermocouple channels and side outlet for pyrometer	38
Figure 14 Free length between full contact jaws	40
Figure 15 Full and partial contact jaws of different shapes	41
Figure 16 Graphical representation of the temperature gradient over the 30 mm free length of the S355J2 steel sample by using full-length copper jaws	41
Figure 17 Graphical representation of the temperature gradient over the 30 mm free length of the S355J2 steel sample by using full-length X5CrNi18-8 steel jaws	42
Figure 18 Allotropic transformation of titanium	44
Figure 19 Micro-hardness HV 0.02 distribution over the diffusion welded joint having parameters (T = 860 °C, F = 0.5 kN, t = 40 min) and Ar gas as protective environment.....	48
Figure 20 Thermocouple welding on sample 316L.....	48
Figure 21 Specimens clamped in the high-temperature copper jaws of Gleeble.....	49
Figure 22 Diffusion bonding operation during holding time	50
Figure 23 Transformer power variations before holding time on sample T870_F0.33_t50 with Ni interlayer	51
Figure 24 Oxidation on the surface of titanium.....	52
Figure 25 SEM image and corresponding EDS line scanning results of the bonded joint of sample no. 1 (T870_F0.5_t40).....	53
Figure 26 Metallography of sample no.1 (T870_F0.5_t40) using optical microscope.....	54
Figure 27 Micro-hardness HV 0.1 distribution over the diffusion welded joint of sample no. 1 (T870_F0.5_t40).....	54

Figure 28 Deformation on titanium side and evaporation of Ag interlayer of sample no. 2 (T850_F0.9_t20).....	55
Figure 29 SEM and OM image of sample no. 3 (T820_F0.7_t20)	56
Figure 30 Micro-hardness HV 0.1 distribution over the diffusion welded joint of sample no. 3 (T820_F0.7_t20).....	56
Figure 31 SEM image of sample no. 4 welded in furnace	57
Figure 32 Metallography of sample no. 5 welded in furnace.....	57
Figure 33 Micro-hardness HV 0.1 distribution over the diffusion welded joint in furnace of sample no. 5.....	58
Figure 34 SEM image and corresponding EDS line scanning results of the bonded joint in furnace of sample no.6.....	58
Figure 35 Micro-hardness HV 0.1 distribution over the diffusion welded joint in furnace of sample no. 6.....	59
Figure 36 Higher deformations on the titanium side of sample no. 1 (T870_F0.5_t40).....	60
Figure 37 broken sample no. 2 (T850_F0.5_t30).....	60
Figure 38 SEM image and corresponding EDS line scanning results of the bonded joint of sample no. 3 (T820_F0.7_t60).....	61
Figure 39 Metallography of sample no. 3 (T820_F0.7_t60)	61
Figure 40 Micro-hardness HV 0.1 distribution over the diffusion welded joint of sample no. 3 (T820_F0.7_t60).....	62
Figure 41 SEM image and corresponding EDS line scanning results of the bonded joint in furnace of sample no.4.....	63
Figure 42 Micro-hardness HV 0.1 distribution over the diffusion welded joint in furnace of sample no.4.....	63
Figure 43 SEM image and corresponding EDS line scanning results of the bonded joint of sample T820_F0.7_t60	65
Figure 44 Micro-hardness HV 0.1 distribution over the diffusion welded joint of sample T820_F0.7_t60.....	66

List of Tables:

Table 1 Diffusion welding parameter for various materials and combination of materials	23
Table 2 Solutions for diffusion welding – liquid environment	24
Table 3 Dependence of heating rates on load and sample diameter	38
Table 4 Cooling rates under free cooling for different samples diameters	39
Table 5 Thermocouple type available on Geeble and its temperature range	39
Table 6 Chemical compositions (wt%) of Titanium Grade 2	43
Table 7 Mechanical and physical properties of Titanium Grade 2	44
Table 8 Chemical compositions (wt%) of 316L.....	45
Table 9 Mechanical and physical properties of 316L.....	45
Table 10 Mechanical and physical properties of used interlayers	46
Table 11 Different parameters of diffusion welding using Ni interlayer	52
Table 12 Different parameters of diffusion welding using Ag interlayer	53
Table 13 Different parameters of diffusion welding using Cu interlayer	60
Table 14 Different parameters of diffusion welding using Ag-Cu interlayers	64
Table 15 Chemical composition of the marked regions in Figure 43 (wt%).....	65

List of Abbreviation:

T_m	-	Melting temperature	[°C]
T_w	-	Welding temperature	[°C]
p_w	-	Welding pressure	[MPa]
t_w	-	Welding time	[min]
Cr	-	Chromium	[-]
Al	-	Aluminium	[-]
Cu	-	Copper	[-]
Si	-	Silicon	[-]
C	-	Carbon	[-]
Ni	-	Nickel	[-]
Mo	-	Molybdenum	[-]
Nb	-	Niobium	[-]
W	-	Tungsten	[-]
Ti	-	Titanium	[-]
Ta	-	Tantalum	[-]
Mg	-	Magnesium	[-]
Al-Si 12	-	Alloy of aluminium and silicon	[-]
AlMg6	-	Alloy of aluminium and magnesium	[-]
TiC	-	Titanium carbide	[-]
ZrC	-	Zirconium carbide	[-]
NbC	-	Niobium carbide	[-]
TaC	-	Tantalum carbide	[-]
MoC	-	Molybdenum carbide	[-]
Mo ₂ C	-	Molybdenum carbide	[-]
WC	-	Tungsten carbide	[-]
BaCl ₂	-	Barium chloride	[-]
NaCl	-	Sodium chloride	[-]
Ba ₂ O ₃	-	Barium oxide	[-]
KCl	-	Potassium chloride	[-]
Na ₂ CO ₃	-	Sodium carbonate	[-]
SiC	-	Silicon carbide	[-]
BaF ₂	-	Barium fluoride	[-]
KNO ₃	-	Potassium nitrate	[-]
NaNO ₃	-	Sodium nitrate	[-]
NaOH	-	Sodium hydroxide	[-]

R _a	-	Surface roughness	[μm]
R _m	-	Ultimate tensile strength (UTS)	[GPa]
IMC	-	Intermetallic compound	[-]
DC	-	Direct Current	[-]
AC	-	Alternative current	[-]
Ti-6Al-4V	-	Alloy of titanium	[-]
AISI	-	American Iron and Steel Institute	[-]
316L	-	Steel marking	[-]
OM	-	Optical microscope	[-]
SEM	-	Scanning electron microscope	[-]
EDS	-	Energy dispersive spectroscopy	[-]
XRD	-	X-ray diffraction	[-]
CTE	-	Coefficient of thermal expansion	[K ⁻¹]
Fe	-	Iron	[-]
IPDB	-	Impulse pressure diffusion bonding	[-]
304L	-	Steel marking	[-]
Ag	-	Silver	[-]
s.s	-	Solid solution	[-]
SS	-	Stainless steel	[-]
H _{IT}	-	Indentation hardness	[-]
HAZ	-	Heat affected zone	[-]
DSI	-	Dynamic System Inc.	[-]
LVDT	-	Linear variable displacement transducer	[-]
X5CrNi18-8	-	Steel marking	[-]
S355J2	-	Steel marking	[-]
FeTiO ₃	-	Ilmenite (iron-titanium oxide)	[-]
TiO ₂	-	Titanium dioxide	[-]
N	-	Nitrogen	[-]
O	-	Oxygen	[-]
H	-	Hydrogen	[-]
HCP	-	Hexagonal close packed	[-]
BCC	-	Body centre cubic	[-]
X2CrNiMo17-12-2	-	Steel marking	[-]
S	-	Sulfur	[-]
P	-	Phosphorus	[-]
Mn	-	Manganese	[-]
Co	-	Cobalt	[-]

Ti Gr 2	-	Titanium grade 2	[-]
HV	-	Hardness in Vickers	[-]
wt	-	Weight	[-]

1. Introduction

Welding is one of the most widespread used technology since around 1930 for creating permanent joint. It is a process of metallurgical joining of metals by application of heat or pressure or both. It plays a very significant role in almost every field. During the mid 20th century, there were only few methods to create a joint between two (metal to metal) faying surfaces. Later on, more than 100 techniques of joining materials have already been developed till now.

Lately, distinct welding methods are feasible to join similar and dissimilar materials. Fusion welding, solid state welding and radiant energy welding methods are most suitable choice to form heterogeneous bond between unlike materials. However, during these joining processes, there can occur defects whose magnitude certainly depend on the parent materials to be welded and process variables and have a remarkable influence on the mechanical properties of the final joint. Specifically, joining heterogeneous materials, many difficulties may arise due to different physical, thermal, mechanical and chemical properties (i.e. difference in melting points, thermal expansion, density, reaction with surrounding gases) and may also lead to the formation of intermetallic compounds (IMCs) between joints which impair the mechanical properties of the final weld. These problems can be overcome by adopting special welding techniques, such as diffusion bonding which is one of the method of solid state welding. It was first discovered by N. F. Kazakov in 1953, who was a professor of Moscow Institute of Technology (MIT). The unique feature of diffusion welding technology is to join different combination of materials which are difficult-to-weld. It is also helpful to weld reactive and refractory materials with extremely good quality and retain almost same mechanical properties as base metals.

Diffusion welding is fairly quite a new technology in the research field. It has numerous applications in distinct areas such as aerospace, nuclear, automotive electronics and sensor industries. This has led to increasing the attention for the researcher to develop new and advanced materials.

This diploma work represents the experimental procedure of diffusion bonding for Titanium Grade 2 and AISI 316L austenitic steel using Gleeble 3500 thermal-mechanical simulator machine. The work mainly focused on finding out suitable metallic interlayer with almost no deformation and then achieving enough ductility by employing various interlayers.

2. Theoretical part

2.1. Physical principal of diffusion

Diffusion is the phenomena of material in which the movement and transport of atoms from a higher concentration region to a lower concentration region in the direction of the concentration gradient. Atoms move continuously until each and every atom strives to achieve an equilibrium state, i.e. equilibrium concentration [1,2]. The diffusion process can be divided into two types: self-diffusion and heterodiffusion.

Self-diffusion: It takes place in pure metal. During self-diffusion, atoms migrate randomly throughout the crystal lattice. Due to the random movement of atoms in the grid, concentration gradient arises in crystal lattice but mass of pure metal does not change. This concentration gradient can be expressed by Fick's laws when the Fick's first law (equation 2.1) for metal plate indicates a variation of concentration in the x-direction per unit of time. The diffusion flux J of the atoms per unit time per unit area in the direction of the x-axis is proportional to the concentration gradient. Mathematically, it is expressed as:

$$J = -D \cdot \left(\frac{\partial C}{\partial x} \right) \quad (2.1)$$

In most practical cases, diffusion processes are non-stationary ones because diffusion processes change over time. It can be deduced the relation called Fick's second law (equation 2.2). In mathematical form, it is represented as:

$$\frac{\partial C}{\partial t} = \frac{\partial}{\partial x} \left(D \cdot \frac{\partial C}{\partial x} \right) = D \cdot \frac{\partial^2 C}{\partial x^2} \quad (2.2)$$

Where,

J	-	Diffusion flux	[mol.m ⁻² .s ⁻¹]
D	-	Diffusion coefficient	[m ² .s ⁻¹]
C	-	Concentration	[mol.m ⁻³]
x	-	Diffusion direction	[m]
t	-	Time	[s]

Heterodiffusion: It occurs between two phases of the material. It is more complex phenomenon and possible only if the atom has sufficient amount of energy to displace one position to another one. When the atom moves in the grid, it creates a hole or vacancy in its place. Generally, its displacement is about few micrometers. Figures 1, 2, 3, 4 reveal the movement of atom in crystalline grid with different mechanisms [1,2].

2.1.1. Diffusion mechanisms

Generally, there are four possible ways of diffusion: 1) vacancy mechanism, 2) interstitial mechanism, 3) direct exchange mechanism, 4) ring mechanism.

- 1) Figure 1 depicts vacancy mechanism. It involves the exchange of atom from a normal lattice position to an adjacent vacant lattice one. For taking place this mechanism, it is necessary to present vacancies in crystal lattice. These vacancies directly indicate the number of defects present in the crystal grid. Since diffusing atoms and vacancies interchange their positions, the motion of vacancies is in a direction opposite to that of atoms direction. Both self-diffusion and hetero-diffusion occur by this mechanism [2].

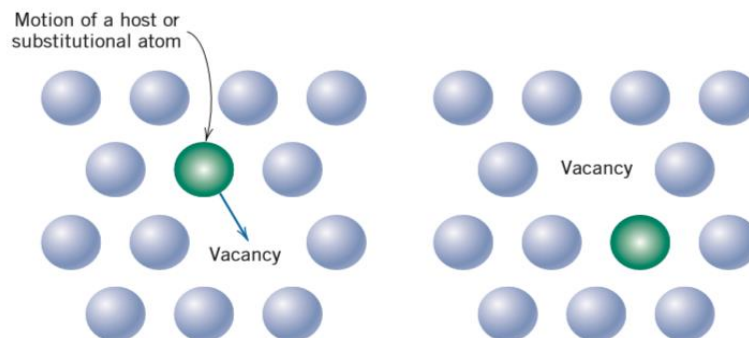


Figure 1 Vacancy mechanism [2]

- 2) Figure 2 schematically presents interstitial mechanism wherein atoms migrate nearby from an interstitial site to neighboring one that is unoccupied. This mechanism is termed as interstitial diffusion. Migrating atoms (called impurities such as hydrogen, carbon, nitrogen and oxygen) are small enough to fit into the interstitial site. Generally, host or substitutional impurity atoms do not diffuse via this mechanism and rarely form interstitials site. In most metal alloys, interstitial diffusion take place quite fast than the vacancy mode due to smaller size of interstitial atoms [2].

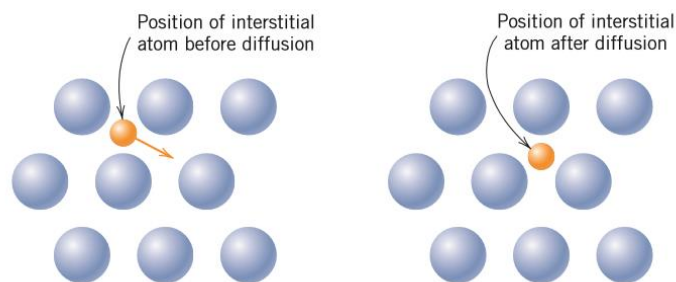


Figure 2 Interstitial mechanism [2]

- 3) Figure 3 shows interchange the place between two adjacent atoms. This would require a quite high amount of energy because each atom must move a distance of two atomic diameters and this would be appreciable for local distortion in the lattice. Therefore this mechanism should be eliminated [1].

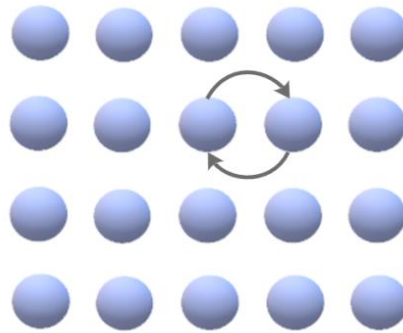


Figure 3 Direct exchange mechanism

- 4) Figure 4 illustrates about circular exchange of four atoms in metal called as ring mechanism. This process likely happens in almost all kind of metals with closed packed structure where four atoms move around at a time. This mechanism is not possible because exceptionally high activation energy would be required. [1].

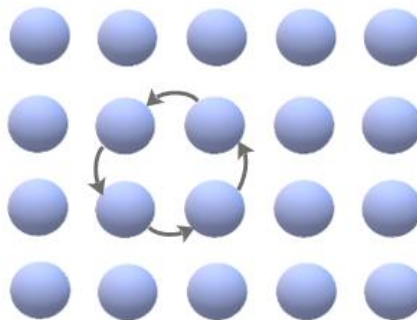


Figure 4 Ring mechanism

2.2. Mechanism of bonding

In diffusion bonding, joint plays a vital role. For bond strength and reliability, the material should have right distance to allow diffusion and atomic bonding. It also depends on the surface of the joining materials. Before bonding, it is necessary to remove the adsorbed layer of gas, water and other substances which are present on the surface of material. Figure 5 illustrates the three stages of joint formation.

First stage: It begins with the initial contact between two metallic surfaces at room temperature. In this stage, the true contact area is small. Bonding is dominated by compressive stress, creep deformation mechanism and also oxide film fracture mechanism. Application of heat and pressure causes the asperities to deform and grow, until a bond plane containing a large number of porosity is formed. However, at the end of this stage, the bonded area is less than 100% and many voids remain in the joint.

Second stage: Diffusion of atoms takes place along the grain boundary. During the second stage, two different but related phenomena occur: (1) shrinkage and spheroidization of some voids and (2) the formation and growth of the first nuclei of

intermetallic compounds. At the end of this stage, many voids are eliminated but lots of voids still remain within the grains.

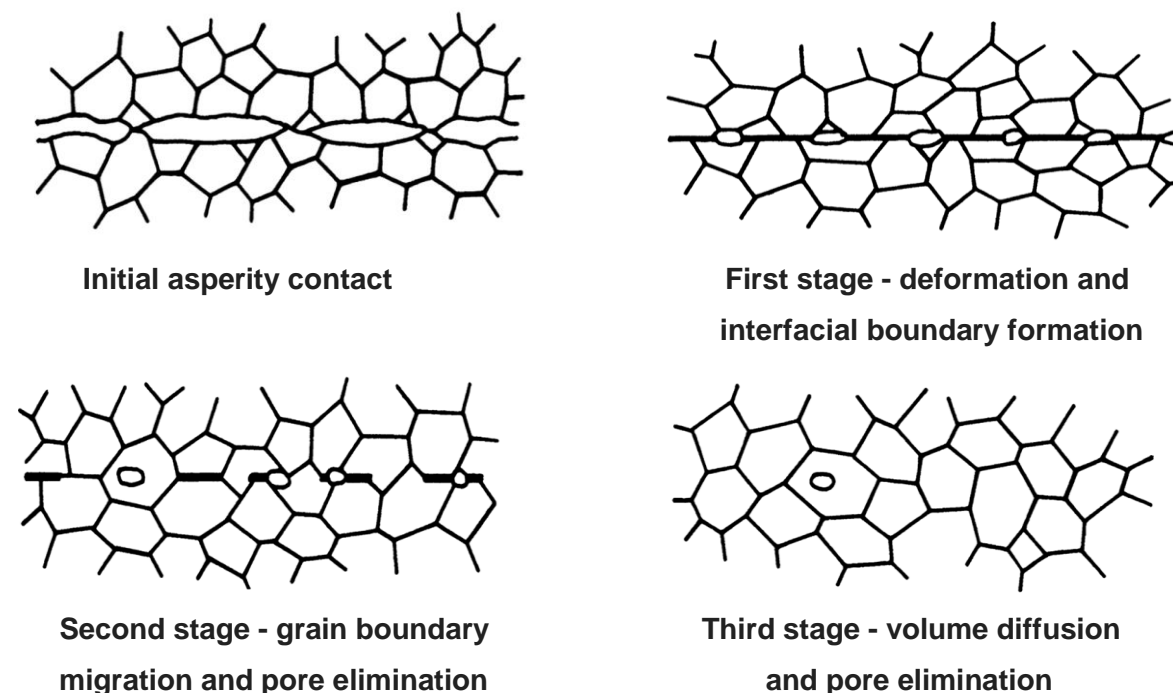


Figure 5 Stages of joint formation [3]

Third stage: In this stage, nuclei continue grow across the bond surface. As a result, porosity is trapped in the center of the crystal. The original interface disappears due to migration of the bond interface. When this phenomena occurs, the only mechanism that persists is the volume interdiffusion between two metallic materials [3,4].

Creating a basic model of diffusion welding is very difficult because it takes place under specific conditions and its result is influenced by the predominant phenomenon. For instance, when exerted pressure at the edge of surfaces is low, a long welding time is obviously required to achieve a high quality joint. When applied pressure and bonding temperature are high enough at the faying surface, the surface asperities first deform and then create a sound weld between specimens within shorter time due to the fact that atoms at the edge of surfaces will make atomic bond.

Diffusion bonding is executed by different materials having distinct mechanical and thermo-mechanical properties, intermetallic phases or sometimes, undesirable structures may form on the weldment surfaces. To avoid such phases, it is favorable to insert suitable metallic interlayers between them in order to achieve a quality joint. Interlayers are mostly found in form of foils, spray coating, galvanic coating or powders.

When diffusion welding is performed with different materials having different coefficient of thermal expansions, residual stresses are generated at the point of contact as specimens cool down. To overcome this problem, selection of appropriate metallic

interlayers having co-efficient of thermal expansion (CTE) value between CTE values of joined components and good plasticity are preferable, which compensates the resulting stresses.

2.3. Principle and technological parameters of diffusion welding.

To create a high-quality joint, it is required to clean both metal surfaces properly which are welded together. Cleaning process also prevents further oxidation with metals during bonding. Afterward, heat is applied to the materials to a predetermined temperature. It is necessary to ensure that process is held at that temperature for a specified period of time until it comes under plastic state. Thereafter, sufficient pressure is applied to create a sound diffusion weld. One thing is to make sure about stability of the vacuum or protective atmosphere during the process. In fact, for producing a high-quality joint between two heterogeneous materials, it is necessary to first carry out several tests with chosen material in order to figure out the appropriate welding parameters for diffusion welding.

2.3.1. Main technological parameters

A successful diffusion bond is controlled by a number of variables. The most influencing variables for diffusion welding technology are temperature, pressure and time. Purity of shielding (inert) gas or vacuum, surface roughness and cleanliness also consider as secondary parameters. These variables are discussed in this section.

Temperature: It is very sensible parameter for diffusion bonding technique. It is determined by the melting temperature of the welded material. When welding is done by dissimilar material, it should be considered as a lower melting temperature of metals. Temperatures between $0.6T_m$ to $0.9T_m$ are best for diffusion welding of many metals and alloys. But the optimum value is considered approximately $0.7T_m$. It affects the diffusion rates of the individual elements in the welded material and also increases plasticity of materials. The aim is to reduce welding temperature as much as possible.

In diffusion process, diffusivity is also a function of temperature. Mathematically, it can be expressed as equation (2.3):

$$D = D_0 \cdot e^{\frac{-Q}{k \cdot T}} \quad (2.3)$$

Where,

D	- Diffusivity, the diffusion coefficient at temperature T	$[m^2 \cdot s^{-1}]$
D_0	- Constant of proportionality	$[m^2 \cdot s^{-1}]$
Q	- Activation energy for diffusion	[J]
T	- Absolute temperature	[K]
k	- Boltzmann's constant	$[J \cdot K^{-1}]$

From equation (2.3), it is obvious that the diffusion processes vary exponentially with temperature. Therefore, very small change in temperature significantly affects the diffusion process [4,5].

Pressure: The welding pressure must be sufficient enough not only to bring mating surfaces close together but also to diffuse material as much as without much deformation. Meanwhile, care must be taken to avoid the formation of macroscopic cracks. Pressure affects several aspects of the process such as final joint, deformation and recrystallization process. The pressure is chosen according to the type of material, the welding temperature, the physical and mechanical properties and the type of interlayer used [4,5].

Time: It is dependent parameter. It is selected according to the pressure and temperature. It is necessary that its choice must be optimal for sufficient diffusion due to the size of the welded surfaces and the different diffusion rates of the individual elements of welded materials. In diffusion welding application, time may vary from few minutes to several hours. For economic reasons, time should be a minimum for best production rates [4,5]. Table 1 shows an example of diffusion welding parameter for different types of materials and combination of materials.

Another important aspect of diffusion welding is the working environment. Welding is done in vacuum chamber or in protective atmosphere by using inert gases such as argon, helium and sometimes nitrogen. When these gases are used, their purity must be very high to avoid recontamination. By employing vacuum, there must be chosen the vacuum pressure according to the type of material which is to be welded. When vacuum pressure is low, sufficient strength can only be obtained by holding the joint for an ample span of time. On contrary, high vacuum pressure increases the cost of the equipment. When welding can be done with insufficient protection, it may create the problem of corrosion due to surrounding oxygen. Therefore, quality of joint could be brittle. There might also be one possibility of welding in free atmosphere, but joint cannot achieve such a quality as joint can produce in vacuum [2]. Table 2 shows special way of diffusion welding in liquid environment.

Table 1 Diffusion welding parameter for various materials and combination of materials [6]

Welded materials	T_w (°C)	p_w (MPa)	t_w (min)
Low carbon steel	950	16	6
Medium carbon steel	1000	12	5
Steel 12060 + steel 19858	1000	20	3
Cr-Al steel	1000	20	5
Austenitic steel + Cu	650	18	40
Al-Si 12 + steel	370	2	10
Cu + steel (0.5% C)	850	5	10
Ni (porous) + austenitic steel	950	5	25
Austenitic steel	1150	14	15
Cu	885	5.6	8
Al + Cu	450	3	8
Mo	1600	10	20
Cu + Mo	900	5	15
Nb	1300	915	10
Mo + Nb	1400	10	20
W	2000	10	20
AlMg6	500	2	10
Graphite + Ti	950	7	20
TiC + Mo	1427	5	10
ZrC + Nb	1400	15	10
ZrC + Ta	2000	5	10
ZrC + W	1800	15	10
NbC + Nb	1600	5	10
NbC + Ta	1700	5	10
NbC + Mo	1800	5	10
NbC + W	1800	5	10
TaC + Nb	1200	5	10
TaC + Ta	1900	5	10
TaC + Mo	1600	5	10
TaC + W	2000	5	10
Mo ₂ C + Mo	1400	5	10
MoC + W	1500	5	10
WC + Mo	1850	5	10
WC + W	1900	5	10

Table 2 Solutions for diffusion welding – liquid environment [6]

Composition of solutions	T_m (°C)	T_w (°C)
100% BaCl ₂	962	1020-1320
90% BaCl ₂ + 10% NaCl	-	950-1300
100% Ba ₂ O ₃	577	1200-1400
100% NaCl	800	850-920
100% KCl	766	820-920
78% BaCl ₂ + 22% NaCl	-	700-950
80% BaCl ₂ + 20% KCl	640	680-1060
70% BaCl ₂ + 30% KCl	-	680-900
53% BaCl ₂ + 20% NaCl + 27% KCl	550	600-900
80% Na ₂ CO ₃ + 10% NaCl + 10% SiC	-	870-900
56% KCl + 44% NaCl	660	700-815
83% BaCl ₂ + 17% BaF ₂	844	900-1000
100% KNO ₃	338	350-600
100% NaOH ₃	317	330-600
100% NaOH	318	350-580

2.3.2. Influence of metallurgical factors

The most important metallurgical factors are allotropic transformation, recrystallization and behaviour of surface oxides.

Allotropic transformation plays a vital role in diffusion bonding because during this transformation, materials will change its volume at some particular temperature. Materials such as steels, tin, titanium, zirconium and cobalt undergo allotropic transformation. This factor is even more important in diffusion welding with dissimilar metals due to preservation the dimensional stability or a creation of good quality weld [5].

Recrystallization is also another important aspect. Recrystallization occurs in pure metal, which has been cold worked, is heated to a sufficiently high temperature usually greater than $0.35T_m$ to $0.4T_m$ [1]. Generally, diffusion rates are higher during allotropic transformation and during recrystallization [5].

Surface oxides are also necessary to be considered during the diffusion welding. Alloys with different compositions vary greatly in the nature of oxides which cover their surfaces. It is needed to assure that some metals such as beryllium, aluminium, chromium and other active elements create strong layer of oxides on the surface. These metals and alloys containing them are more difficult to weld than those which form less stable oxides such as copper, nickel and gold etc. Oxide films make diffusion welding more difficult and

usually require elaborated weld surface preparation. Titanium, zirconium, tantalum and columbium dissolve their own oxides at common diffusion welding temperature even though the films are initially adherent [5].

2.3.3. Impact of surface roughness and cleanliness

Surface preparation in diffusion bonding plays a major role in the final joint quality. Therefore, it is truly imperative to clean the specimen thoroughly prior to welding. For this sort of welding, metal surfaces are generally preferable. They should be properly cleansed with required machining having adequate surface asperities and sufficiently degreased. The more smooth and clean the weld faces are, the better quality of weld joints will be. Hence, they should be first machined with fine cutting tools and then degreased them with acetone. But there is also exception i.e. diffusion welding of steel 19436 to steel 12060 [6].

Figure 6 shows the influence of roughness on the strength of welded joints for dissimilar welding of steel 19436 to steel 12060 at a temperature 950°C, welding pressure 20 MPa and welding time 5 minutes. It can be seen from the figure that the most suitable roughness for this combination is in the range of 1.6 to 3.2 R_a .

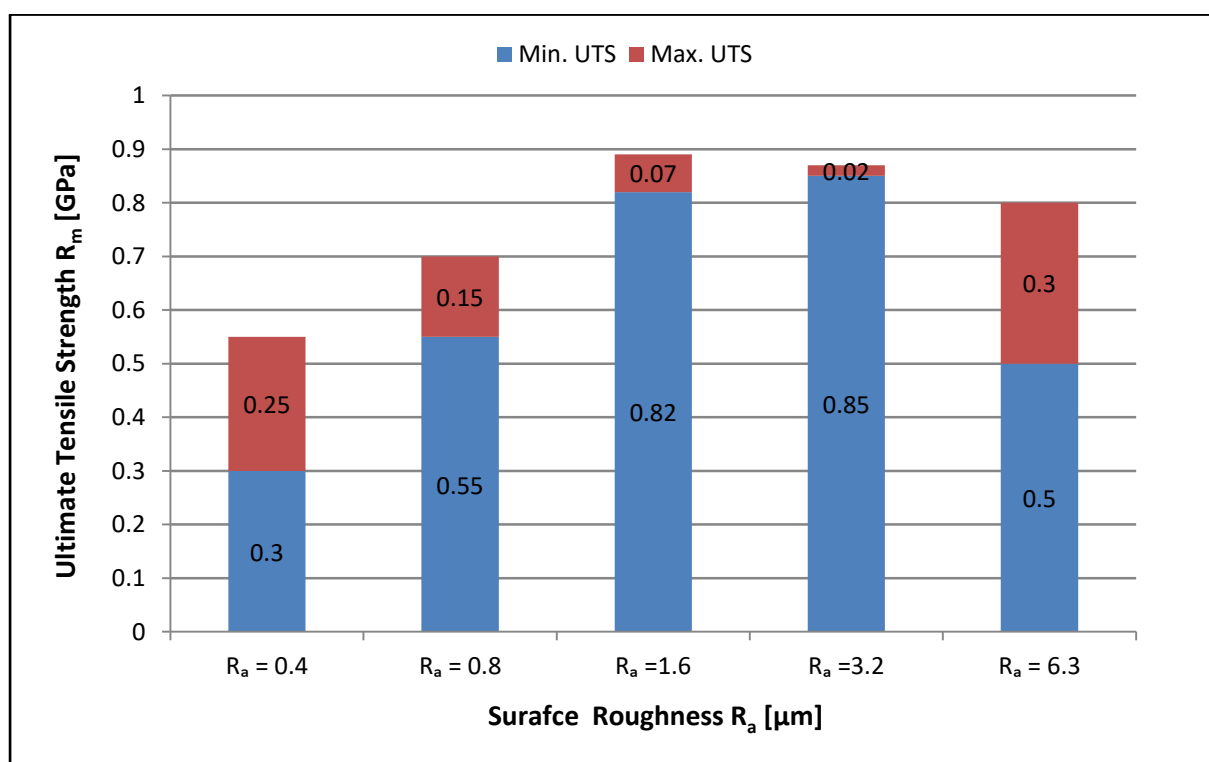


Figure 6 Effect of roughness on the strength of weld joints [6]

There are various form of machining on steel 45 (high quality structural carbon steel) including rough-turning, semi-finish turning, grinding and polishing. It is apperant from the figure 7 that the most suitable method for preparing surface cleaning with machining operation is semi-finish turning and polishing. Another method is, for example, cleaning

mating surface by ultrasonically by which flexural strength of diffusion bonded joints rises from 686-784 MPa to 784-1274 MPa [1].

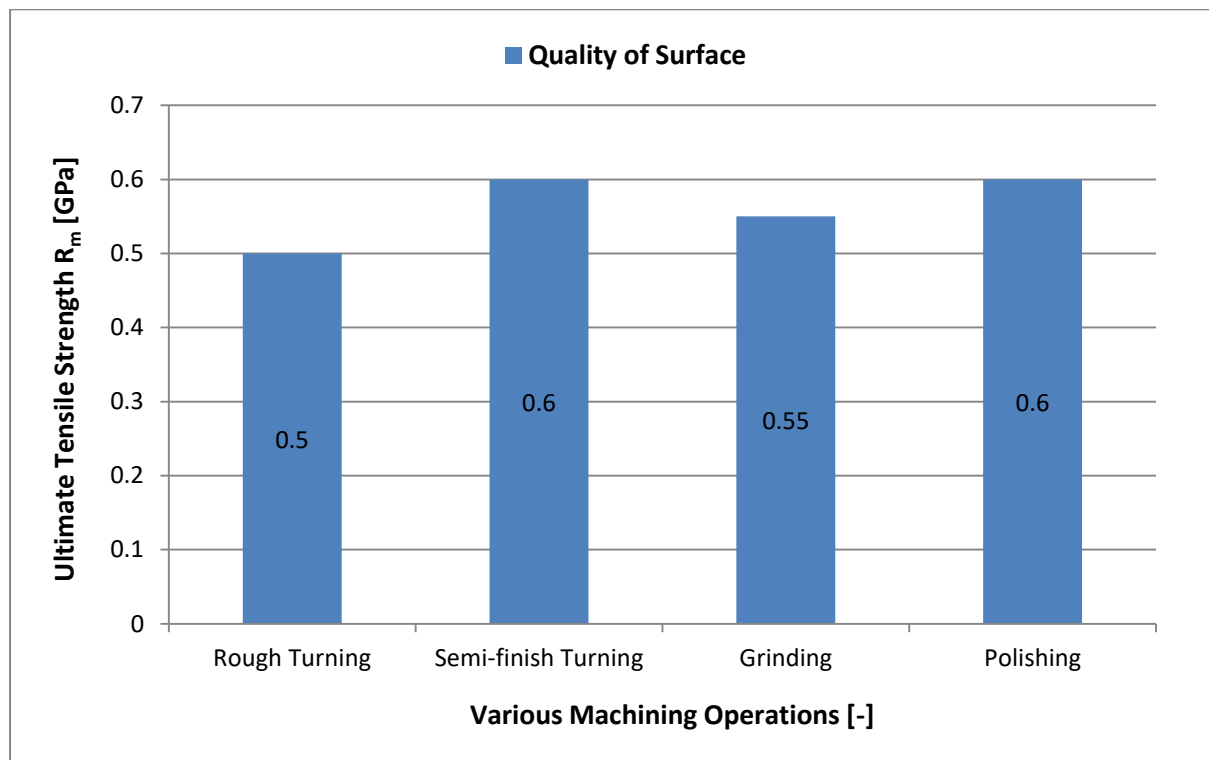


Figure 7 Strength of joints in steel 45 as a function of surface preparation for bonding [1]

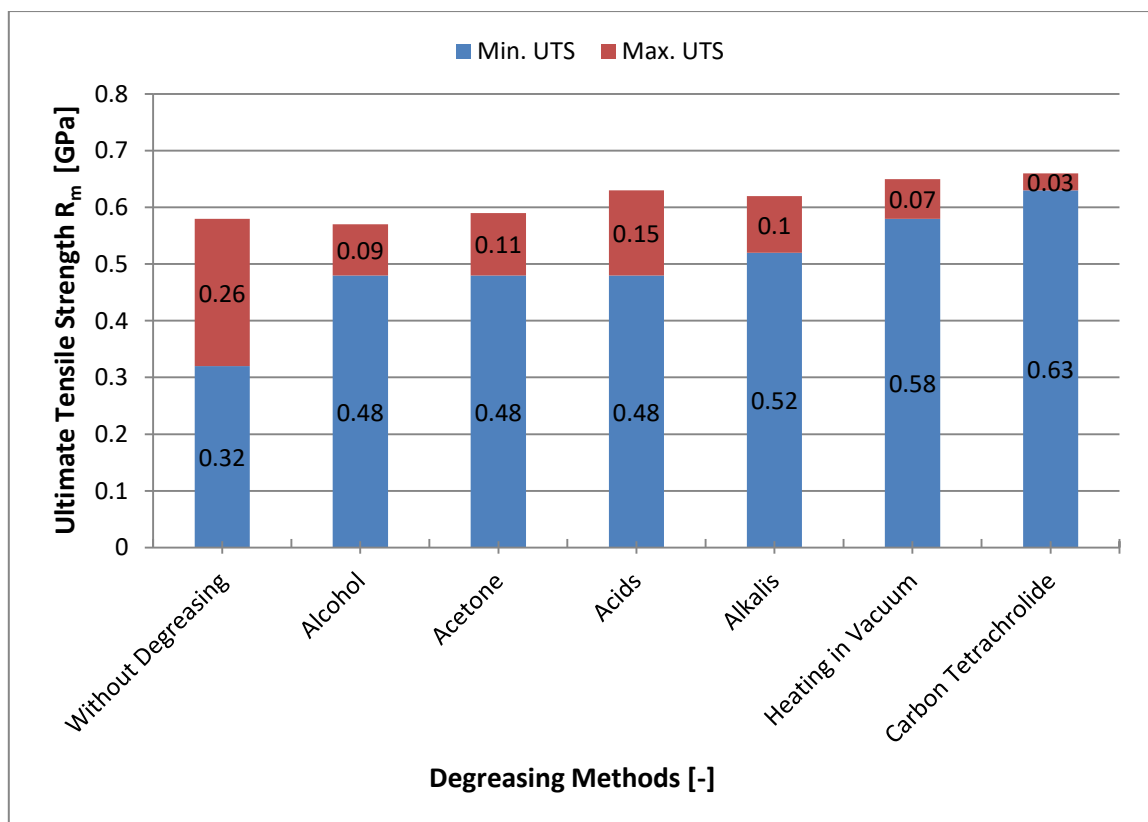


Figure 8 Joint strength of steel 45 as a function of chemical treatment of the mating surfaces [1]

Strength of diffusion bonding can also be affected by the surface conditions. There are adsorbent layers (oil, grease, dust, dirt, rust, paint, etc.) on the surfaces, which must be removed. These layers prevent sufficient contact between two mating surfaces. Hence, the quality of joint can be reduced. Figure 8 illustrates how the adsorbent layers can be removed by different techniques such as chemical etching (pickling) with acids and alkalis, degreasing with alcohol, acetone, carbon tetrachloride and heating under vacuum [1].

2.4. Diffusion welding with interlayer

Recently, the use of interlayers in diffusion bonding technology is expanding in distinct areas such as aerospace, nuclear, sensor and micro-electronics industries. Figure 9 illustrates the mechanism of interlayer in diffusion bonding technology. Although interlayers confer certain advantages in proper joining of welds, wrongly chosen interlayer can also give such disadvantages. They provide some features, in certain applications, which are given below [5]:

- Reduce the effect of diffusion welding parameters
- Speed up diffusion process in contact area
- Solve alloying compatibility problems when joining dissimilar metals
- Minimize the formation of intermetallic compounds (IMCs)
- Remove undesirable elements

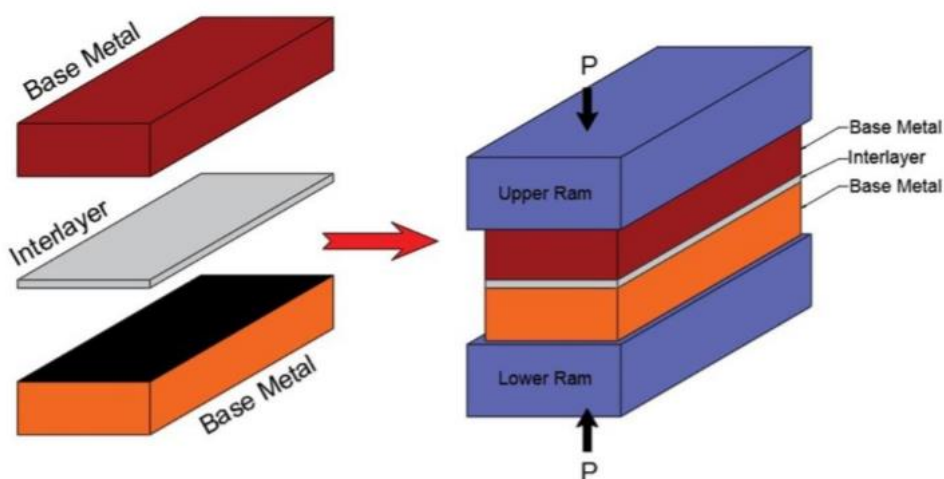


Figure 9 Scheme of diffusion welding with interlayer [7]

Interlayers are used in several forms – as electroplated to the welded surfaces, as foil inserts, as coatings and even as powdered fillers. They are generally kept thin to minimize the effect of heterogeneity at the weld region after the joint is made. Commonly used thickness for interlayer should not exceed 0.25 mm [5].

Interlayers are used to minimize or eliminate problems caused by specific chemical or metallurgical characteristics of the metals to be joined. This requires the careful selection of the interlayer for specific application. Mostly, interlayer is used in pure form of metal. For example, pure titanium is frequently used as an interlayer with titanium alloys. Nickel is used as an interlayer with chromium containing nickel-base superalloys. Silver, however, has been used as an interlayer with aluminum alloys. Another kind of interlayer that has been suggested is with rapid diffusing elements. Alloys containing beryllium have been suggested for the use with nickel-base alloys to increase the rate of joint formation [5,7]. Improperly chosen interlayers can result in the following adverse effect [5]:

- Decrease the temperature capability the joint
- Decrease the strength of the weldment
- Cause microstructural degradation
- Risk of corrosion problem at the joint.

2.5 Advantages, disadvantages and applications of diffusion welding

Diffusion welding offers quite a few advantages over the more commonly used welding processes as well as a number of distinct limitations.

Following are some of the advantages of this process [1,3,4,8]:

- It can turn out weldments in which there is no porosity or discontinuity across the interface. As a result, weldments have extended service life, quality and reliability.
- The joints retain same mechanical and physical properties as parent materials by selecting proper welding process variables.
- It can be used to join not only similar but also dissimilar metals, alloys which have different in physical-mechanical characteristics and also non-metals such as glass, ceramic, quartz, cermets, graphite and semi-conductors.
- Deformation of the component is kept minimal but sometimes, little machining is required.
- Highly qualified technicians are not required because the process can be almost fully automated.
- It is possible to produce intricate shapes and high precision components with good dimensional tolerances.
- Materials to be joined may vary in thickness from a few micrometres (foil) to several meters.
- It does not need any electrodes, solders, special grades of wire and fluxes.
- Final product does not gain in weight as happens with ordinarily welded and brazed components.

Following are some limitations of this process that should be considered [3,4,8]:

- It increases capital cost with increasing component size because bigger size of vacuum chamber is necessary.
- Thermal cycle time is quite large compare to conventional fusion welding and brazing processes.
- It requires careful surface preparation and fit up of the workpieces as well as high quality vacuum and protective environment.
- Suitable interlayers and procedures have not yet been developed for all metals and alloys.
- Components are verified by non-destructive testing for proper execution of joints in many cases.

Although diffusion welding is the special welding methods, its potential applications should not be underestimated by other welding technology. It is mainly used in the following applications [5,9]:

- Diffusion bonding is primarily used in aerospace, nuclear and electronics industries.
- It is being used in fabrication of honeycomb, rocket engines, turbine components, structural members, composites and laminates.
- It is developed for commercial use for the creation of compact heat exchangers with high performance.
- Diffusion bonding, in conjunction with superplastic forming, is also used when creating complex sheet metal forms.
- It is also useful in the micro-electronics field bonding of power device heat sinks.
- In the sensor industry, it has been used for the manufacture of oxygen analysing sensors used for monitoring oxygen concentrations in the power generation and metallurgical processing plant.
- It is used to weld ferrous and non-ferrous alloys, reactive and refractory metals.
- It can also be employed to join dissimilar materials to materials such as metals to glass, ceramics, ferrites, graphite and semi-conductors.

2.6. Types of diffusion bonding furnaces

Nowadays, dissimilar metals and alloys can be joined for special purpose applications. To make them by diffusion welding, one needs specially designed furnace which have different sources of heating and different protective environments.

The key components of vacuum diffusion welding unit comprise a vacuum chamber, a vacuum pump system, heating source, hydraulic system for exerting pressure and other accessories, such as pressure and vacuum gauges, thermocouple, cooling unit and monitoring device [1]. Different diffusion bonding furnaces are shown in figure 10.

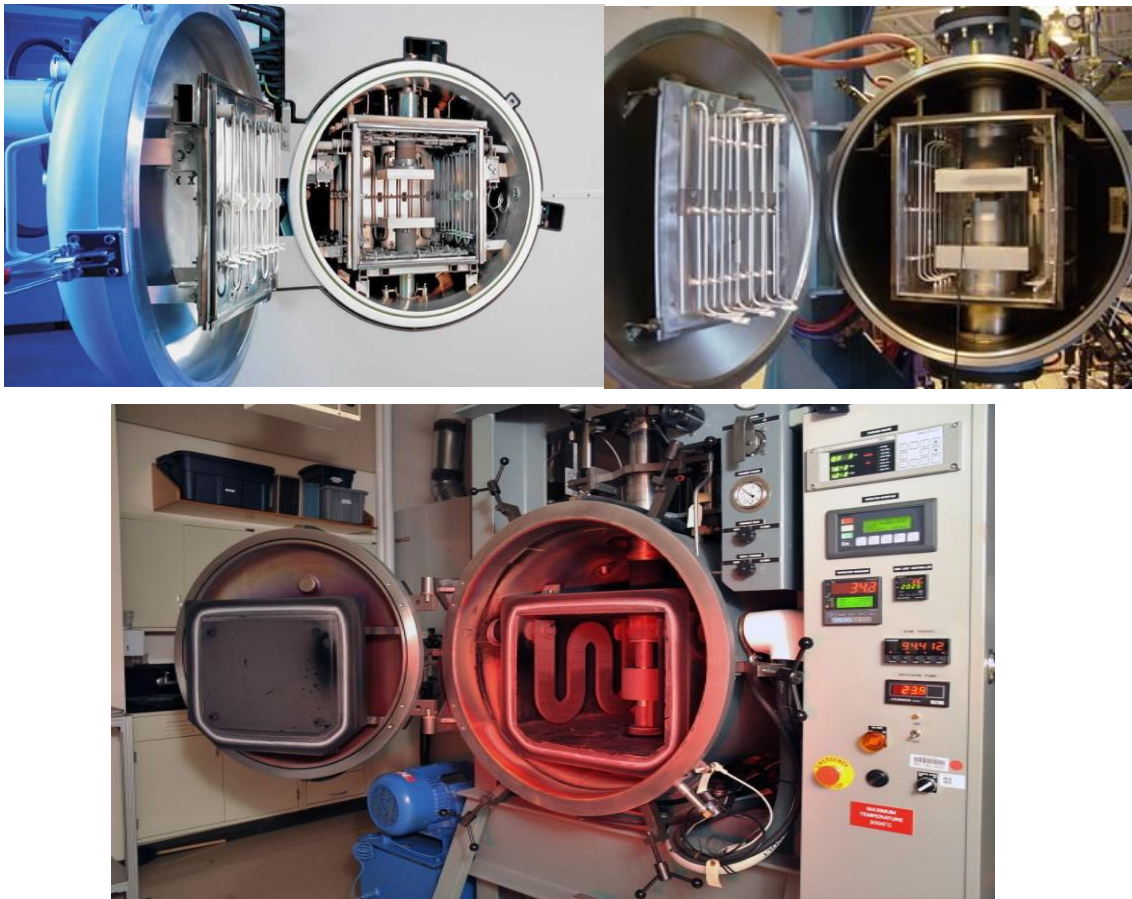


Figure 10 Diffusion bonding furnace [10,11,12]

2.6.1. Device separation according to vacuum

Vacuum is an environment where the gas or steam pressure is considerably lower than the atmospheric pressure. In the case of diffusion welding, the vacuum is easily formed by evacuating gases and vapours from the vacuum (welding) chamber. The resulting vacuum is then required to be maintained throughout diffusion bonding process. This is achieved by adequate sealing of the walls and also by the use of special getter which absorbs the oil and water vapour. At present, there are three basic ways to create a vacuum: a vacuum diffusion pump, special gas scavengers and cryogenic traps [1].

Classification of vacuum according to its usage

- 1) Low vacuum – 1.3×10^{-1} Pa or less
- 2) Medium vacuum – 1.3×10^{-1} to 1.3×10^{-4} Pa
- 3) High vacuum – 1.3×10^{-4} to 1.3×10^{-7}
- 4) Ultra high vacuum – 1.3×10^{-7} to 1.3×10^{-10}
- 5) Reduced or elevated pressure of shielding gases

Classification of vacuum by workpiece placed in vacuum chamber

- 1) Welded part covered with fully vacuum
- 2) Welded part covered with partly or locally vacuum

2.6.2 Basic types of heat sources and methods of heating

In vacuum diffusion bonding, work pieces can be heated into two different groups. First, heat is transferred to the two work pieces by radiation or thermal conduction using external heat sources. Second, heat is generated in the work pieces themselves by conversion of electrical energy to thermal one. Methods of heating can be divided into the following categories:

Resistance heating: Suitable heat source for this heating method is a welding transformer. Electric current flows through the workpieces and heats them up. Consequently, final weld is done. It is therefore obvious that the workpieces must be electrically conductive. Mostly, this type of heating is used to weld thin sheets or layers from different materials [1].

Induction heating: It is the predominant method in both industries and research areas. Workpieces which are placed inside an inductor coils are heated by high frequency electro-magnetic current. Heat source is in most cases a high-frequency generator capable to achieve temperatures above 1500 °C. More than 40 types of these devices have been developed from which approximately 90% are universal and the rest are special. [1].

Radiation heating: It is also well-known method. This method is suitable for cyclic operation. Heat source is a rod, a thin-foil or a ribbon such as tungsten, tantalum or molybdenum, which is heated by the passage of the electric current. Heat is then radiated (just like the bulb). Very good joints are created by this method using diffusion welding equipment. It serves to connect relatively small components with a sensitive temperature gradient such as ceramics, semiconductor or glass [1].

Electron beam heating: It requires sufficient high vacuum in the process chamber. It is used for joining refractory metals (such as tungsten, molybdenum and zirconium). This type of device comprises electron optical systems. Three devices are equally spaced 120° apart from each other and are located outside the working chamber. Workpieces usually play a role of anode and beams themselves acts as a cathode. The DC and AC voltages are applied to achieve movement of the electron beam. This method of heating allows semi-automatic production and has special protection against X-rays [1].

Solar heating: This appliance uses concentrators and heliostat for heating. The solar furnace allows local heating over 3000 °C. The intensity of solar energy can be changed by obscuring the mirror or by moving the sample out of focal length. The specificity of this type of furnace is that the sample is heated only on one side, so for proper heating samples must be rotated during heating. Hence, tubes and rods products can be rotated continuously in diffusion bonding solar furnace. Therefore, it can be expected that diffusion welding with this type of heating can be produced some better results than with electric heating because bonding process is done without any influences of surroundings [1].

Gas heating: The use of carbon dioxide for diffusion welding has been a lasting trend. Carbon dioxide significantly reduces the welding process. Unlike others, diffusion bonding machine therefore contains a protective gas tank and gas distribution. The protective gas passes from the reservoir, the reducer and the dryer into the welding chamber, where it displaces all air. This type of heating device is most often applied to the welding of less demanding materials such as copper, nickel, lead, medium and low carbon steel. Tubes and rods are welded to a diameter of 50 mm [1].

2.7 Research focus on diffusion welding with the use of interlayers

Diffusion welding is one of the by far most adopted technologies in distinct areas of manufacturing for joining dissimilar metals. Since diffusion welding is emerging field, many researches have been carried out in the last few years. High melting temperature metals (Mo, W, Ta, Nb) and metals with high affinity to oxygen (Al, Mg, Ti) are difficult to weld by conventional welding technology or sometimes, the weld does not have a sufficient quality. That is the reason, why this technology is often chosen for joining dissimilar materials. Also, it is one of the few methods wherein metals can be joined with non-metals such as ceramics, graphite and glass. As discussed in detailed information about this methodology here in this section, some of the research works are explained here, which are closely related to experiment in order to make it more accurate in both decision based and result oriented.

The research paper titled with **“Microstructure and Mechanical properties of vacuum diffusion bonded joints between Ti-6Al-4V alloy and AISI 316L stainless steel using Cu/Nb multi-interlayer”** was printed in ELSEVIER publication in the Vacuum 145 (2017) 68-76 by T.F. Song, X.S. Jiang and their other colleagues.

The main purpose of this article was to gain high mechanical strength of the joint of these two materials through optimizing the welding process parameter.

The experiment was carried out between these two dissimilar metals by using Cu/Nb as a multi-interlayer in the temperature range of 850-950 °C with interval of 50 °C for 90 min and 900 °C with a bonding period of 30-120 min under a uniaxial load $(2-8) \times 10^{-1}$ Pa in vacuum chamber. Vacuum hot pressing furnace was used for heating the samples. The thickness of Cu and Nb foils is 20 µm and 25 µm with purity of 99.9 %. Optical microscopy (OM), scanning electron microscope (SEM), energy dispersive spectroscopy (EDS) and X-ray diffraction (XRD) techniques were carried out to analyze the micro-structure characteristics of final welded joints. Universal testing machine (WDW-3100) and micro-vickers hardness tester (HXD-100TM/LCD) was employed to evaluate the mechanical properties such as maximum tensile strength and hardness of the bonded joints.

This research work was primarily focused on the microstructures and mechanical properties of the final joints with respect to various bonding time and temperature. When the bonding temperature was 900 °C or below, joint formed no intermetallic compounds (IMCs)

and it revealed strong TiA/ α - β Ti/Nb/Cu/SS diffusion bond by inserting a Cu/Nb multi-interlayer. Fracture analysis results demonstrate fracture at Cu/Nb interface at lower temperature and remnant Cu layer at 900 °C for 90 min.

To sum up, maximum tensile strength 489 MPa and minimal hardness value 99 HV were measured at the welded joint at 900 °C for 90 min. Analysis from fracture morphology, joint displays extensive dimples on the surface, indicating a ductile nature at 900 °C for 90 min whereas at 950 °C for 90 min, it shows cleavage and lamellar fracture, exhibiting a brittle fracture [13].

Second article takes from the "RARE METALS" journal with its title "**Impulse pressuring diffusion bonding (IPDB) of titanium to 304 stainless steel using Ni interlayer**". It was published by Fang-Li Wang and his other colleagues in the Rare Metals (2016) 35(4) 331–336.

The main aim of this article was to obtain successful bonding within a dramatically reduction of time with improved strength of joint.

The experiment was done between these two dissimilar metals by using pure Ni as an interlayer with 200 μ m thick foil at a temperature 850 °C for different ranges of time (60-150 s) under impulse pressure (8-20 MPa) in vacuum. Diffusion bonding test was conducted on the Gleeble 1500D thermal-simulation experiment machine. SEM, EDS analyzer, XRD and tensile testing machine were utilized to investigate metallography, chemical compositions, fracture morphology and tensile strength of samples, respectively. In this experiment, four samples were heated to 850 °C temperature at 60 s, 90 s, 120 s and 150 s. From the metallography, it was observed that the resultant joints were detected with no IMCs. There was generated Ni-Fe solid solution on steel side whereas Ti_2Ni , TiNi and $TiNi_3$ IMCs formed at the Ti/Ni interface. One important information was also found from metallography that the thickness of the interlayer increases gradually with the increase of bonding time.

At the end, the maximum tensile strength 358 MPa was achieved by IPDB for 90 s. Fracture took place along the Ti_2Ni and TiNi phase upon tensile loading. The existence of cleavage pattern on the fracture surface exhibits the brittle nature of the joints [14].

The journal paper named "**Diffusion bonding of commercially pure titanium to 304 stainless steel using copper interlayer**" was published in ELSEVIER publication in the volume of Materials science and Engineering A 407(2005) 154-160 by S. Kundu and his other colleagues.

As per its title, the main goal of this research work was to improve the quality of joint between these two dissimilar metals by using Cu as an interlayer of thickness 300 μ m. Since copper did not only generate any intermetallic compound with iron but also had a lower

melting point than Ti, Fe and Ni which in turn increased the flow ability at high temperature helped to create good contact between the faying surface.

The experiment was carried out between these two dissimilar metals by using Cu as interlayer in the temperature range 850-950 °C for 1.5 h under uniaxial pressure of 3 MPa in vacuum chamber. Heating was done by electric resistance created between the two samples. Scanning electron microscope (SEM) was used for analyzing microstructure of the transition joints and chemical compositions were also determined by energy dispersive spectroscopy (EDS). For better accuracy of the result, four samples were tested for each process parameter.

The research paper was basically focused on temperature. Three different temperature ranges 850 °C, 900 °C, 950 °C were kept to compare the result. At lower bonding temperature 850°C, both bond strength and breaking strain of the diffusion couple was observed very low. During the bonding temperature 900 °C, considerable improvement was found in both ultimate tensile strength and breaking strain while at temperature 950 °C, Fe-Cu-Ti and Cu-Ti bases intermetallic were not found in diffusion interfaces.

Thus, this research paper reveals that with increasing temperature (950 °C), bond strength decreases because of enhanced volume fraction of brittle intermetallic compound. On the other side, at lower temperature (850 °C), it shows very poor bond strength due to incomplete coalescence of mating surface. The most accurate result was found at the temperature 900 °C which gives bond strength of 318 MPa and ductility of 8.5 % [15].

Another article related to diffusion welding is “**Evaluation of the microstructure and mechanical properties of diffusion bonded joints of titanium to stainless steel with a pure silver interlayer**”. It was printed in ELSEVIER publication in the volume of Materials and Design 46 (2013) 84–87 by Yongqiang Deng and his colleagues. According to the title, the main intention of this research work was to achieve optimal mechanical strength of the joint between these two dissimilar metals by using Ag as an interlayer of thickness 50 µm.

The experiment was conducted between these two dissimilar metals by using Ag as interlayer between temperatures of 825-875 °C for 20 min under uniaxial pressure of 8 MPa in vacuum. A Gleeble 1500D thermal–mechanical simulator was adopted to bond the specimens. SEM with back-scattered mode, EDS, tensile testing machine and micro-hardness measuring device were selected to reveal the microstructure of the reaction layers, to determine the chemical composition across the joint, to evaluate the strength of the joints and to measure the hardness distribution along the bonded joint, respectively.

In the experimental part, three samples were heated to the different temperature (825 °C, 850 °C and 875 °C). It was observed from the metallographic samples that resultant joints were detected no IMCs on steel side. They were composed of not only remnant Ag

interlayer at the middle but also Ti-Ag intermetallic phase and Ti-Ag substrate (s.s.) on the Ti side. It was reported from the EDS analysis that fracture took place through the remnant Ag interlayer upon tensile loading and it was evident that Ti-Ag phase had no detrimental effect on the bonding strength which exhibited that joints were in ductile nature. One important thing was also noticed in this research paper that all samples were achieved almost the same value of average tensile strength.

To summarize, the Ag interlayer can effectively block the formation of brittle IMCs between Ti and SS, thus formed joints were composed of SS/Ag/Ti-Ag/Ti s.s./Ti. Notably improved bonding strength of more than 410 MPa was achieved. Therefore, Ag can be considered as a desirable interlayer for bonding dissimilar materials like Ti to SS [16].

Last but not least, an article titled with **“The influence of nickel interlayer for diffusion welding of titanium alloy (Ti-6Al-4V) to austenitic stainless steel 304L”** was published by Czech Technical University, Prague in 2013.

The main purpose of this research paper was to attain best mechanical properties e.g. micro hardness of final joint of these two dissimilar metals without and with Ni interlayer.

The experiment was performed between these two dissimilar metals without and with nickel interlayer (thickness 20 μm electroplated on steel sample) at a temperature 900 $^{\circ}\text{C}$ for 15 min under pressure of 2.5 bar using Argon as an inert gas with shielding environment. Heating is enabled by use of high frequency inductor and graphite crucible. Metallography, chemical compositions and mechanical properties were evaluated by SEM, EDS analyzer and micro-hardness measuring device, respectively.

From the metallography, it was observed that welded sample composed of different intermetallic phases with having some thickness value in micrometer. Diffusion of Ti alloy compositions to steel part and diffusion of steel elements to Ti alloy part was measured by EDS analyzer.

Sample without Ni interlayer, TiNi_3 IMC was created in direction to steel, which was very brittle, having hardness value of this layer $H_{IT} = 14$ GPa was much higher than base metal $H_{IT} = 5$ GPa. In direction of Ti alloy, Ti_2Ni IMC was also created.

Sample with Ni interlayer, no intermediary phase was created in direction to steel. Only Cr, Fe diffused into electroplated Ni. On the other hand, in the direction of Ti alloy, TiNi IMC was created having hardness value of this phase $H_{IT} = 10$ GPa.

In conclusion, with the help of Ni interlayer, positive influence was observed on final welded joint which is resulted in reducing hardness value on intermediary layer to 10 GPa, compared to sample without interlayer with hardness 14 GPa. Therefore, resulting weld with Ni interlayer would be more ductile, so use of Ni interlayer was advantageous for this kind of diffusion welding [17].

3. Gleeble simulator machine for diffusion welding

The Gleeble device was firstly introduced in 1957 to simulate the heat-affected zone (HAZ) of arc welding. It was developed by American company Dynamic System Inc. (DSI). It is one of the most used systems in the world to determine the properties of materials, to improve a material's performance or to enhance a material's fabrication process. In past, DSI mainly used in America and Japan but nowadays, it has been expanding to Europe, Russia, China, India and South Korea [18]. This device can be simulated, for example, continuous casting, hot rolling, weld HAZ cycles, diffusion bonding, forging, heat treating and many others processes [19].

Gleeble device performs physical simulation of material processing in which small sample of material is used. The simulation process is then carried out in the gleeble device. When the simulation result is accurate, this result can be immediately transferred from the laboratory to the actual production process to solve real-world problems [19].

In the laboratory of the Technical University of Liberec, there is Gleeble 3500 device, which was purchased in the year 2013 and it is the second device in the whole Czech Republic of a similar type.

3.1. Gleeble 3500 Thermal-Mechanical Simulator

The Gleeble simulator, is located at the Technical University of Liberec, make up of several main parts such as control panel, the main unit (including the hydraulic pump, vacuum pump, water cooler, mobile unit, vacuum chamber and transformer). Gleeble 3500 Thermal-Mechanical Simulator as shown in figure 11.



Figure 11 Gleeble 3500 Thermal-Mechanical Simulator [20]

This device is fully integrated with digital closed loop control with thermal and mechanical testing system. Easy-to-use Windows based computer software, combined with an array of powerful processors, provides an extremely user-friendly interface to create, run and analyse data from thermal-mechanical tests and physical simulation programs. Specimen sizes that can be tested by this device should be in maximum 20 mm diameter in round shape, 400 mm² in square, 2 mm x 50 mm in flat strip [19].

3.2. Basic components of the Gleeble system

The entire system is not a single device as shown in figure 12. It consists of a main unit, a transformer for heating, a console, a hydraulic pump, a water cooler, a mobile unit (include the Hydrowedge II) for temperature and mechanical tests, a vacuum system for creating vacuum environment in vacuum chamber, a compressor for compressed air and a thermocouple welder machine for welding thermocouples on the specimen surface.

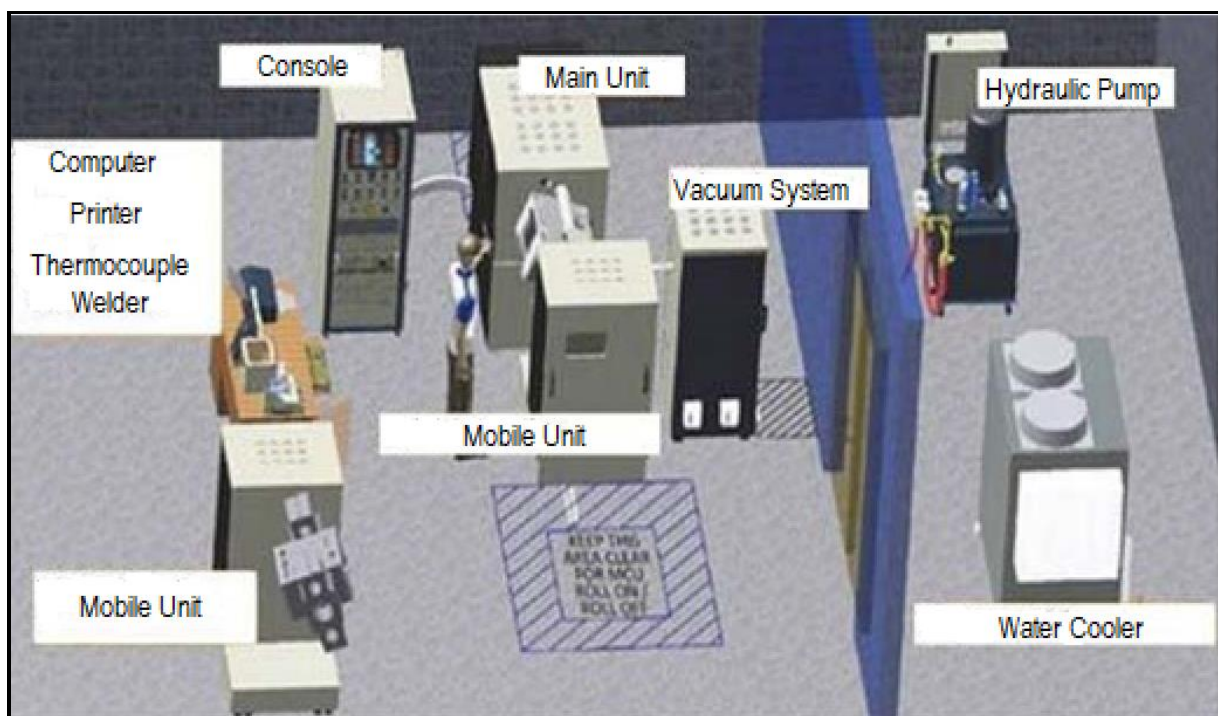


Figure 12 Arrangement of the Gleeble system [21]

Generally, hydraulic servo system is attached to the mobile unit and the console with the hardware and software for the management and control of the entire system. This is followed by the hydraulic pump to maintain adequate pressure in the hydraulic unit [19]. The vacuum system is capable of reaching the sufficient amount of vacuum (higher than 10^{-1} Pa) in a vacuum chamber.

For controlling and monitoring of temperature of the specimen during the test, four thermocouples are used in a standard Gleeble device. There are two possibilities (figure 13) for measuring the temperature, with either four thermocouple channels or one pyrometer channel and three thermocouple channels.



Figure 13 Four thermocouple channels and side outlet for pyrometer [21]

3.3. Operation of Gleeble 3500

The Gleeble device can be operated totally by manually, totally by computer or by any combination of manual or computer control which is needed to provide maximum versatility in materials testing. However, the device is always operated manually when loading and unloading a test specimen.

Working of Gleeble device is based on two systems. First, thermal system in which, test specimen can be heated directly by resistance heating. Second, mechanical system allows the operator to program changes from one control mode to another during the test with respect to time [19].

3.3.1. Gleeble thermal system

The Gleeble 3500 simulator device generates a wide range of temperature profiles with wide range of heating and cooling rates. It can create gradients with high slope but relatively flat gradients. Heating rate for different loads on different samples diameter is given in table 3.

Table 3 Dependence of heating rates on load and sample diameter [21]

Sample heating rates	
Tensile load, diameter 6 mm	10,000 °C.s ⁻¹
Tensile load, diameter 10 mm	3,000 °C.s ⁻¹
Compression load, diameter 6 mm	50 °C.s ⁻¹
Compression load, diameter 10 mm	5 °C.s ⁻¹

There are two types of cooling: free (uncontrolled) cooling and controlled (programmed) cooling. During free cooling, heat dissipates from the samples with help of cooled high-temperature jaws when the transformer is off. In controlled cooling, the samples are first heated and then cooled according to program set by computer. Highest cooling rate can be achieved by combination of compressed air and water. Free cooling depends on the type and material of the high temperature jaws, the thermal conductivity of the samples and

free span between jaws [21]. An example of the achieved cooling rates using full-contact copper jaws for different samples diameters is given in table 4.

Table 4 Cooling rates under free cooling for different samples diameters [21]

Free (controlled) cooling	
Sample diameter 6 mm	140 °C.s ⁻¹ , range between 1,000 °C to 800 °C
	78 °C.s ⁻¹ , range between 800 °C to 500 °C
Sample diameter 10 mm	300 °C.s ⁻¹ , range between 1000 °C to 800 °C
	200 °C.s ⁻¹ , range between 800 °C to 500 °C

The direct resistance heating system of Gleeble 3500 can heat specimens at rates of up to 10,000 °C.s⁻¹ or can hold steady-state equilibrium temperatures. High thermal conductivity jaws (made of copper or austenitic steel) are used to hold the specimen, making the device capable of high cooling rates. An optional quench system can achieve cooling rates up to 6,000 °C.s⁻¹ at the specimen surface. Generally, heating and cooling rates are kept at a temperature not exceeding ±1 °C.s⁻¹ for uniform heating and cooling of the samples. Thermocouples or optional pyrometer provide signals for accurate feedback control of specimen temperatures [19].

Several types of thermocouples (K,S,R,B and E) are possible to use in Gleeble device. Their temperature ranges are shown in table 5. Four thermocouple channels can be used at one time and any one of them can be used for temperature control. The most used thermocouples in Gleeble testing are Type K, Type S and Type R. Thermocouples are welded at the centre on the sample surface by the thermocouple welder machine to achieve a uniform temperature gradient [19].

Table 5 Thermocouple type available on Gleeble and its temperature range [19]

Thermocouple type	Description	Operating range
Type K	Ni-Cr(+) vs. Ni-Al(-)	0-1,250 °C
Type S	Pt-10%Rh (+) vs. Pt(-)	0-1,450 °C
Type R	Pt-13%Rh (+) vs. Pt(-)	0-1,450 °C
Type B	Pt-30%Rh (+) vs. Pt-6%Rh(-)	0-1,700 °C
Type E	Cu-Ni(+) vs. Ni-Cu(-)	0-900 °C

3.3.2 Gleeble mechanical system

The Gleeble 3500 mechanical system also offers fully integrated hydraulic servo system capable of exerting as much as 10 tons of force in tension and in compression. Displacement rate as fast as 1,000 mm.s⁻¹ and displacement as much as 100 mm can be achieved. However, it is never possible to achieve the maximum displacement and

maximum force. Linear variable displacement transducer (LVDT), load cells, or non-contact laser extensometer provide feedback to ensure accurate performance and repeatability of the mechanical test program [19].

The mechanical system allows the operator to change program from one control mode to another during the test. This capability provides the versatility that is necessary to simulate many thermal-mechanical processes. The program can switch between control variables at any time and as often as required during the test. Control modes that are available include stroke displacement, force, various extensometers, true stress, true strain, engineering stress, and engineering strain [19].

3.3.3 Temperature gradient and high temperature jaws

Gleeble 3500 device is able to control temperature distribution along the axis of the specimen, i.e. the temperature gradient. Several factors affect the temperature gradient – the type of testing material, its thermal and electrical resistance, the surface and volume ratio, the length of the sample, the cross section and free length (the distance between the edges of the jaw contacts as shown in figure 14). The shorter contact between the clamping jaws and the specimen generates the more uniform temperature gradient along the axis of the specimen [21].

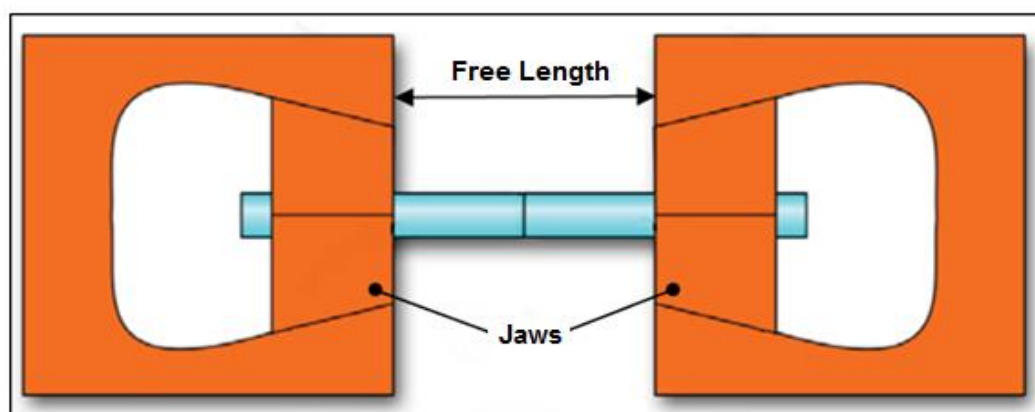


Figure 14 Free length between full contact jaws [22]

The high temperature jaws have a great effect on the temperature gradients and heat dissipation process. Jaws have many different types and variety of shapes as shown in figure 15. Therefore, it is necessary to select appropriate jaws and specimen according to their temperature and shapes. Typically, copper (Cu 99%) and austenitic steels (X5CrNi18-8) jaws are used because they have different thermal conductivity, which in turn different temperature gradient can be obtained. Jaws can be divided into full-contact and partial contact [21].



Figure 15 Full and partial contact jaws of different shapes

Figure 16 shows a temperature gradient on a sample of S355J2 steel having 12 mm diameter by using full contact copper jaws and free span 30 mm. Figure 17 shows a temperature gradient on a sample of S355J2 steel having 12 mm diameter by using full contact (X5CrNi18-8) austenitic steel jaws and same span as copper jaws have. Both graphs are generated from Origin software between temperature ranges from 200 °C to 1200 °C.

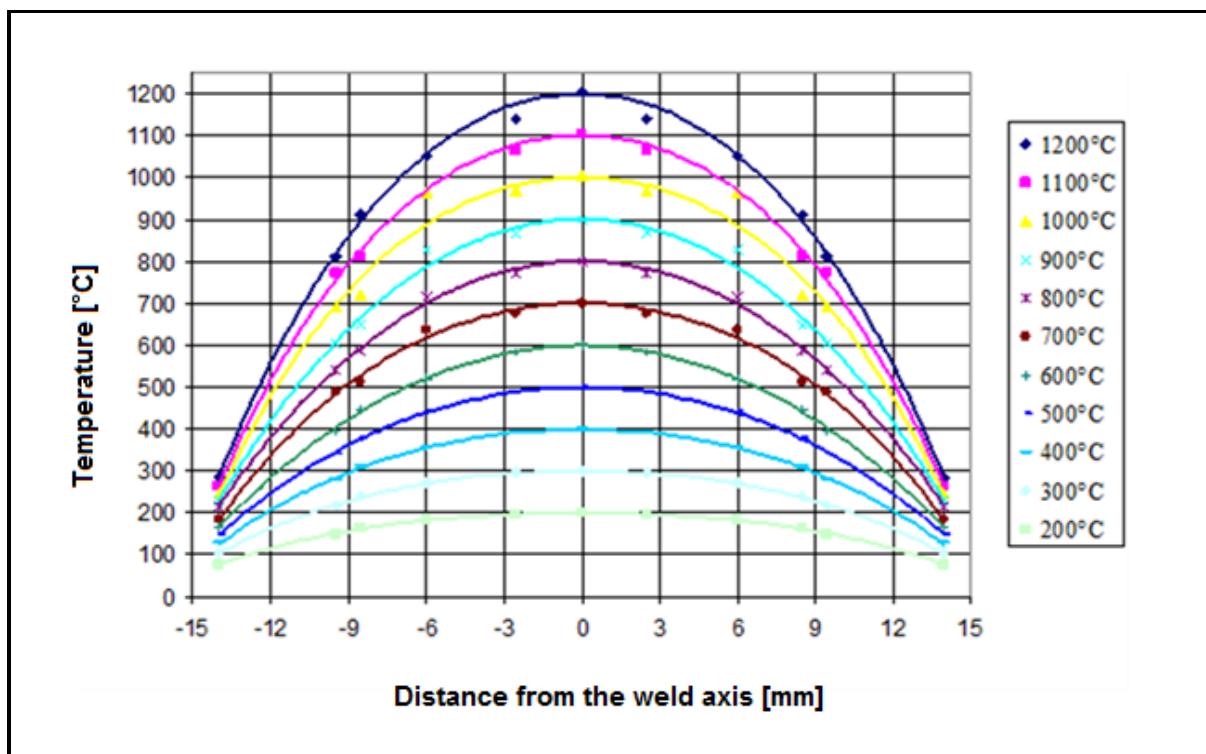


Figure 16 Graphical representation of the temperature gradient over the 30 mm free length of the S355J2 steel sample by using full-length copper jaws [21]

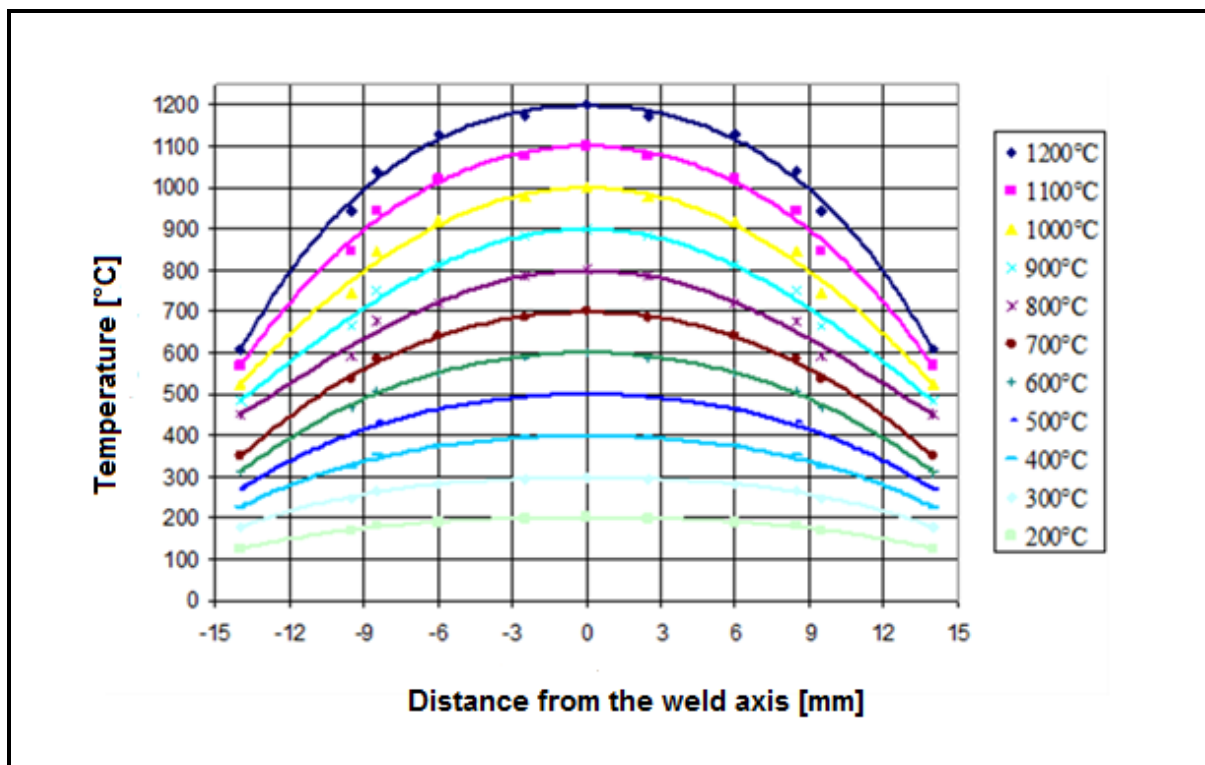


Figure 17 Graphical representation of the temperature gradient over the 30 mm free length of the S355J2 steel sample by using full-length X5CrNi18-8 steel jaws [21]

4. Experimental part

Main intention behind this diploma work was to figure out suitable metallic interlayers having negligible deformation and then improve ductility of heterogeneous joint by adopting diffusion welding technology between these two dissimilar materials, commercially pure Titanium Grade 2 and Austenitic Stainless Steel 316L, by choosing suitable welding process parameters. Consequently, it might be reduced the heterogeneity of the weld joint area which in turn, enhances life span of such joint. In this chapter, different materials' and distinct interlayers' properties have been discussed.

4.1 Titanium Grade 2

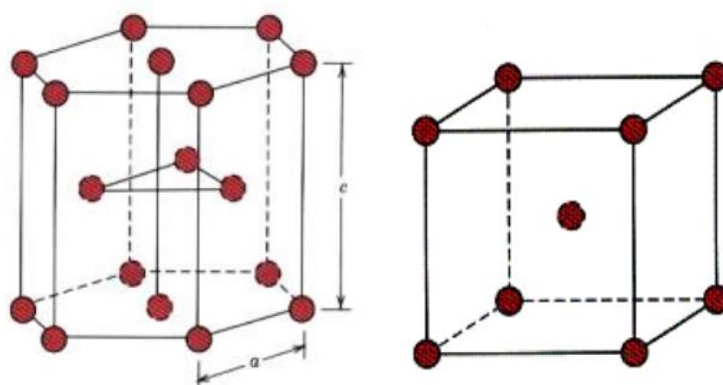
Titanium was first discovered in the late 18th century. English W. Gregor and German M.H. Klaporh both independently discovered it from the mineral ores named as ilmenite (FeTiO_3) and rutile (TiO_2) around the same time. However, it was not purified until early 1900s. In year of 1910, M.A. Hunter developed his method for extracting metal from the ore but was not successful. During 1938, metallurgist William Kroll invented "Kroll Process" wherein magnesium is employed as the reducing agent instead of sodium. This process is still widely used in industry for mass production of titanium [23].

Titanium Grade 2 is designated as UNS R50400, European Standard EN 10204-3.1. Pure titanium is a silver-grey colour allotropic metal that melts at approximately 1665 °C and boils at 3260 °C. Furthermore, it has low coefficient of thermal expansion and low conductivity as well. As a result, it can minimize the possibility of distortion due to welding. It has great affinity to absorb gases such as oxygen, hydrogen and nitrogen from the surrounding premises and tends to make oxides, hydrides and nitrides, respectively. Consequently, it requires shielding such as inert gas or vacuum atmosphere during welding. Titanium tends to form a tight microscopic film of oxides reacting with oxygen on freshly prepared surfaces even at room temperature as do magnesium and aluminium. This effect provides natural passivity to further reaction with media, which imparts in parts for its excellent corrosion resistance to salt, oxidizing acid solutions and mineral acids. It has good ductility and non-magnetic. Moreover, it has a 60 % low density compare to steel or nickel base-superalloys. It is 60 % heavier but two times stronger than aluminium. It can be operated at a temperature 427 °C with continuous service and 538 °C to 595 °C during intermittent service. Titanium Grade 2 chemical compositions are shown in below table 6.

Table 6 Chemical compositions (wt%) of Titanium Grade 2 [27]

C	N	H	Fe	O	Ti
0.08	0.03	0.01	0.30	0.25	balance

Titanium has two crystal structures commonly known as alpha and beta. At room temperature, it presents in α -phase which has a hexagonal close-packed (HCP) grid (shown in figure 18(a)). At temperature 882 °C, it starts to convert to β -phase which contains a body-centred cubic (BCC) crystal structure (shown in figure 18(b)). Titanium has a wide variety of applications such as aerospace, medical, chemical and marine industries. Typical products such as airframe and aircraft engine parts, reactor vessels, heat exchangers and condenser tubing. It also utilizes for offshore oil installation water pipe lines, honeycomb, bellows, gaskets, exhaust pipe shrouds, implantation and prosthesis [24,25,26]. Mechanical and physical properties Titanium Grade 2 are shown in table 7.



(a) HCP structure

(b) BCC structure

Figure 18 Allotropic transformation of titanium [2]

Table 7 Mechanical and physical properties of Titanium Grade 2 [27]

Properties	Value (in Unit)
Melting point	1665 °C
Density	4.51 g/cm ³
Yield strength	275 GPa
Ultimate tensile strength	344 GPa
Hardness	145 HV
Modulus of elasticity	105 GPa
Izod impact	114-171 J
Elongation at break	20%

4.2 Steel AISI 316L (X2CrNiMo17-12-2)

Steel AISI 316L belongs to austenitic stainless steel. It is called as austenitic chromium-nickel stainless steel that contains between two and three percentage of molybdenum. It can also be found under different designation such as 1.4307, X2CrNiMo17-12-2.

Typically, it contains minimal 16% Cr, 10% Ni and maximum 18% Cr, 14% Ni. In addition to, some other elements or (impurities) such as Mo, Mn, C, S, Si, P and N are added to improve other properties. It has superior corrosion resistance to most chemicals, salts and acids environments. Moreover, molybdenum content also helps to increase immunity towards marine ones. It is extensively employed for weldments as it contains extra-low carbon 0.030% which aids to minimize detrimental effect of chromium carbide precipitation due to welding process. Consequently, it has a very high resistance to corrosion point. It also provides higher creep, stress to rupture and tensile strength at elevated temperature. It has excellent impact strength, very good machinability and excellent formability as well. High hardness and strength can be achieved by work hardening process. It is non-magnetic. It can be operated in air at a temperature 870 °C with intermittent service and up to 925 °C during continuous service. The chemical compositions of 316L are shown in table 8.

Table 8 Chemical compositions (wt%) of 316L [29,30]

C	Si	Cr	Ni	Mo	S	P	Mn	N	Cu	Co	Fe
0.03	1.00	18.50	13.10	2.20	0.02	0.05	1.96	0.11	1.02	0.19	balance

AISI 316L has been widely used in handling many chemicals used by the process industries, including pulp and paper, textile, food pharmaceutical. Moreover, it is also used for marine, nuclear, power generation, high performance, oil and gas industry. Typical products includes heat exchangers, condensers, tanks, pipes, tubes, turbines, valves and pumps parts, exhaust manifolds, jet engines etc. It is also preferable for medical implantation, including pins, screws and orthopaedic implants like total hip and knee replacement [28,29,30,31]. Mechanical and physical properties of 316L are shown in table 9.

Table 9 Mechanical and physical properties of 316L [32]

Properties	Value (in Unit)
Melting point	1375-1400 °C
Density	8 g/cm ³
Yield strength	205 GPa
Ultimate tensile strength	515 GPa
Hardness	155 HV
Modulus of elasticity	193 GPa
Izod impact	150 J
Elongation at break	60%

4.3 Feasible interlayers for experiments

Three interlayers were utilized for testing such as Nickel (Ni), Copper (Cu) and Silver (Ag). Their mechanical and physical properties are given in table 10.

Table 10 Mechanical and physical properties of used interlayers [33,34,35]

Properties	Ni	Cu	Ag
Melting point	1453 °C	1085 °C	962 °C
Density	8.9 g.cm ⁻³	8.93 g.cm ⁻³	10.50 g.cm ⁻³
Yield strength	150 MPa	33.3 MPa	54 MPa
Ultimate tensile strength	400 MPa	210 MPa	154 MPa
Hardness	100 HV	50 HV	25 HV
Modulus of elasticity	200 GPa	110 GPa	76 GPa
Poisson ratio	0.312	0.343	0.370
Thermal conductivity	91 W.m ⁻¹ .K ⁻¹	385 W.m ⁻¹ .K ⁻¹	419 W.m ⁻¹ .K ⁻¹
CTE (linear)	13.3 x 10 ⁻⁶ K ⁻¹	16.4 x 10 ⁻⁶ K ⁻¹	19 x 10 ⁻⁶ K ⁻¹

5. Diffusion welding of Titanium Grade 2 to AISI 316L Steel

The following chapter demonstrates how to find out suitable metallic interlayer diffusion welding technology between commercial pure Titanium Grade 2 to high-alloy Austenitic stainless steel 316L by adopting different metallic interlayers having thickness (0.1 mm) to obtain good ductility at the joint with almost no deformation. It also explains the preparation of specimens with the help of thermocouple welding machines, actual welding process and the evaluation of the metallography using optical microscope (OM) and scanning electron microscope (SEM) with energy dispersive spectroscopy (EDS) and micro-hardness test for analysing mechanical behaviour of specimens.

5.1 Reason for using different interlayers

An experiment was performed by Michal Novak and his professor titled with **“Diffusion welding of heterogeneous welds between Titanium Grade 2 to Austenitic stainless steel 316L”**. More than 10 samples were carried out between these two materials. After completing experiments, samples were removed from the Gleeble device and machined for further steps. Static tensile test was conducted on TIRA test 2300 machine. Maximum tensile strength 254 MPa was achieved on sample having parameters 860 °C temperature, 0.5 kN force and 40 minutes. But it is less than half of the tensile strength of titanium or steel. For further improvement, another experiment was performed with the same parameters and device with polishing on titanium side using Ar gas as a protective environment. It was found from the static tensile test that maximum tensile strength (336.18 MPa) of this sample was slightly improved, which is 80 MPa more than the sample welded in vacuum atmosphere. Although the final strength of the joint was sufficient, ductility was extremely bad. It fractured within a small time after ultimate strength. Only 0.2% elongation was hardly achieved. It indicates that the joint was in brittle nature. This fact can also be found out from the figure 19. It reveals that the hardness at the joint interface was suddenly increased which was also evident of brittle joint. Very low ductility might create a problem during cyclic or continuous repeated load. For that reason, it is decided to overcome this problem employing suitable interlayers and it will be further helpful to improve the ductility [36].

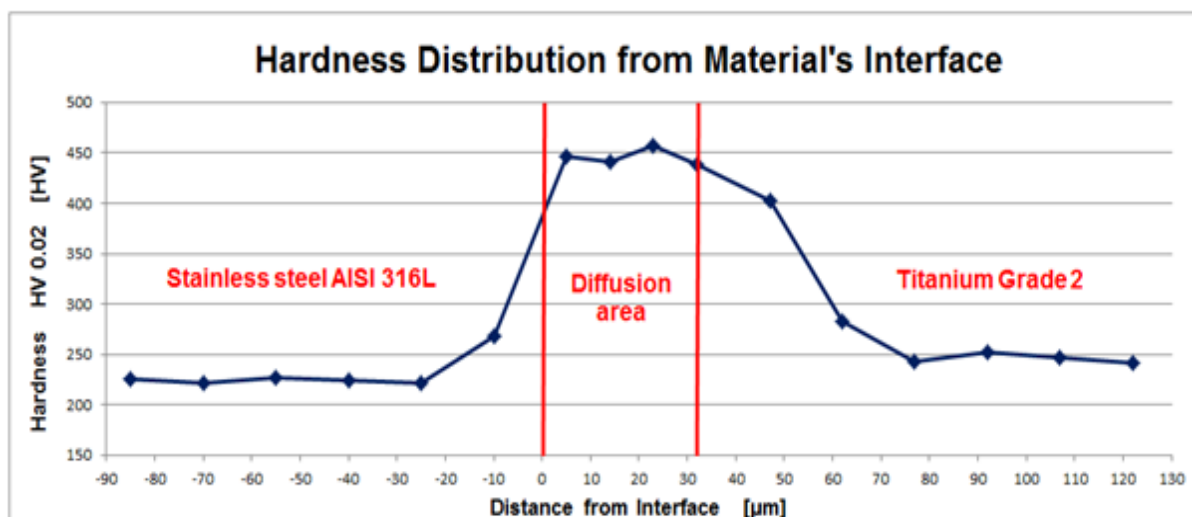


Figure 19 Micro-hardness HV 0.02 distribution over the diffusion welded joint having parameters ($T = 860\text{ }^{\circ}\text{C}$, $F = 0.5\text{ kN}$, $t = 40\text{ min}$) and Ar gas as protective environment [36]

5.2 Sample preparation

The cylindrical samples of commercially pure Titanium Grade 2 and AISI 316L Steel with the dimension of 12 mm in diameter and 50 mm in length were used. These samples were cut and machined from the bar stock. By fine-turning operation, the average roughness (316L $R_a = 1.14\text{ }\mu\text{m}$ and Titanium Grade 2 $R_a = 0.81\text{ }\mu\text{m}$) was achieved on the front of contact faces.

The following step is to fasten the type-K thermocouples. They should be placed as close as possible to the edge of the sample (i.e. 0.5 to 0.7 mm). Samples must be properly cleaned with acetone prior attaching the thermocouples on the surfaces and thermocouples are then welded via thermocouple welding machining at a voltage of 31 V. They are made up of two wires (chromel and alumel) having diameter 0.25 mm. Both wires are insulated by ceramic tube to prevent the contact between them. Thermocouple welded sample is shown in figure 20.

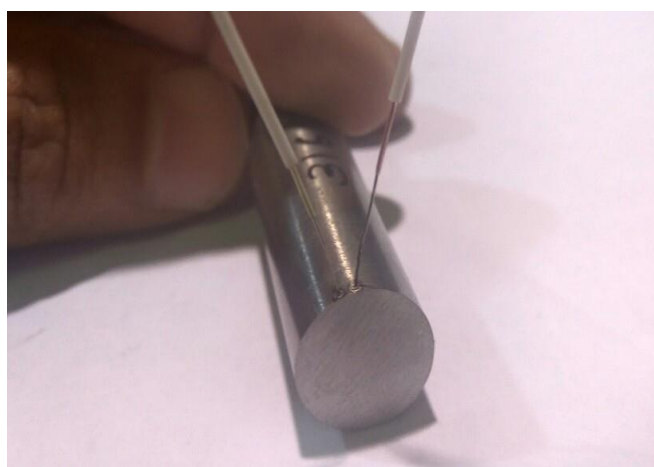


Figure 20 Thermocouple welding on sample 316L

5.3 Design and Implementation of the experiment

The right conditions, interlayers and process variables of diffusion welding were primarily determined by researches, metals properties, theory of diffusion bonding and from real world experiments. In the case of diffusion bonding, the welding temperature generally ranges from 50 to 90 % of the melting point of the materials. When welding different materials, lower melting temperature of materials should be considered. Titanium Grade 2 and AISI 316L Steel have a melting point of about 1665 °C and 1400 °C. From the mathematical calculation, it was found that the welding temperature should be in the range of 770 to 1260 °C. The Gleeble system enables to maintain steady and also variation in pressure throughout the process. Process parameters are chosen according to the type of materials in order to obtain the necessary local plastic deformations meanwhile avoiding excessive deformations or macro cracks.

5.3.1 Realization of experiment

After fastening the thermocouples on the sample 316L, the samples were inserted into full-length copper jaws which were then clamped into the clamping jaws of Gleeble as shown in figure 21. These jaws were used in all experiments due to steeper temperature gradient.

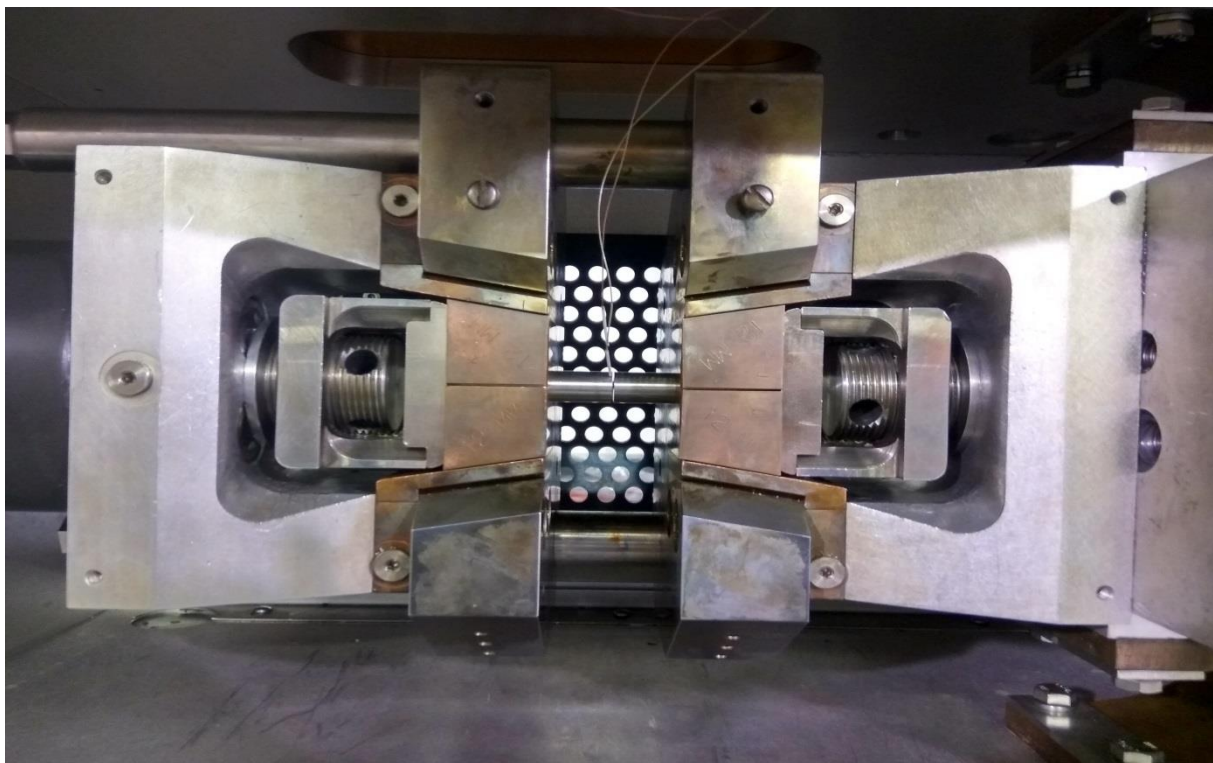


Figure 21 Specimens clamped in the high-temperature copper jaws of Gleeble

The samples were inserted into the copper jaws in such a way that their end faces were in the same plane as the end faces of the copper jaws. Then specimens were fixed with copper jaws and copper jaws were attached to clamping jaws with bolt spacers. As a

result, specimens cannot be displaced during the experiments and the sufficient amount of heat can be transfer from the specimens, jaws and devices. This would give a accurate result and also provide safety to the Gleeble system.

The mating surfaces of specimen were prepared by conventional grinding and polishing techniques. Samples must be cleansed and degreased with acetone prior executing the process because of dirty or greasy surfaces. Therefore, final result would be better in context of mechanical properties. The clean and dried specimens were then mechanically approached so that the faces were in contact. Subsequently, the chamber was first evacuated and then filled with vacuum pressure about $1.8 - 2.8 \times 10^{-3}$ Torr.

Diffusion welding is relatively tedious process itself and requires visual check for the separation of the thermocouple or large deformation throughout its time. Whenever this sort of problem arise during operation, it should be necessary to terminate the whole program or system. The segregation problem of thermocouple arises during the heating of samples to the welding temperature, but it may also fall off during the holding at a particular temperature. Figure 22 displays the operation of diffusion welding of titanium to steel with nickel interlayer, with the titanium on the right side.



Figure 22 Diffusion bonding operation during holding time

During the welding process, the current power variation (PowAngle) can also be observed during the heating cycle of temperature owing to inadequate contact between surfaces of materials and interlayer. This condition can be observed until a partial diffusion of the material and interlayer. It will then stabilize and increase the required power of the

transformer at the starting of holding time. During the exposure of temperature, power of transformer is constant and thereafter it will decrease as cooling process will start. An example of a transformer power variation is shown in figure 23. The data are obtained by welding sample T870_F0.33_t50; i.e. at a welding temperature 870 °C, a compressive force 0.33 kN for 50 minutes holding time. As can be seen from figure, at first few min transformer power rises sharply, that is, the system's rise time, then it fluctuates, oscillates and rises continuously up to approximately 30 min (this correspond to a welding temperature of almost 870 °C).

During cooling process, transformer is off. Therefore, power goes down sharply. Once the joint forms, the vacuum pressure can be released from the vacuum chamber and the sample can be removed from the Gleeble device.

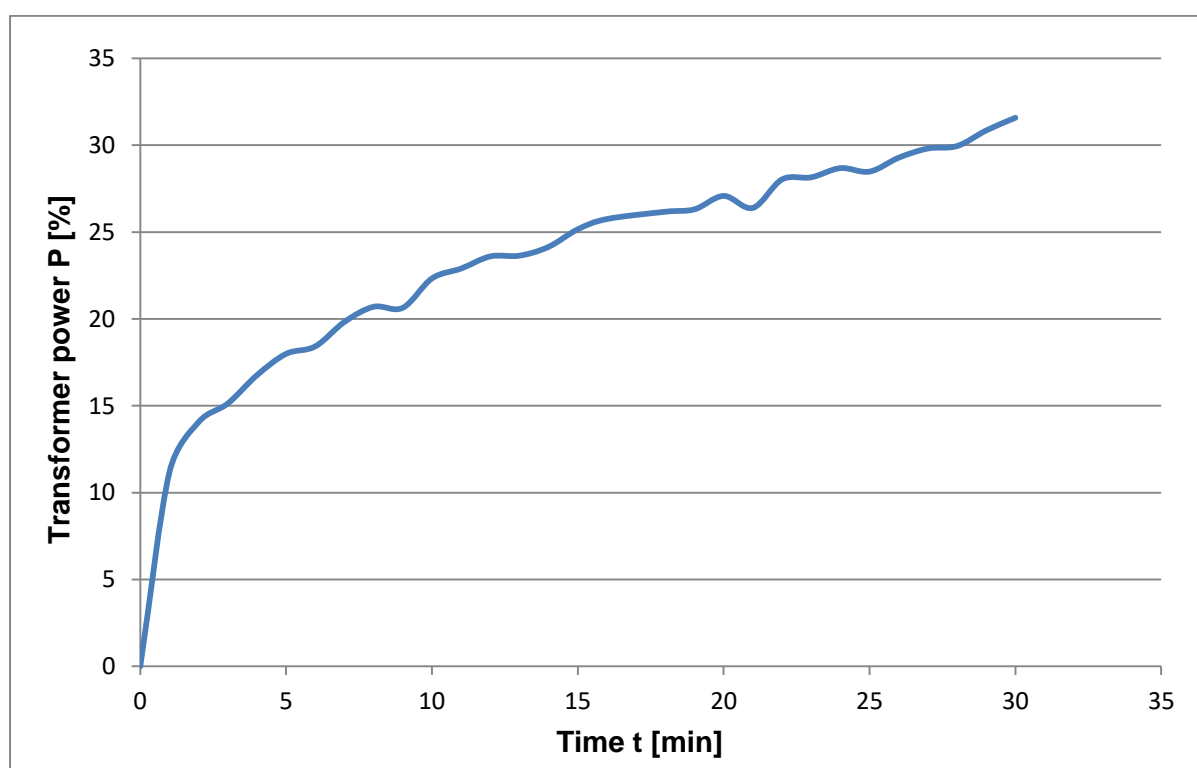


Figure 23 Transformer power variations before holding time on sample T870_F0.33_t50 with Ni interlayer

5.3.2 Diffusion bonding with Ni interlayer

From the research paper of S. Kundu and his colleagues, it is investigated that the diffusion bonding between commercially pure Ti Gr 2 and 304SS with the help of Ni interlayer reveals good result on final welded joint in view of ductility [37]. In this respect, Ni can be considered as a useful interlayer owing to its satisfactory corrosion resistance. Different parameters of Ni interlayer used in this experiment are shown in table 11.

Table 11 Different parameters of diffusion welding using Ni interlayer

	Temperature (°C)	Exerted Force (kN)	time (min)
Sample no. 1	900	0.33	40
Sample no. 2	870	0.33	50
Sample no. 3	870	0.5	30

Firstly three samples (table 14) were performed on the Gleeble device as primarily to figure out the right variables. Sample no. 1 (T900_F0.33_t40) indicates that the experiment was done at the temperature 900 °C, compressive force 0.33 kN and time 40 minutes. By inputting this process parameter, specimen started to deform sharply on titanium side around temperature 875 °C due higher plastic deformation and experiment was immediately terminated. Clicking sound was heard while taking out of this sample from the device. It is evident that the final joint would not get sufficient bonding between them. There was also found no deformation on steel 316L side.

Sample no. 2 (T870_F0.33_t50) labeled with reduction in temperature and higher time was used for next trial. However, even with this sample, there was still not good bonding and interlayer slipped out after removing the sample. On the positive side, almost negligible deformation of 0.08 mm was observed during 50 minutes holding time from the recorded data. For the sample no. 3, force was increased by some extent whereas time was reduced. As a result, very less deformation (0.2 mm) was achieved but sample was broken due to insufficient bonding during cutting process. During the welding process, remaining oxygen in welding chamber reacted with titanium and formed titanium oxide on its surface as shown in Figure 24.



Figure 24 Oxidation on the surface of titanium

From the experiment with Ni interlayer, it is investigated that titanium grade 2 starts deformation at temperature 875 °C. Thus, it is not possible to use Ni interlayer along with Ti Gr 2 at higher temperature than 870 °C. But, it is shown in the research paper of S. Kundu that Ti Gr 2 is successfully bonded at 900 °C with aid of Ni interlayer [44].

5.3.3 Diffusion bonding with Ag interlayer

From the research paper of Yongqiang Deng and his colleagues, it is reported that the diffusion bonding between commercially pure Titanium Grade 2 and 304 Stainless Steel with the aid of Ag interlayer exhibits good result in light of micro-hardness distribution of bonded joint. It is evident that bonded joint is in ductile nature [16]. Thus it is expected that the Ag can be considered as a more effective intermediate material for the diffusion bonding of Ti Gr 2 and SS 316L. Table 12 shows different variables of Ag interlayer used in this experiment.

Table 12 Different parameters of diffusion welding using Ag interlayer

	In Gleeble device			In vacuum furnace	
	Temperature	Exerted Force	Time	Temperature	Time
	(°C)	(kN)	(min)	(°C)	(hour)
Sample no. 1	870	0.5	40	-	-
Sample no. 2	850	0.9	20	-	-
Sample no. 3	820	0.7	20	-	-
Sample no. 4	870	0.5	40	870	10
Sample no. 5	850	0.9	20	850	5
Sample no. 6	820	0.7	20	850	5

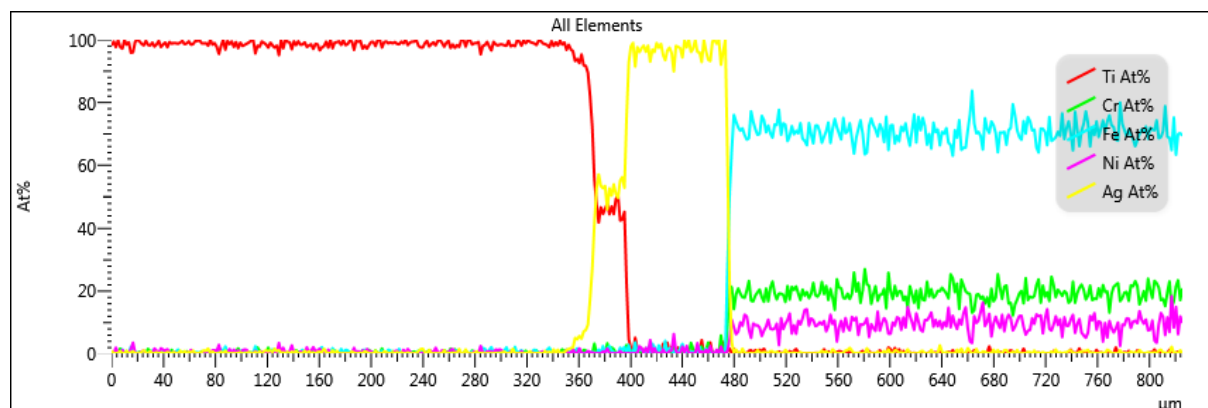
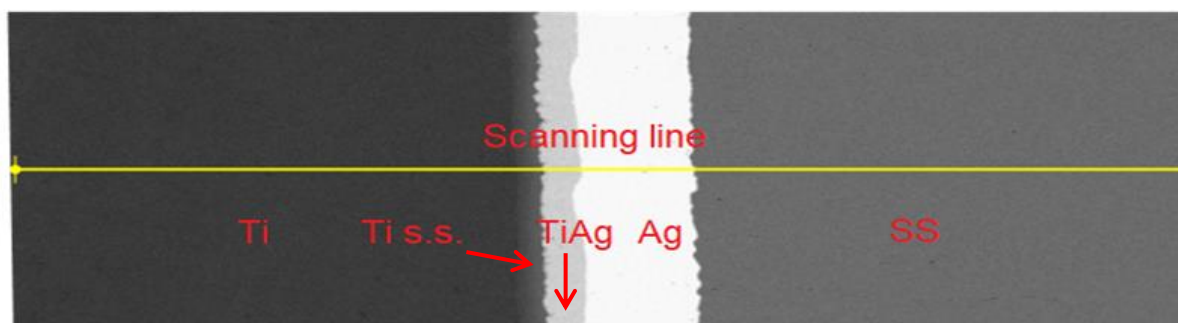


Figure 25 SEM image and corresponding EDS line scanning results of the bonded joint of sample no. 1 (T870_F0.5_t40)

Three samples were firstly bonded in Gleeble device and then this process was continued in vacuum furnace. Figure 25 reveals the SEM image with EDS scanning line of sample no. 1 (T870_F0.5_t40) in Gleeble device at temperature 870 °C, force 0.5 kN and time 40 minutes. Several distinct layers from left to right side, Ti/Ti s.s/TiAg/Ag/SS, were observed. Titanium solid solution (Ti s.s) 19.55 μm, Ti-Ag IMC (TiAg) 28.33 μm and Ag interlayer 82.62 μm thicknesses were measured at the joint of interface. It can be seen from the EDS that there is small amount of Ag diffuse into Ti. On opposite side, Ag is not diffused into SS because it is not soluble in the Fe at this temperature.

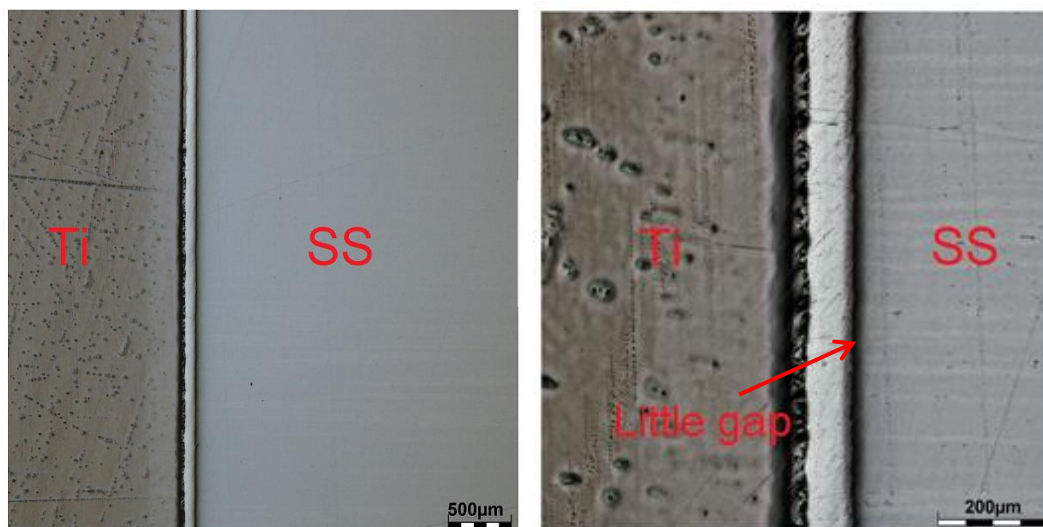


Figure 26 Metallography of sample no.1 (T870_F0.5_t40) using optical microscope

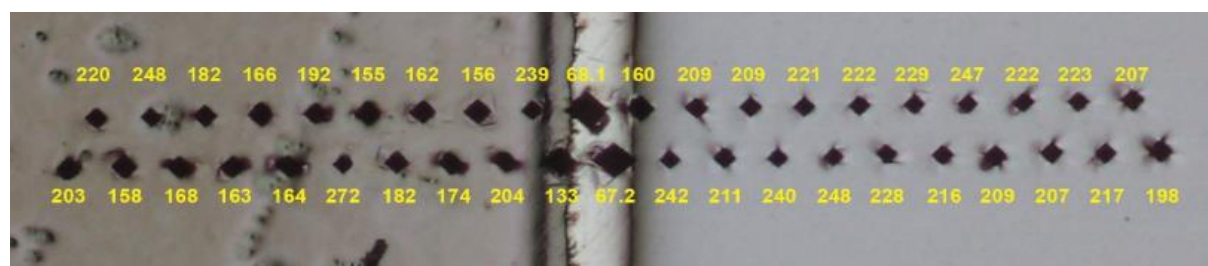
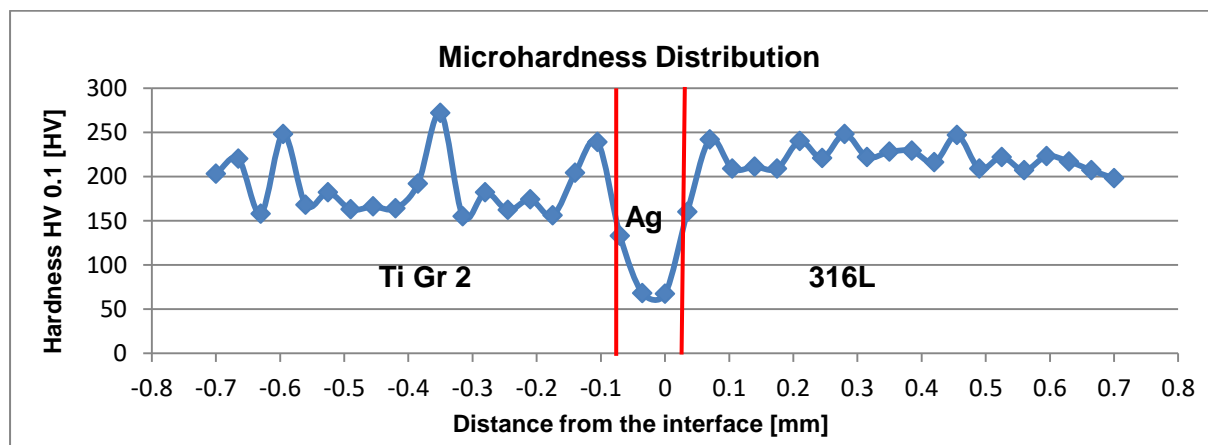


Figure 27 Micro-hardness HV 0.1 distribution over the diffusion welded joint of sample no. 1 (T870_F0.5_t40)

From the metallographic evaluation, it is clearly visible that there is a little gap between Ag interlayer and SS (figure 26). It indicates that there is no sufficient bonding between Ag interlayer and SS. At the Ag interface, low hardness values are observed (figure 27). It indicates ductile nature of joint.

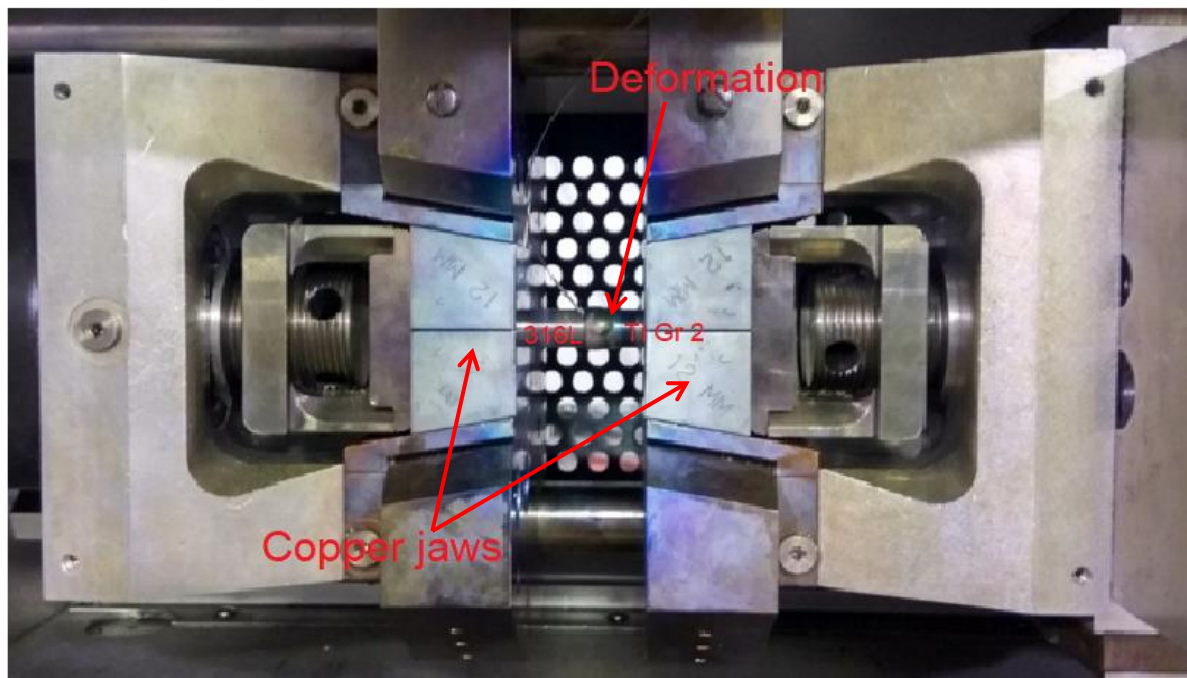
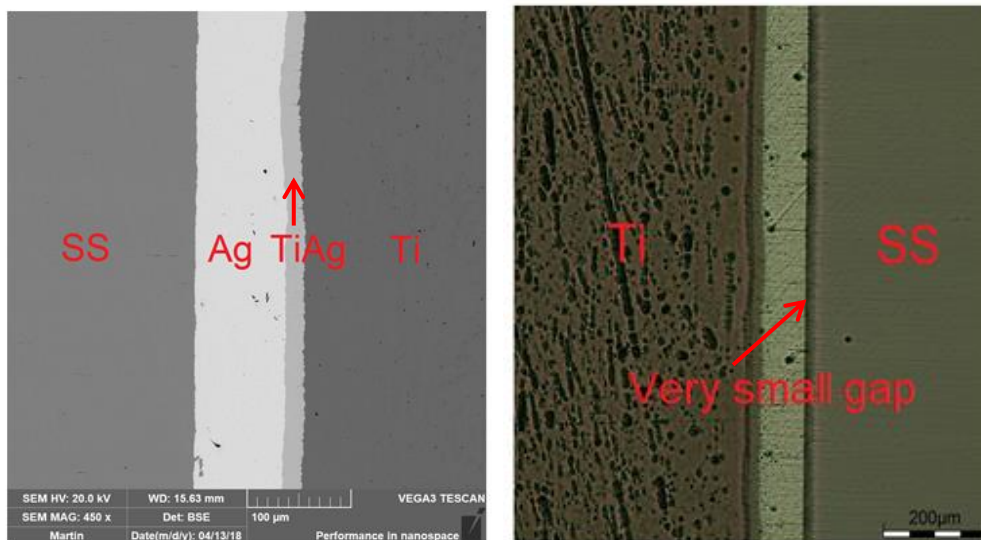


Figure 28 Deformation on titanium side and evaporation of Ag interlayer of sample no. 2 (T850_F0.9_t20)

Compared to sample no. 1 in Gleeble device, sample no.2 (T850_F0.9_t20) was slightly reduced bonding temperature and time. Compressive pressure was noticeably increased due to the gap on the side of 316L. The problem arose during increasing temperature between 600 °C to 850 °C. As can be displayed in figure 28, it can notably be found deformation on the titanium side and evaporation of Ag interlayer on the sample and also on the copper jaws.

Sample no.3 (T820_F0.7_t20) was with a little bit reduced temperature, force and same time as previous one due to evaporation and deformation. Very small deformation (0.2 mm) was measured during the holding time. As can be seen from figure 29(a), there was found only two layers TiAg IMC and Ag interlayer but no Ti s.s. As shown in figure 29(b), very small gap on the side SS was examined during the microstructural evaluation. It is evident that joint was not properly bonded but it shows good result and also diminishes thickness of TiAg IMC compare to sample no.1 (figure 25).

From the micro-hardness graphs (figure 30), hardness is quite similar to sample no. 1 (figure 27) at the Ag interface. According to Fe-Ag binary phase diagram (see in appendix), Ag cannot form IMCs with the Fe but it cannot be soluble either in it. This is considered as primary reason for inadequate contact between SS and Ag interlayer.



(a) SEM

(b) OM

Figure 29 SEM and OM image of sample no. 3 (T820_F0.7_t20)

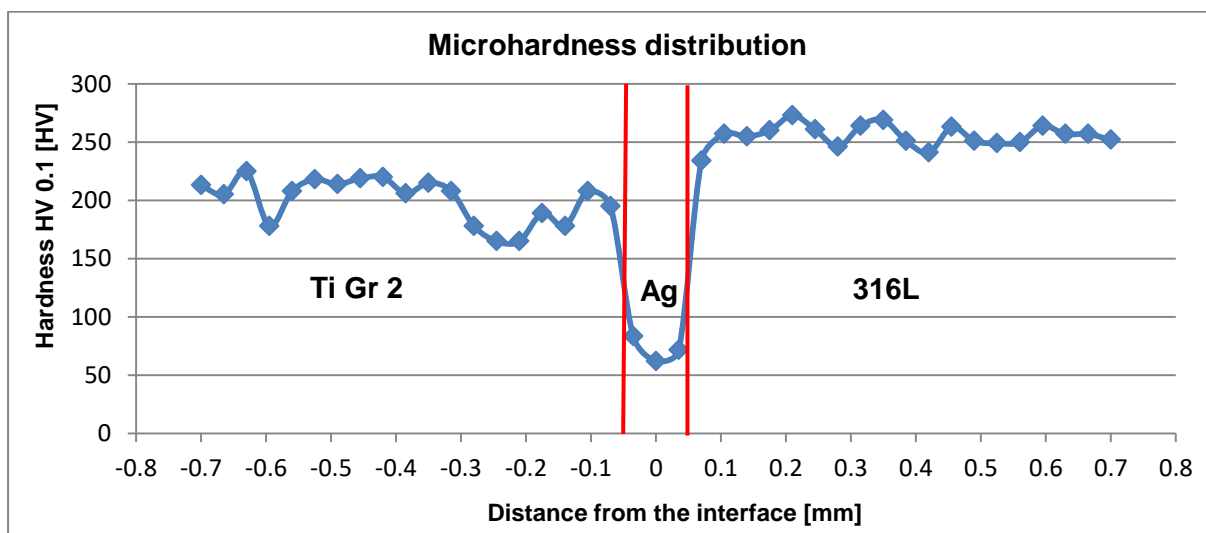


Figure 30 Micro-hardness HV 0.1 distribution over the diffusion welded joint of sample no. 3 (T820_F0.7_t20)

After welding on the Gleeble device, the sample no. 4 was bonded in furnace having temperature 870 °C for 10 hours to find out diffusion rate during holding time. From the SEM images (figure 31), it can be easily found crack at the diffusion area. It is evident that longer holding time would probably not produce effective result in light of diffusion.

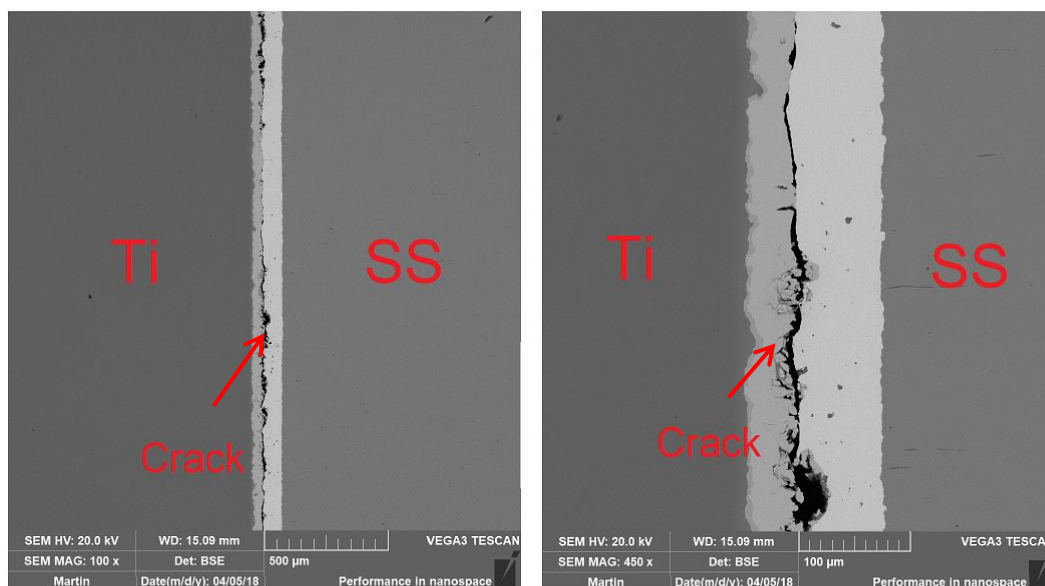


Figure 31 SEM image of sample no. 4 welded in furnace

Sample no. 5 was bonded in furnace having temperature 850 °C for holding time 5 hours to check rate of diffusion. Figure 32(a) represents diffusion of Ag into Ti during bonding. It also displays two portions at the Ag interface. Upper portion reveals the TiAg IMC while lower portion shows fully diffusion of Ag into Ti. The magnified view of upper portion is shown in figure 32(b).

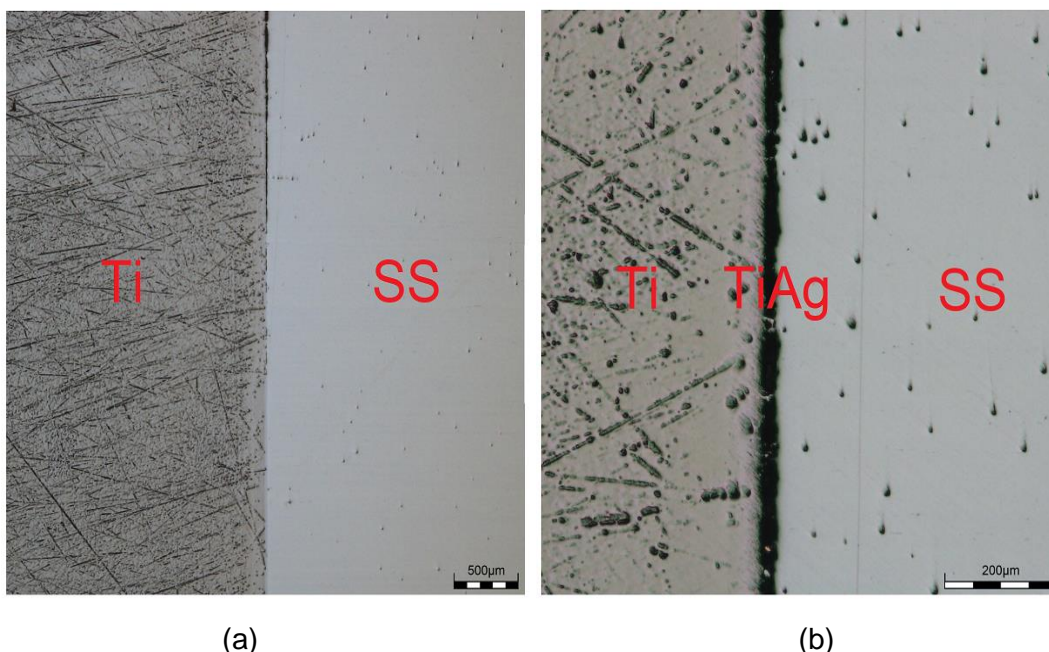


Figure 32 Metallography of sample no. 5 welded in furnace

From the micro-hardness graph (figure 33), higher value of hardness (423 HV) near Ti-Ag interface was evaluated during hardness measurement. Also, adjacent to Ag interlayer, TiAg IMC was formed due to diffusion of Ag into Ti. This IMC shows significantly high hardness value (348 HV and 382 HV). It proves the brittle nature of bonded joint.

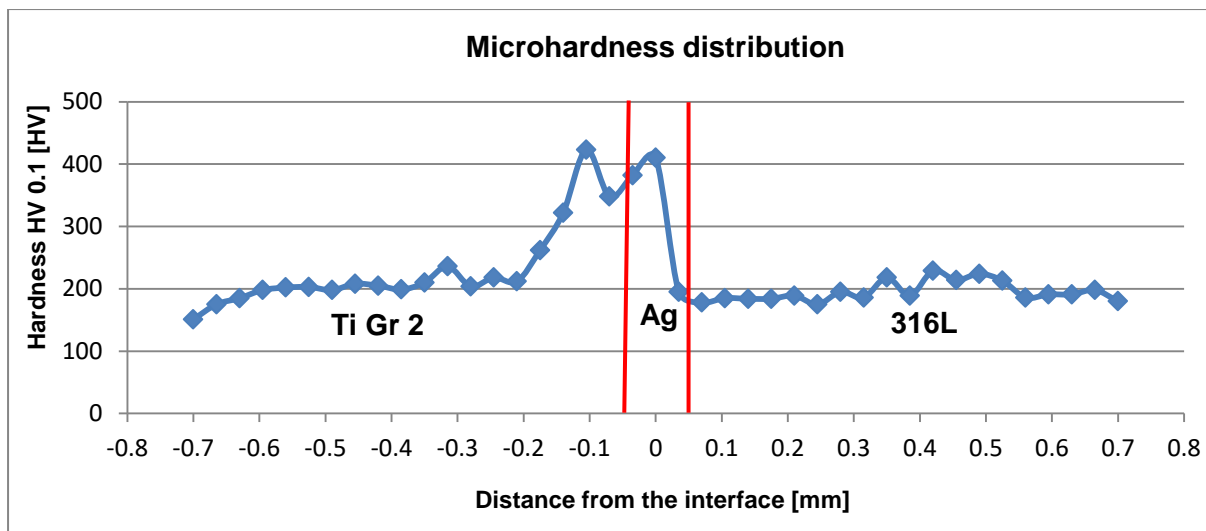


Figure 33 Micro-hardness HV 0.1 distribution over the diffusion welded joint in furnace of sample no. 5

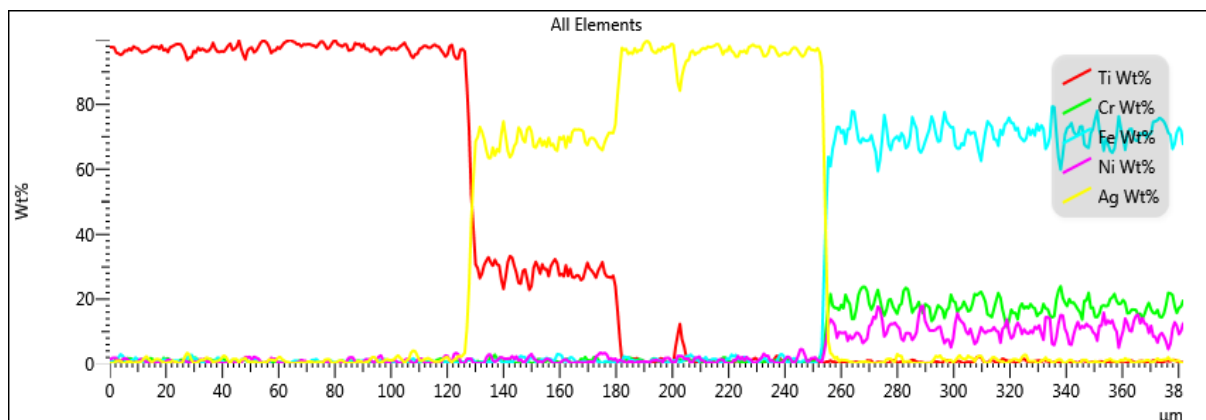
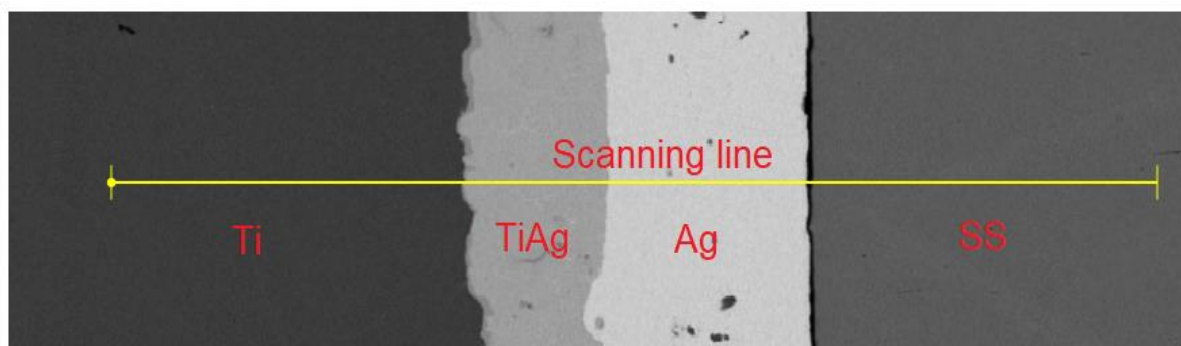


Figure 34 SEM image and corresponding EDS line scanning results of the bonded joint in furnace of sample no.6

Sample no. 6 was put into the furnace for 850 °C for 5 hours. Figure 34 reveals the microstructure and corresponding EDS line scanning results of the Ti/Ag/SS interface of the bonded joint. From SEM, two layers (TiAg, Ag) were observed. If this sample is compared to sample no. 3 (figure 29(a)), sample no.6 exhibits higher diffusion rate and also higher thickness of TiAg IMC.

Figure 35 displays the value of micro-hardness at the material interface. On the side of titanium, hardness values gradually increase while they are nearly same on the side of stainless steel. Impact of hardness on the Ag interface is steeply decreased and appeared the extremely low value around 50 HV which is less than 200 HV from previous impact. This exhibits a ductile nature of the joint.

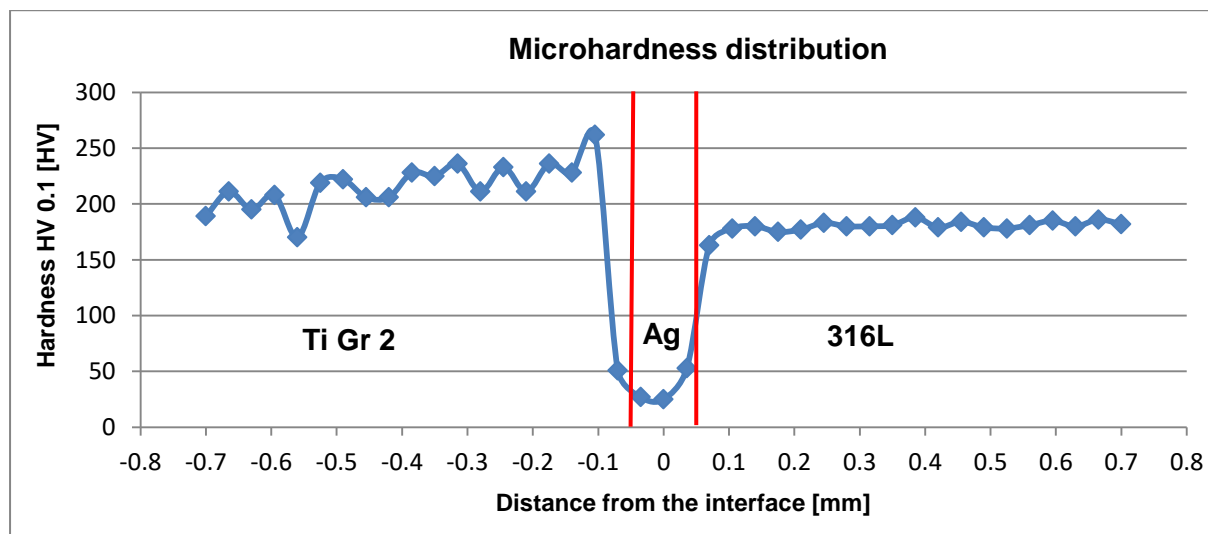


Figure 35 Micro-hardness HV 0.1 distribution over the diffusion welded joint in furnace of sample no. 6

From the experiment with Ag interlayer, it is deduced that Ag interlayer cannot form adequate bond with SS. But it is shown that Ag formed good joint with SS from the research paper of Yongqiang Deng [16]. Diffusion rate increases with increasing the holding time and also temperature in furnace but longer holding time generates crack at the interface.

5.3.4 Diffusion bonding with Cu interlayer

From the research paper of S. Kundu and his colleagues, it is documented that the diffusion bonding between commercially pure Ti Gr 2 and 304 SS with the help of Cu

interlayer reveals good result on final welded joint in view of ductility [15]. Therefore, it is anticipated that the Cu can be estimated as a potential candidate to be used as interlayer to improve the joint ductility. Different parameters of Cu interlayer used in this experiment are shown in table 13.

Table 13 Different parameters of diffusion welding using Cu interlayer

	In Gleeble device			In vacuum furnace	
	Temperature	Exerted Force	Time	Temperature	Time
	(°C)	(kN)	(min)	(°C)	(hour)
Sample no. 1	870	0.5	40	-	-
Sample no. 2	850	0.5	30	-	-
Sample no. 3	820	0.7	60	-	-
Sample no. 4	870	0.5	40	850	10

Sample no. 1 (T870_F0.5_t40) was carried out in Gleeble device. During execution of experiment, higher deformation was displayed on L-Gauge. As a result, test was immediately terminated. Here, higher deformation is clearly shown on the titanium side (figure 36).



Figure 36 Higher deformations on the titanium side of sample no. 1 (T870_F0.5_t40)

Sample no. 2 labelled with T850_F0.5_t30 was experimented with slight changes in diffusion bonding variable. This sample was successfully welded in Gleeble device. But during the machining operation, it was broken at the joint area (figure 37).



Figure 37 broken sample no. 2 (T850_F0.5_t30)

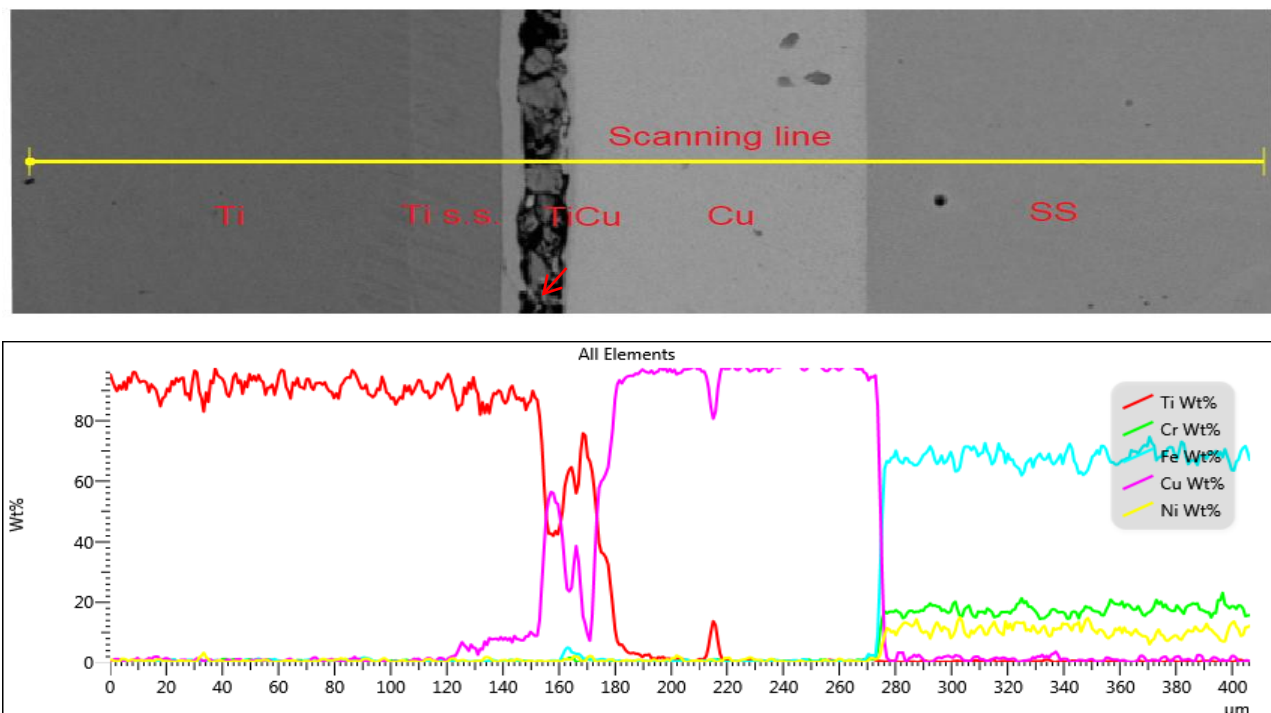


Figure 38 SEM image and corresponding EDS line scanning results of the bonded joint of sample no. 3 (T820_F0.7_t60)

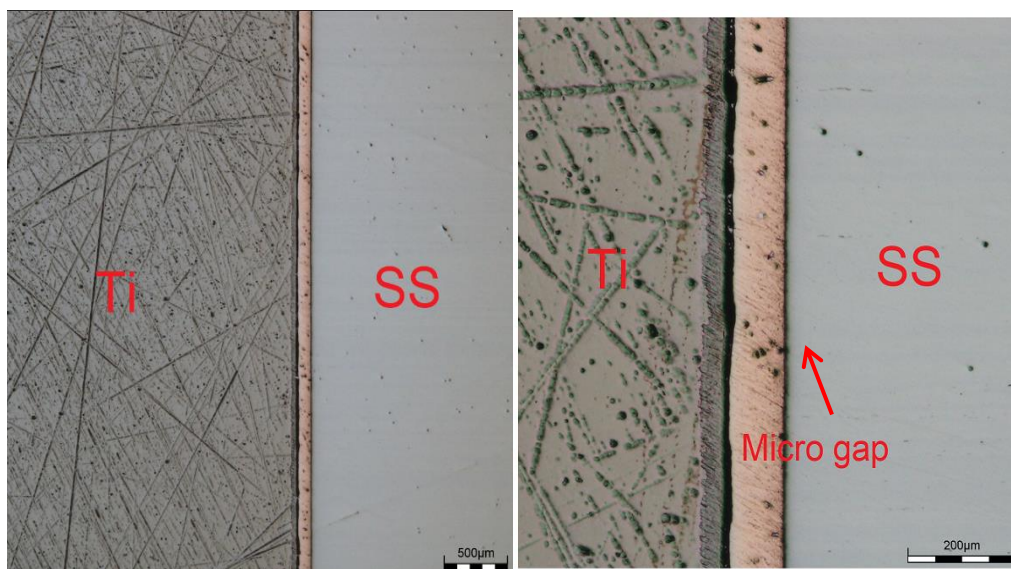


Figure 39 Metallography of sample no. 3 (T820_F0.7_t60)

Sample no. 3 (T820_F0.7_t60) with slight decrease in temperature and increase in applied force and holding time was performed in Gleeble simulator machine. The microstructure and corresponding EDS line scanning results of the Ti/Cu/SS interface of the joint bonded are given in figure 38. The Cu/SS interface is planar in character, indicating the presence of solid solution without any IMC in diffusion zone, which is good condition with the Fe-Cu binary phase diagram. Adjacent to the Cu/SS interface, the elemental concentration profile reveals no element other than Cu. Therefore, this is the remnant Cu interlayer. Close to the remnant Cu interlayer, distinct layers are observed. There is a

plateau in the corresponding elemental profile of this area. EDS analysis of this layer reveals a composition of Cu (56.2 wt%) and Ti (43.8 wt%). According to the Ti-Cu phase diagram, this is a Ti-Cu IMC layer. Between the Ti-Cu IMC layer and Ti, a thin light shaded layer is observed. According to the elemental concentration profile, this region mainly contains Ti with a small amount of Cu, and the concentration profiles of both Ti and Cu exhibit smooth and continuous variations. Therefore, this is a Ti solid solution (Ti s.s) alloyed with Cu. The inter-diffusion of elements indicates the occurrence of mass transfer and good metallurgical bonding is achieved across the bonding interface but there is still micro-gap (figure 39).

As can be seen from micro-hardness graph (figure 40), hardness values at the area of interface are increased at higher number on side of titanium. It indicates the IMC of Ti-Cu. But at the remnant Cu interface, hardness graph is gone much steeper. There is found a very low hardness around 80 HV which is nearly 200 HV lower than previous measured value. It is evident of the ductile nature of the joint.

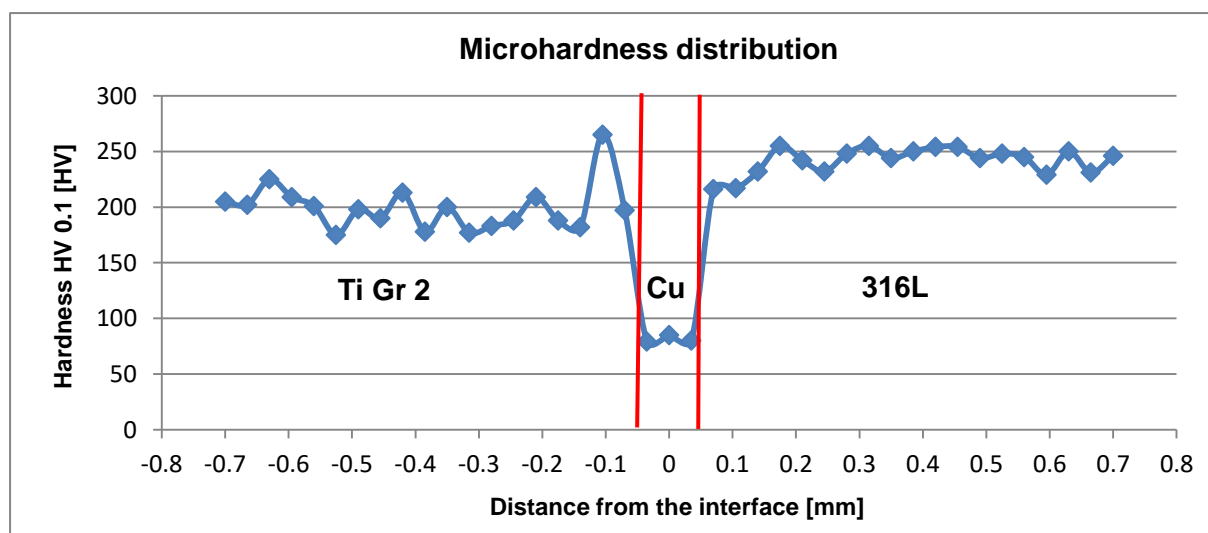


Figure 40 Micro-hardness HV 0.1 distribution over the diffusion welded joint of sample no. 3 (T820_F0.7_t60)

Sample no. 4 with Cu interlayer was carried out in furnace at 850 °C for 10 hours to figure out the rate of diffusion during the holding time. Figure 41 represents 4 regions in SEM. From the EDS analysis, numbers 1, 2, 3 and 4 show SS region, SS with less than 30 wt% of Ti, Ti with lamellar structure with 7.6 wt% of Fe and Ti region, respectively. It was also examined that the titanium diffuses up to region 2 and Fe diffuses

up to region 3. It is surprisingly shown that there is no Cu element found in any region. It indicates that the copper is fully diffused into the joint.

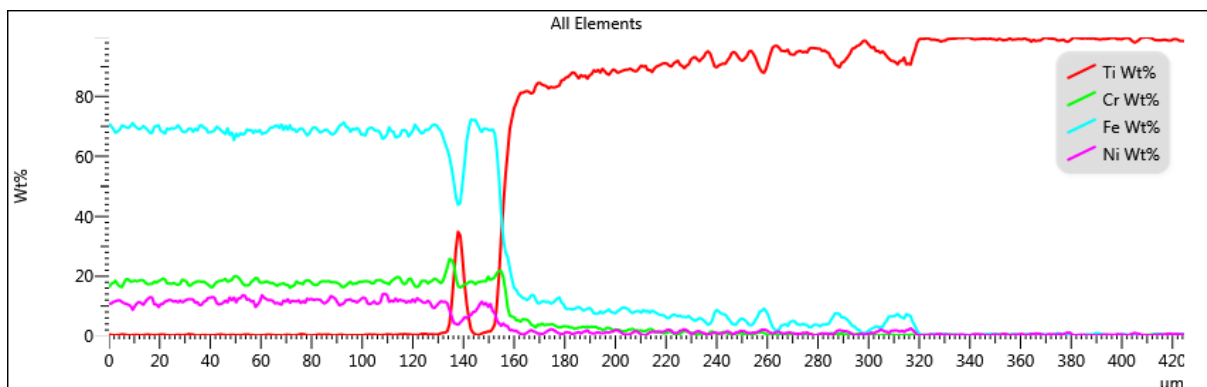
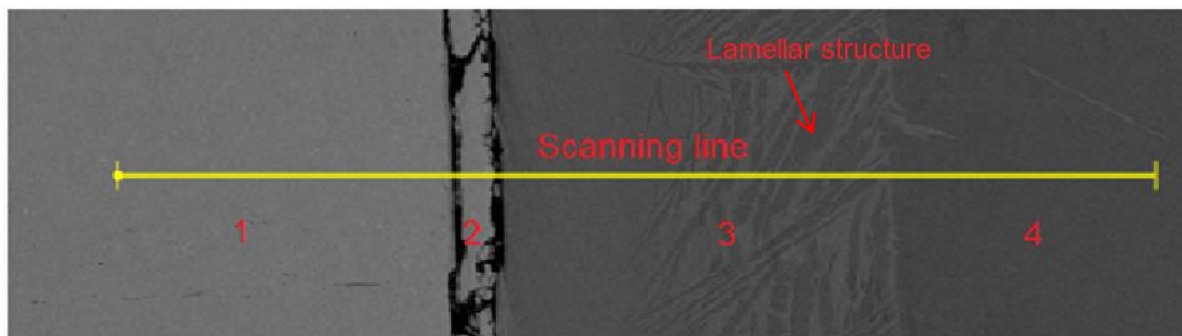


Figure 41 SEM image and corresponding EDS line scanning results of the bonded joint in furnace of sample no.4

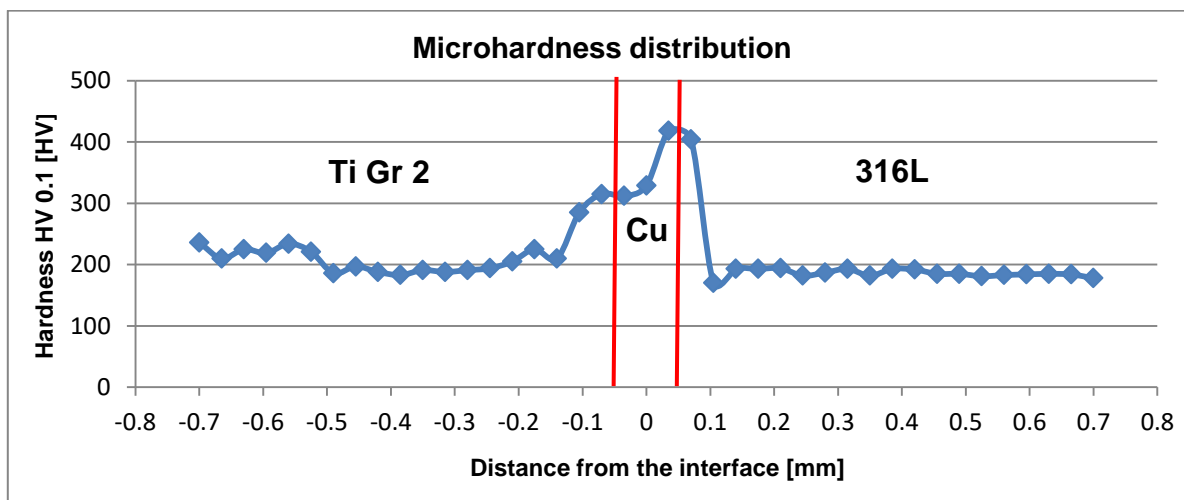


Figure 42 Micro-hardness HV 0.1 distribution over the diffusion welded joint in furnace of sample no.4

As shown in micro-hardness graph (figure 42), both sides (Ti Gr 2 and 316L) hardness values are nearly homogeneous. From side of Ti interface to side of 316L interface, they are continuously increased. On side of Cu/316L interface; higher values (404 HV, 418 HV) are measured. It indicates the formation of Fe-Ti IMC layer which is very brittle nature.

From the experiment with Cu interlayer, it is inferred that it produces good bond between these two materials at the temperature of 820 °C with micro gap on the side of SS. But from the report of S. Kundu, it is investigated that Cu interlayer make sufficient joint between titanium grade 2 and 304 SS at the temperature of 900 °C [15]. Longer holding time shows fully diffusion of Cu into Ti in furnace.

5.3.5 Diffusion bonding with Ag-Cu multi-interlayers

From the above experiment with Ag and Cu interlayers, it could be noticed that interlayer as mentioned above can still form intermetallic compounds with one of the parent metals, which makes it difficult to achieve high quality joints. Insertion of a multi-interlayer has been considered as a practical approach to prevent or to reduce the formation of undesired intermetallic compounds in joints. Ag and Cu have good plasticity. Therefore, they can be considered as a potential intermediate structure to joint titanium to stainless steel.

From the experiment with Ag and Cu interlayers, Ag formed good bonding with Ti and Cu produced sufficient bonding with SS. As a reason, it was decided to attempt both interlayers together, Ag on the side of Ti and Cu on the side of SS. Different parameters of Ag-Cu interlayers used in this experiments are shown in table 14.

Table 14 Different parameters of diffusion welding using Ag-Cu interlayers

	Temperature (°C)	Exerted Force (kN)	time (min)
Sample no. 1	820	0.7	60
Sample no. 2	820	0.7	30

Both samples were tested in Gleeble device. The SEM image and corresponding EDS line scanning results of the Ti/Ag/Cu/SS interface of the bonded joint of first sample (T820_F0.7_t60) are shown in figure 43. The Cu/SS interface is planner in character, indicating no IMC which reveals adequate bonding between Cu and SS. Adjacent to the Cu/SS interface, several layers were observed. As shown in table 15, due to solid state inter-diffusion of Ti and Cu and also solubility of Ag in both materials, continuous IMC layers including $TiCu_4$, $TiCu$, and Ti_2Cu_3 are generated. According to the elemental concentration profile, region 5 mainly contains Ti with a small amount of Cu. Therefore, this is a Ti solid solution (Ti s.s) alloyed with Cu. From the EDS, there is a good diffusion of Cu

into Ti but almost less than 5 wt% Ag diffused into Ti and remaining Ag is soluble in both elements (Ti and SS).

Table 15 Chemical composition of the marked regions in Figure 43 (wt%)

Region No.	1	2	3	4	5	6	7
Ti	1.0	16.9	32.8	42.6	91.2	99.5	33.4
Cu	96.4	80.5	64.7	53.6	7.5	0.5	64.1
Possible phase	Cu	TiCu ₄	Ti ₂ Cu ₃	TiCu	Ti s.s.	Ti	Ti ₂ Cu ₃

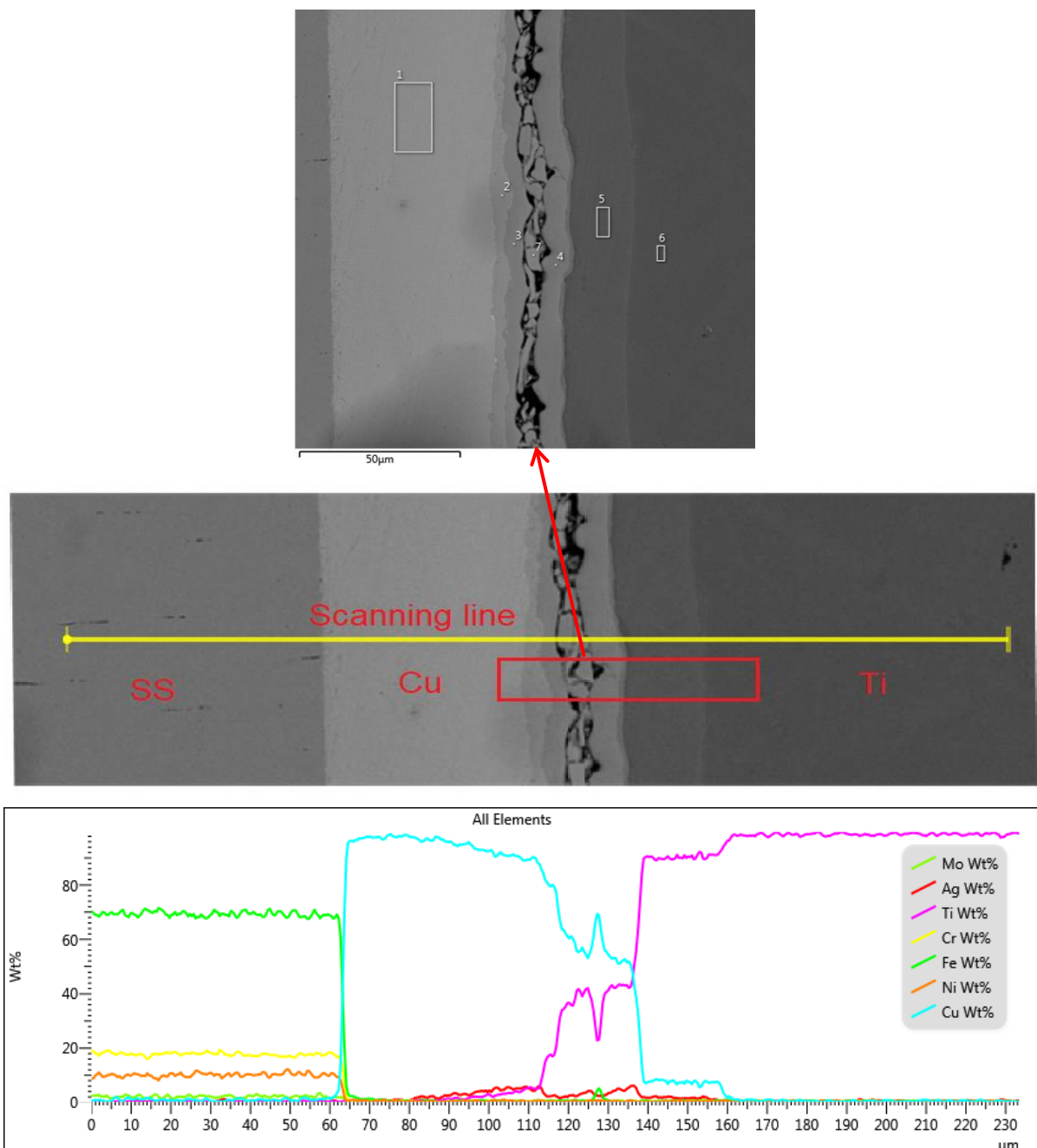


Figure 43 SEM image and corresponding EDS line scanning results of the bonded joint of sample T820_F0.7_t60

From the micro-hardness graph as shown in Figure 44, impact of hardness values at the Ag-Cu interface are increased a little bit compare to Ag and Cu interlayer. Adjacent Ag interface, on the side of titanium, there is found an IMC of Ti_2Cu_3 . Its value of hardness is around 186 HV and 188 HV. It is evident the brittle nature of the joint.

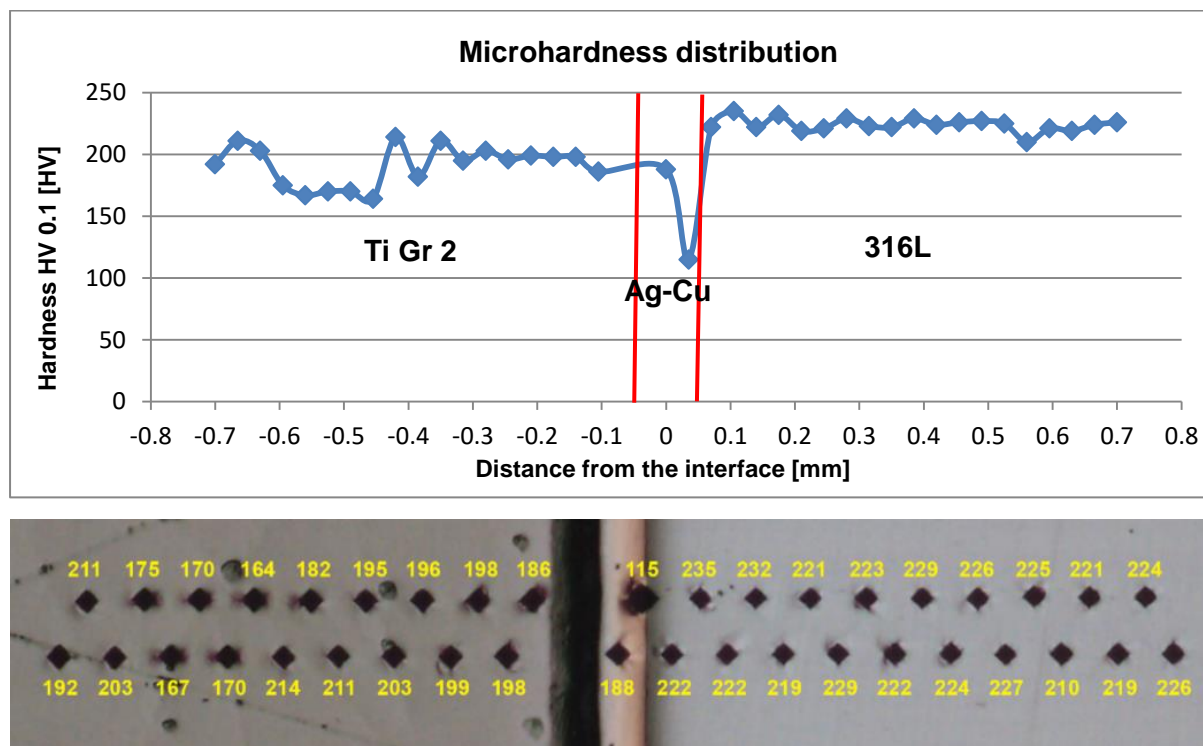


Figure 44 Micro-hardness HV 0.1 distribution over the diffusion welded joint of sample T820_F0.7_t60

For second sample (T820_F0.7_t30), all parameters were similar as sample no. 1 except holding time (change from 60 min to 30 min). From SEM and EDS analysis (see in appendix), it is found that it reveals same result as first sample.

From the experiments with multi-interlayer, it is derived that a lot of IMC formed at the Ag-Cu interface. As a reason, hardness value at this point is increased around 100 HV compare to Ag and Cu interlayer alone. Thus, it can be considered that the final joint could be ductile in nature.

6. Conclusion

Diffusion welding is the by far most adopted technology in different areas of manufacturing and also in research for welding similar and dissimilar materials. It is also helpful to join reactive and refractory materials. Intricate shapes and high precision components with good dimensional tolerances are also produced by employing this technology. Sometimes, it is difficult to join two dissimilar materials with conventional welding technology owing to formation of intermetallic compounds (IMCs) which impair the strength of final joint and also ductility. To overcome this problem, it is necessary to use very thin foil or interlayer.

The main objective of this diploma work was to figure out suitable metallic interlayer with very small deformation and good ductility of joint using diffusion welding between titanium grade 2 and high-alloy AISI 316L.

In the experimental part, three different interlayers (Ni, Ag, and Cu) and multi-interlayers (Ag-Cu) were employed to check the suitability with these two materials. OM and SEM, EDS and Q60 hardness tester machine were used to investigate the micro-structure, to analyze the chemical compositions and to measure the micro-hardness of joints, respectively.

Results of experimental part are as following:

- 1) It is derived from the experiments with Ni interlayer that Ni interlayer is not suitable at temperature 870 °C and below this temperature because it did not make sufficient bonding between titanium grade 2 and stainless steel. Above this temperature, it started to deform on the side of titanium.
- 2) With the aid of Ag interlayer, it is concluded that Ag could be considered as potential candidate because at the interface region, minimal value of hardness (62 HV) was measured in Gleeble device but it did not join completely on the side of SS owing to less solubility at the temperature 820 °C. Also, rate of diffusion increases with increasing holding time.
- 3) It is deduced from the result of Cu interlayer that it makes good joint with 0.56 mm deformation between these two materials but there is still micro-gap on the side of SS. It also generates IMC on side of Ti, though it reveals a very less hardness value (80 HV). This result exhibits the ductile nature of the joint. Longer holding time in furnace shows total diffusion of Cu into Ti.
- 4) Last experiment with Ag-Cu multilayers, it is shown that Cu produces many IMCs with Ti and Ag is almost fully soluble at the temperature 820 °C. Therefore, they cannot prevent to form IMC with Ti.

Discussion of results:

It is found from the experiments that obtaining results are quite similar to the articles of S. Kundu and Yongqiang Deng in context of SEM image. According to metallography evaluation, it is confirmed that there is a still micro-gap in Cu interlayer but it was not shown in their articles.

To sum up, Cu is the most effective interlayer to produce quality weld with negligible deformation (0.56 mm). Moreover, it lessens the hardness compare to Ag-Cu which indicates the ductile nature of the joint. Thus, it is manifest from the result that Cu can be considered as suitable interlayer among three interlayers.

Recommendations for future work:

- 1) To use Cu interlayer with electroplating methods on side of SS.
- 2) To use Nb/Cu multi-interlayers due to Nb does not form any IMC with Ti and also Cu with SS.
- 3) To use titanium grade 5 instead of titanium grade 2. It is more expensive but mechanical properties by temperature range 800 - 1000°C are better than by titanium grade 2.

7. References

- [1] **Kazakov, N.F. 1985.** *Diffusion Bonding of Materials*. Moscow : Mashinostroenie Publishers, 1985. ISBN 0-08-032550-5 .
- [2] **William D. Callister, Jr. 2007.** *Materials Science and Engineering : an introduction* . USA : John Wiley & Sons, Inc., 2007. ISBN-13: 978-0-471-73696-7 .
- [3] **Campbell, F.C. 2011.** *Joining—Understanding the Basics* . United States of America : ASM International, 2011. ISBN-13: 978-1-61503-825-1 .
- [4] **Kearns, W. H. 1980.** *Welding Handbook: Resistance and Solid-State Welding and Other Joining Processes* . United Kingdom : American Welding Society, 1980. ISBN 978-1-349-04961-5 .
- [5] **A. O'Brien, C. Guzman,. 2007.** *Welding Handbook: WELDING PROCESSES, PART 2, Ninth Edition Volume 3*. Miami : American Welding Society, 2007. ISBN: 978-0-87171-053-6.
- [6] **Moravec, Jaromir. 2009.** *Teorie svařování a pájení II: Speciální metody svařování*. Liberec : Technical University of Liberec, 2009. ISBN 978-80-7372-439-9.
- [7] **Enes Akca, Ali Gursel. 2015.** The importance of interlayers in diffusion welding - A review. *PERIODICALS OF ENGINEERING AND NATURAL SCIENCES*. 2015, Vol. 3, 2.
- [8] **T. Violeta, L. Mariana, L. Lucia, A. Georgeta. 2007.** *Materials bonding by diffusion welding technology*. Timisoara, Romania : INCDIE ICPE-CA, Bucuresti, 2007.
- [9] **S. B. DUNKERTON, R. M. CRISPIN, R. PEARCE, D. J. STEPHENSON. 1990.** *DIFFUSION BONDING 2*. England : ELSEVIER SCIENCE PUBLISHERS LTD, 1990. ISBN 1-85166-591-9.
- [10] **2015.** Kyra Wiens. *U.S. Naval Research Laboratory*. [Online] 23 April, 2015. [Cited: 17 February, 2018.] https://www.nrl.navy.mil/PressReleases/2015/37-15r_hotpress_3000x1997.jpg
- [11] **Herring, Daniel H. 2017.** Diffusion Bonding: The Equipment (part 2). [Online] Industrial Heating, 10 May, 2017. [Cited: 16 March, 2018.] <https://www.industrialheating.com/ext/resources/Issues/Issues2/2017/May/ih0517-htdr-fig4-900.jpg>.

- [12] 3520 SERIES Diffusion bonding hot press. [Online] Centorr Vacuum Industries. [Cited: 16 March, 2018.] <https://vacuum-furnaces.com/Websites/centorr/images/3520Series-2.jpg>.
- [13] **T.F. Song, X.S. Jiang, Z.Y. Shao, Y.J. Fang, D.F. Mo, D.G. Zhu, M.H. Zhu. 2017.** *Microstructure and mechanical properties of vacuum diffusion bonded joints between Ti-6Al-4V titanium alloy and AISI316L stainless steel using Cu/Nb multi-interlayer*. 145, China : School of Materials Science and Engineering, Southwest Jiaotong University, Chengdu, Sichuan 610031, China, 2017. *Vacuum* 145 (2017) 68-76.
- [14] **Fang-Li Wang, Guang-Min Sheng, Yong-Qiang Deng. 2014.** *Impulse pressuring diffusion bonding of titanium to 304 stainless steel using pure Ni interlayer*. China : College of Materials Science and Engineering, Chongqing University, Chongqing 400040, China, 2014. *Rare Met.* (2016) 35(4):331–336.
- [15] **S. Kundu, M. Ghosh, A. Laik, G.B. Kale. 2005.** *Diffusion bonding of commercially pure titanium to 304 stainless steel using copper interlayer*. Mumbai, INDIA : Department of Metallurgy and Material Engineering, Bengal Engineering and Science University, Shibpur, Hawrah 711103, West Bengal, India., 2005.
- [16] **Yongqiang Deng, Guangmin Sheng, Chuan Xu. 2012.** *Evaluation of the microstructure and mechanical properties of diffusion bonded joints of titanium to stainless steel with a pure silver interlayer*. 46, Chongqing, China : College of Material Science and Engineering, Chongqing University, 2012.
- [17] **Ladislav KOLAŘÍK, Marie KOLAŘÍKOVÁ, Pavel NOVÁK, Martin SAHUL, Petr VONDROUŠ. 2013.** *THE INFLUENCE OF NICKEL INTERLAYER FOR DIFFUSION WELDING OF TITANIUM AND AUSTENITIC STAINLESS STEEL*. Brno, Czech Republic, EU : *Metal* 2013, 2013, *Metal* 2013.
- [18] About us: Gleeble. [Online] Dynamic Systems Inc. [Cited: 25 March, 2018.] <https://www.leeble.com/about-us1/about-dsi.html>.
- [19] **2012.** *Gleeble User Training 2012: Gleeble Systems and Applications*. Poestenkill, New York, USA : Dynamic Systems Inc., 2012.
- [20] GLEEBLE® 3500-GTC SYSTEM. [Online] Dynamic Systems Inc. [Cited: 25 March, 2018.] <https://www.leeble.com/products/leeble-systems/leeble-3500.html>.

- [21] **J. Moravec, J. Bradac. 2014.** *Možnosti a využití teplotněnapěťového simulátoru Gleeble při výzkumu technologické zpracovatelnosti materiálů.* Liberec : Technical University of Liberec , 2014. ISBN 978-80-7494-138-2.
- [22] **D. E. Clark, R. E. Mizia. 2012.** *Diffusion Welding of Alloys for Molten Salt Service.* Idaho : Idaho National Laboratory , 2012. DE-AC07-05ID14517.
- [23] Titanium Overview – History, Developments, and Applications. [Online] Titanium Processing Center. [Cited: 10 February, 2018.]
<https://titaniumprocessingcenter.com/titanium-technical-data/titanium-history-developments-and-applications/>.
- [24] **Griffing, Len. 1972.** *Welding Handbook: section four Metals and Their Weldability, sixth edition.* Miami, Florida, USA : AMERICAN WELDING SOCIETY, 1972. B000H19E4U.
- [25] **Matthew J. Donachie, Jr. 2000.** *Titanium: A Technical Guide second edition.* Ohio,USA : ASM International, 2000. ISBN: 0-87170-686-5 .
- [26] Titanium Grade 2. *AMERICAN SPECIAL METAL CORPORATION.* [Online] [Cited: 03 March, 2018.] <http://www.americanspecialmetals.com/Titanium-Grade-2.html>.
- [27] Titanium Grade 2. *ASM Aerospace Specification Metals, Inc.* [Online] [Cited: 03 March, 2018.] <http://asm.matweb.com/search/SpecificMaterial.asp?bassnum=MTU020>.
- [28] **Metals, Atlas Specialty.** Stainless Steel - Grade 316L - Properties, Fabrication and Applications (UNS S31603). <https://www.azom.com/article.aspx?ArticleID=2382>. [Online] [Cited: 16 February, 2018.]
- [29] Specification Sheet: Alloy 316/316L. <https://www.sandmeyersteel.com/images/316-316L-317L-spec-sheet.pdf>. [Online] [Cited: 16 February, 2018.]
- [30] Type 316, Type 316L. <http://www.outokumpu.com/SiteCollectionDocuments/Datasheet-316-316L-imperial-hpsa-outokumpu-en-americas.pdf>. [Online] [Cited: 16 February, 2018.]
- [31] **Corporation, AK Steel. 2007.** AK STEEL 316/316L STAINLESS STEEL DATA SHEET. www.aksteel.com. [Online] 2007. [Cited: 20 February, 2018.]
http://www.aksteel.com/pdf/markets_products/stainless/austenitic/316_316L_data_sheet.pdf.
- [32] AISI Type 316L Stainless Steel, annealed bar. [Online] ASM Aerospace Specification Metals, Inc. [Cited: 20 February, 2018.]
<http://asm.matweb.com/search/SpecificMaterial.asp?bassnum=MQ316Q>.

[33] Nickel (Ni): Material Information. [Online] GoodFellow. [Cited: 21 March, 2018.]
<http://www.goodfellow.com/E/Nickel-Metal.html>.

[34] MatWeb MATERIAL PROPERTY DATA. [Online] [Cited: 12 May 2018.]
http://www.matweb.com/search/datasheet_print.aspx?matguid=9aebe83845c04c1db5126fa da6f76f7e.

[35] Silver (Ag) - Properties, Applications. [Online] AZO Materials. [Cited: 21 March, 2018.]
<https://www.azom.com/article.aspx?ArticleID=9282>.

[36] **Novak, Michal. 2016.** *Difúzní svařování heterogenních svarů v kombinaci vysokolegovaná ocel a titan*. Liberec : Technical University of Liberec, 2016.

[37] **Chatterjee, S. Kundu & S. 2006.** *Effect of bonding temperature on interface microstructure and properties of titanium–304 stainless steel diffusion bonded joints with Ni interlayer*. 10 , Howrah, India : Materials Science and Technology, 2006, Vol. VOL 22 .
ISSN: 0267-0836 .

[38] **H.Baker. 1992.** *Alloy Phase Diagrams. Volume 3*. Materials Park, Ohio : ASM International, 1992. ISBN: 0-87170-381-5.

8. Appendix

List of Attachments:

Figure 1 Temperature cycle of sample T870_F0.5_t30 with Ni interlayer	74
Figure 2 Deformation during holding time of sample T870_F0.5_t40 with Ni interlayer	74
Figure 3 Temperature cycle of sample T820_F0.7_t20 with Ag interlayer	75
Figure 4 Deformation during holding time of sample T870_F0.5_t40 with Ag interlayer	75
Figure 5 Temperature cycle of sample T820_F0.7_t60 with Cu interlayer	76
Figure 6 Deformation during holding time of sample T820_F0.7_t60 with Cu interlayer	76
Figure 7 Temperature cycle of sample T820_F0.7_t60 with Ag-Cu multi-interlayers	77
Figure 8 Deformation during holding time of sample T820_F0.7_t30 with Ag-Cu multi-interlayers.....	77
Figure 9 SEM image and corresponding EDS line scanning results of the bonded joint of sample no. 4 (870 °C for 10 hours) in furnace with Ag interlayer	78
Figure 10 Micro-hardness HV 0.1 distribution over the diffusion welded joint of sample no.4 (850 °C for 10 hours) in furnace with Ag interlayer	78
Figure 11 Metallography of sample no. 6 welded in furnace (at 850 °C for 5 hours) with Ag interlayer.....	79
Figure 12 Metallography of sample no. 4 welded in furnace (at 850 °C for 10 hours) with Cu interlayer	79
Figure 13 Metallography of sample no. 1 (T820_F0.7_t60) with Ag-Cu multi-interlayers	80
Figure 14 SEM image and corresponding EDS line scanning results of the bonded joint of sample no. 2 (T820_F0.7_t30) with Ag-Cu multi-interlayers	80
Figure 15 Fe-Cu binary phase diagrams	81
Figure 16 Fe-Ag binary phase diagrams	81

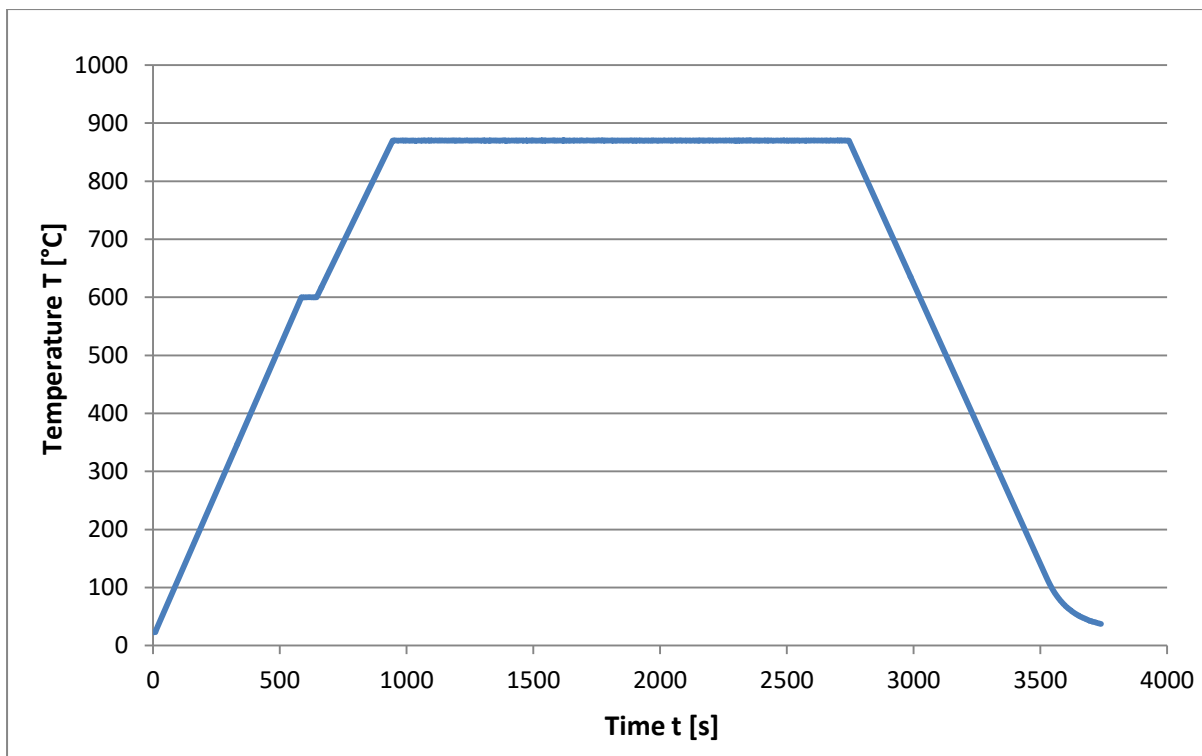


Figure 1 Temperature cycle of sample T870_F0.5_t30 with Ni interlayer

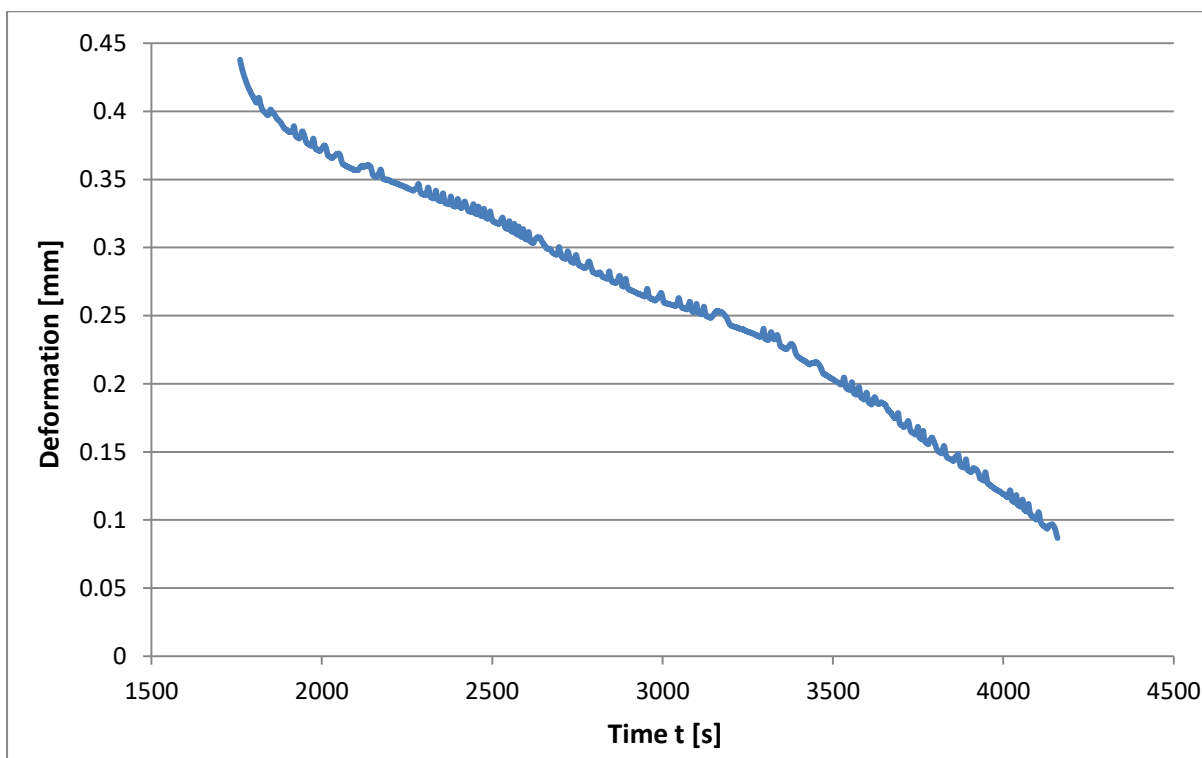


Figure 2 Deformation during holding time of sample T870_F0.5_t40 with Ni interlayer

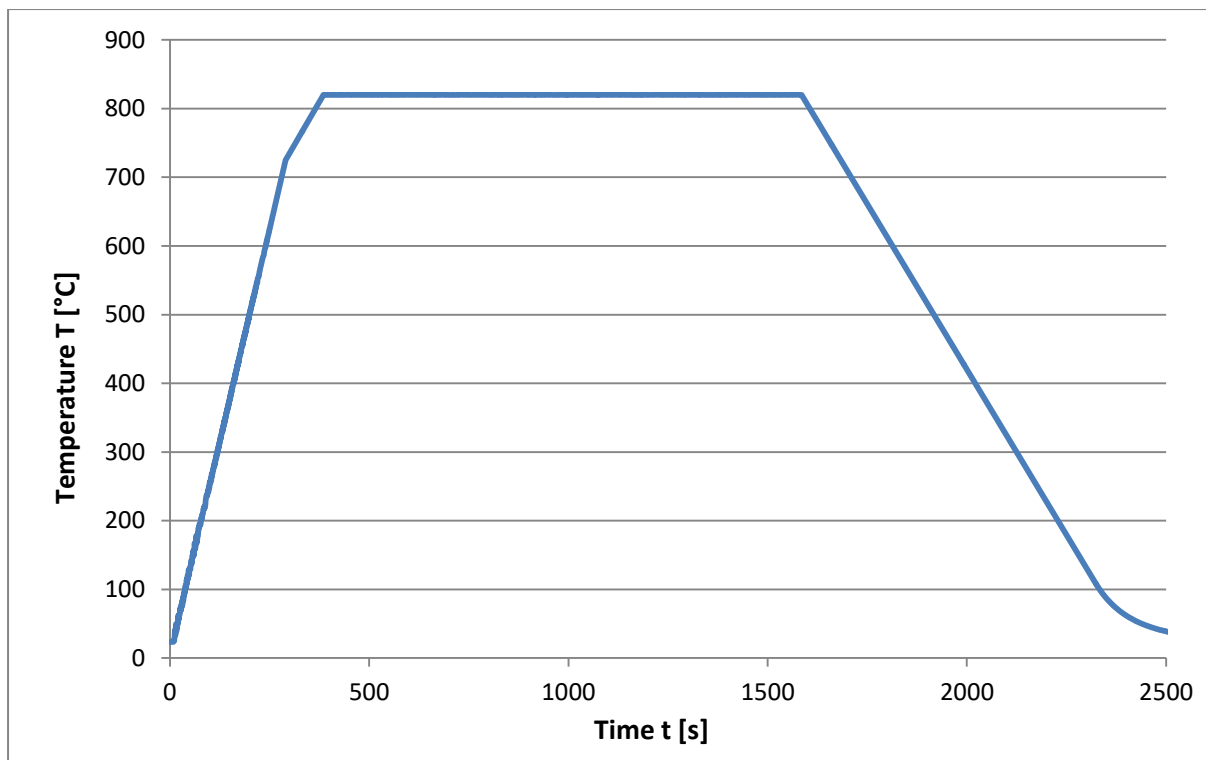


Figure 3 Temperature cycle of sample T820_F0.7_t20 with Ag interlayer

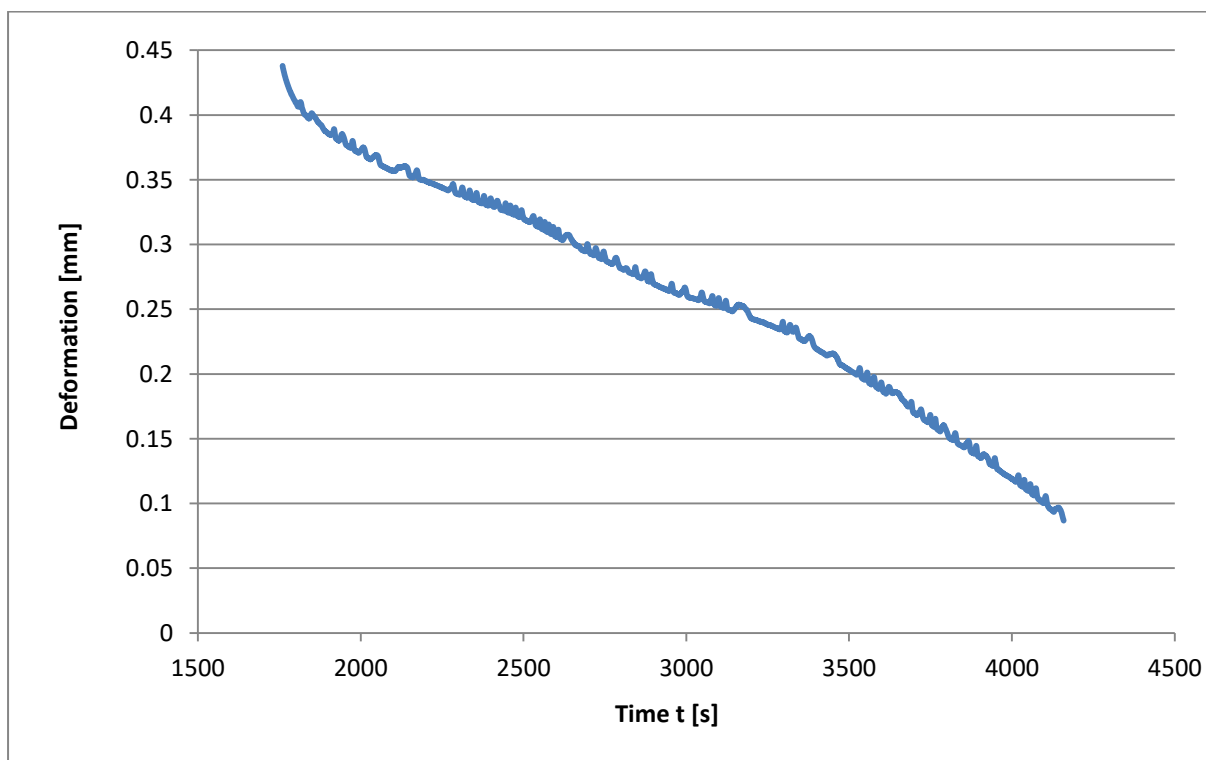


Figure 4 Deformation during holding time of sample T870_F0.5_t40 with Ag interlayer

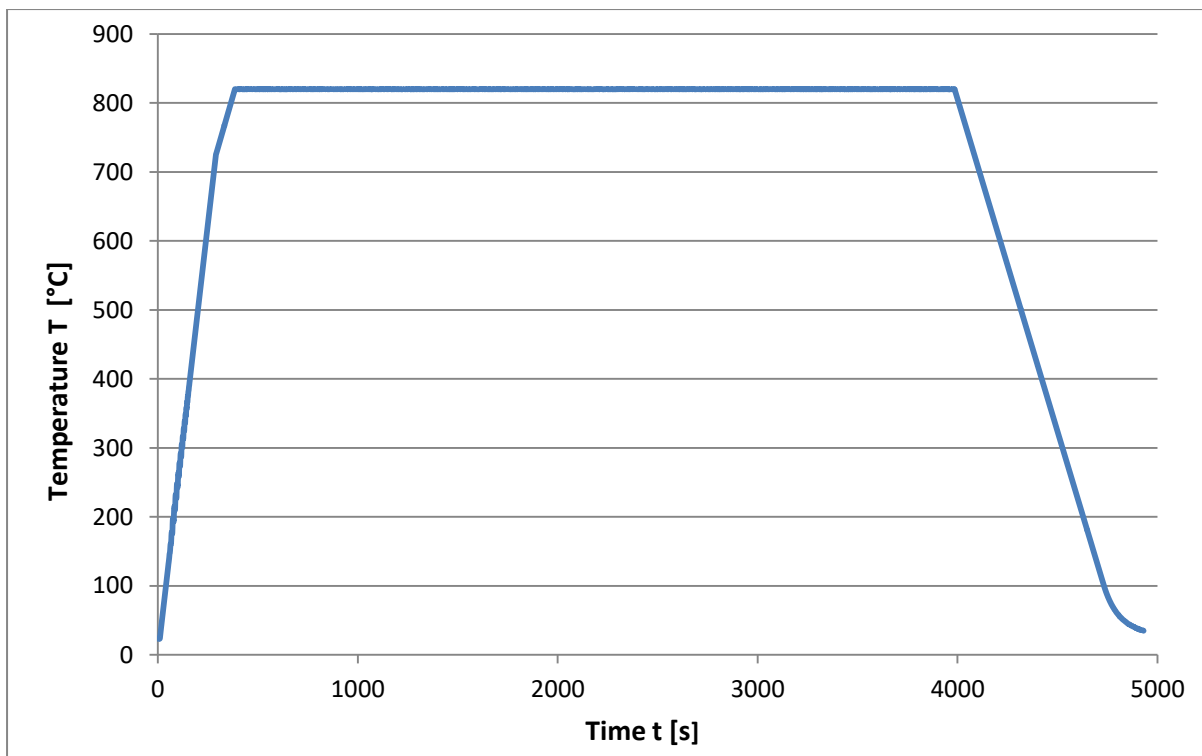


Figure 5 Temperature cycle of sample T820_F0.7_t60 with Cu interlayer

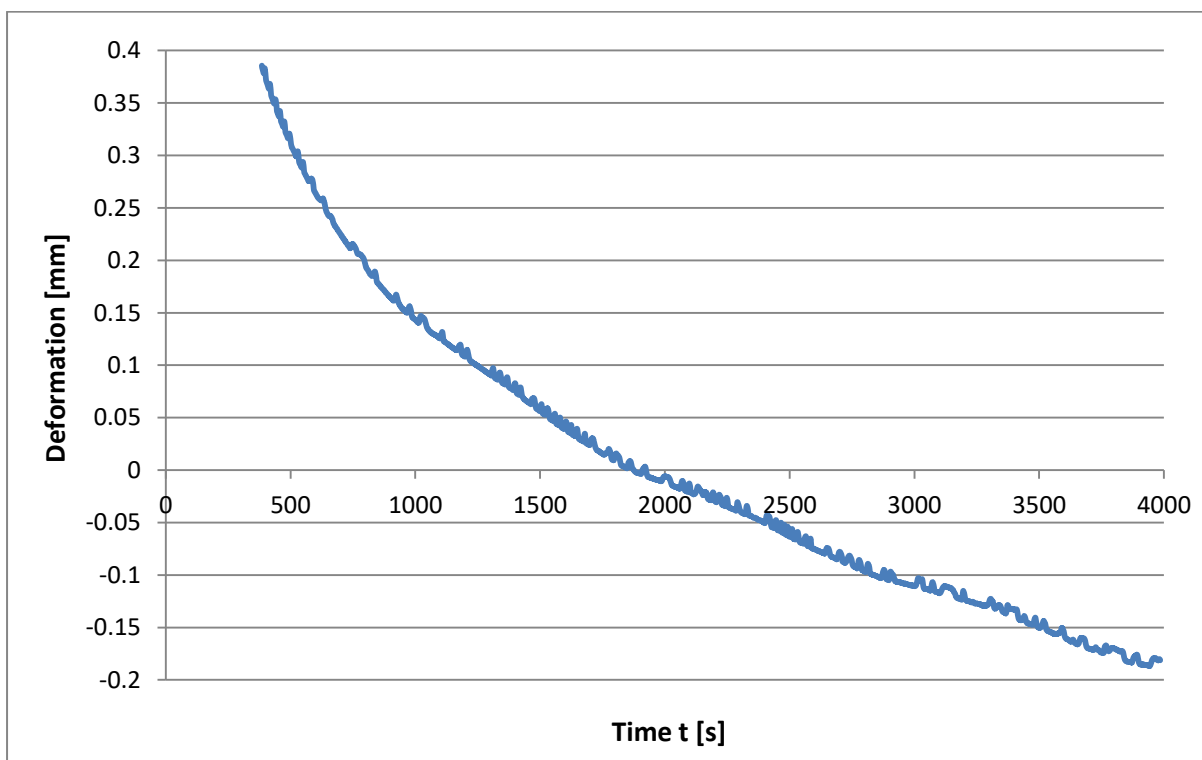


Figure 6 Deformation during holding time of sample T820_F0.7_t60 with Cu interlayer

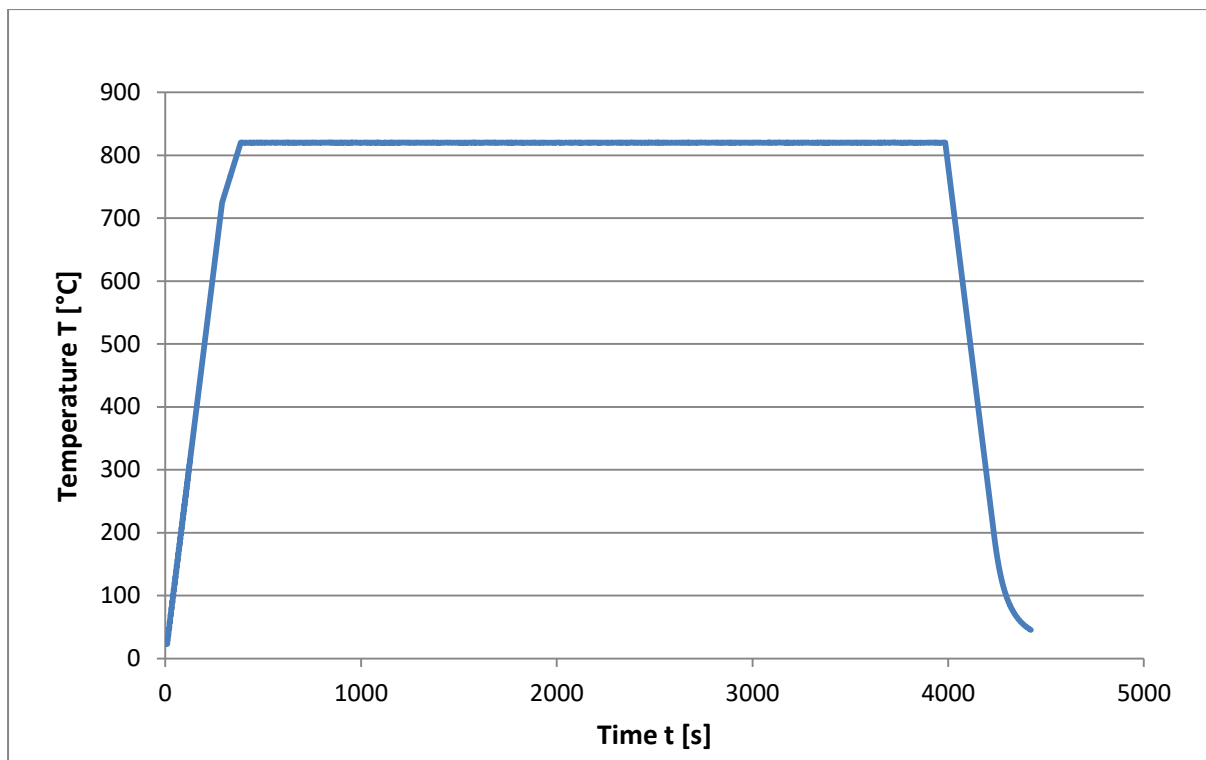


Figure 7 Temperature cycle of sample T820_F0.7_t60 with Ag-Cu multi-interlayers

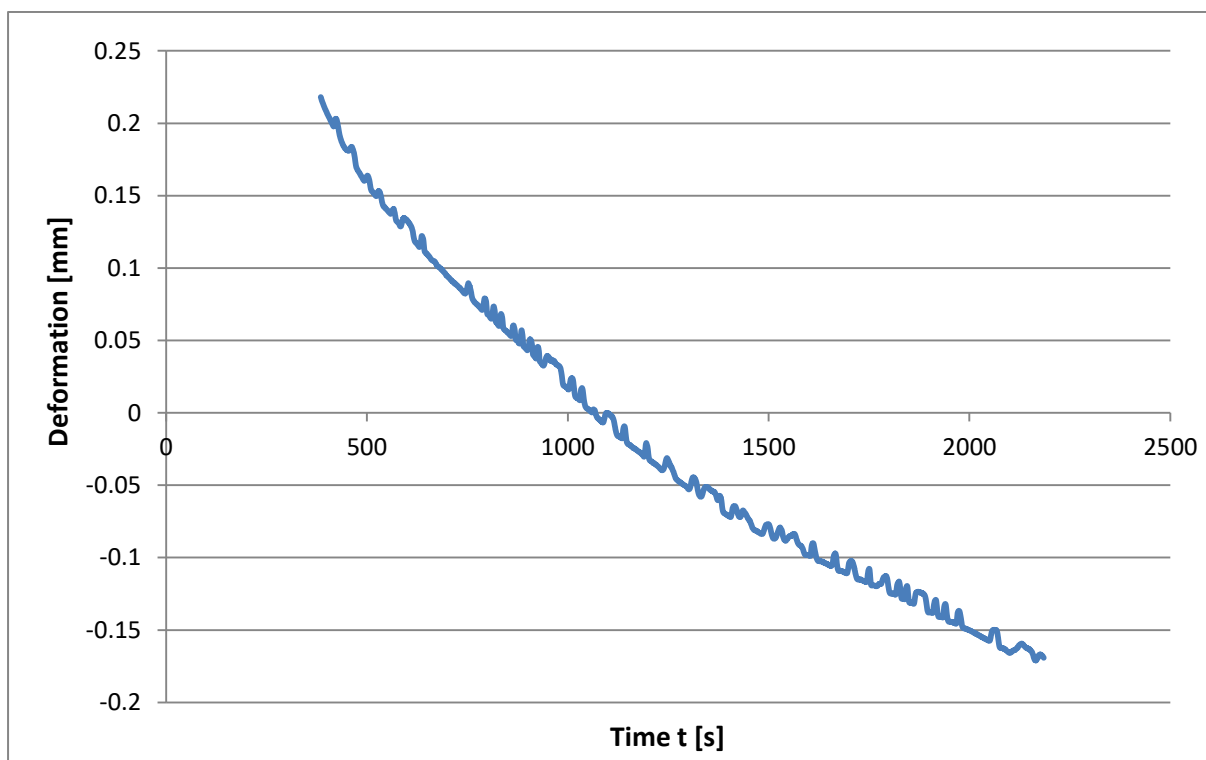


Figure 8 Deformation during holding time of sample T820_F0.7_t30 with Ag-Cu multi-interlayers

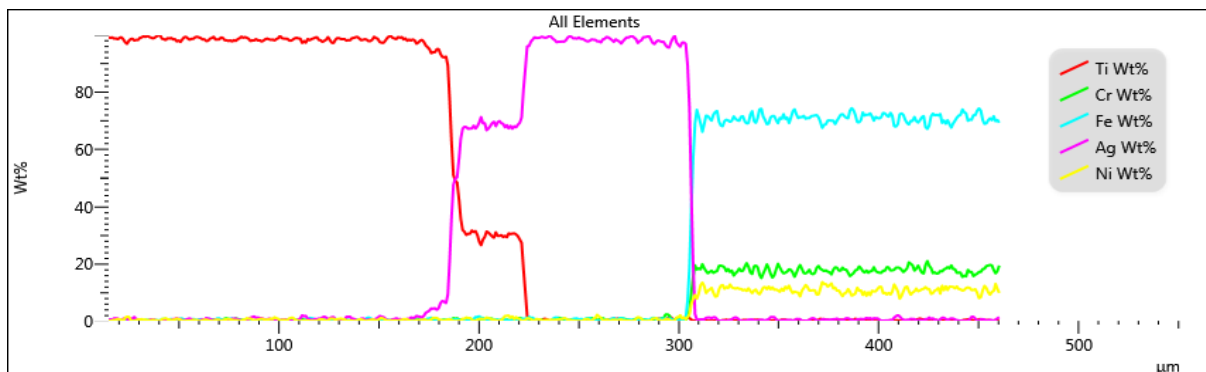
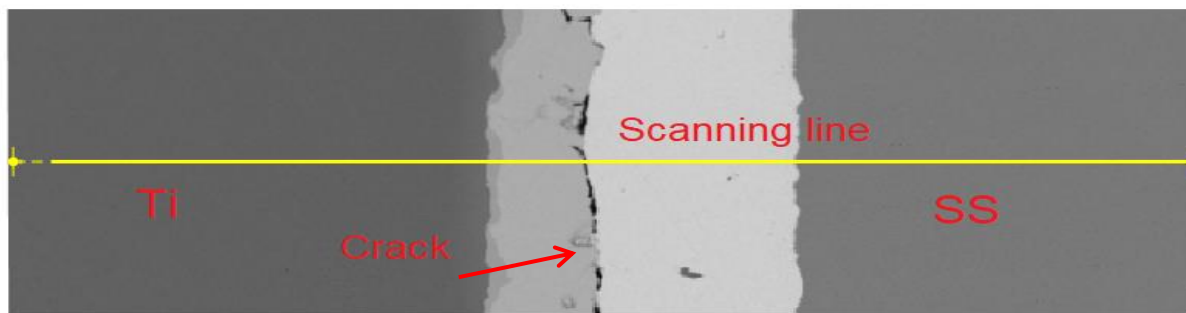


Figure 9 SEM image and corresponding EDS line scanning results of the bonded joint of sample no. 4 (870 °C for 10 hours) in furnace with Ag interlayer

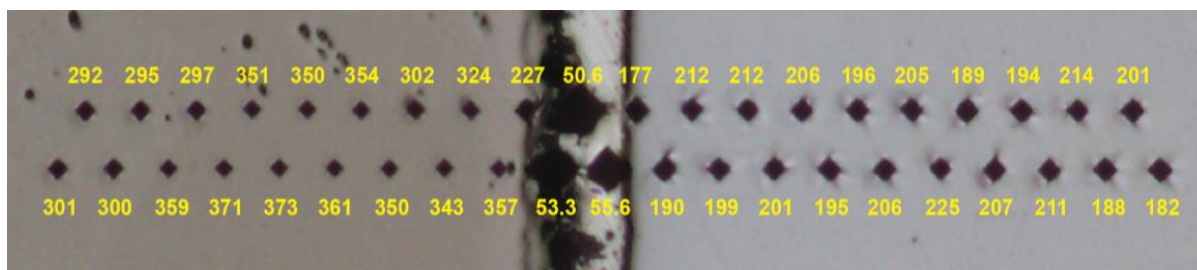
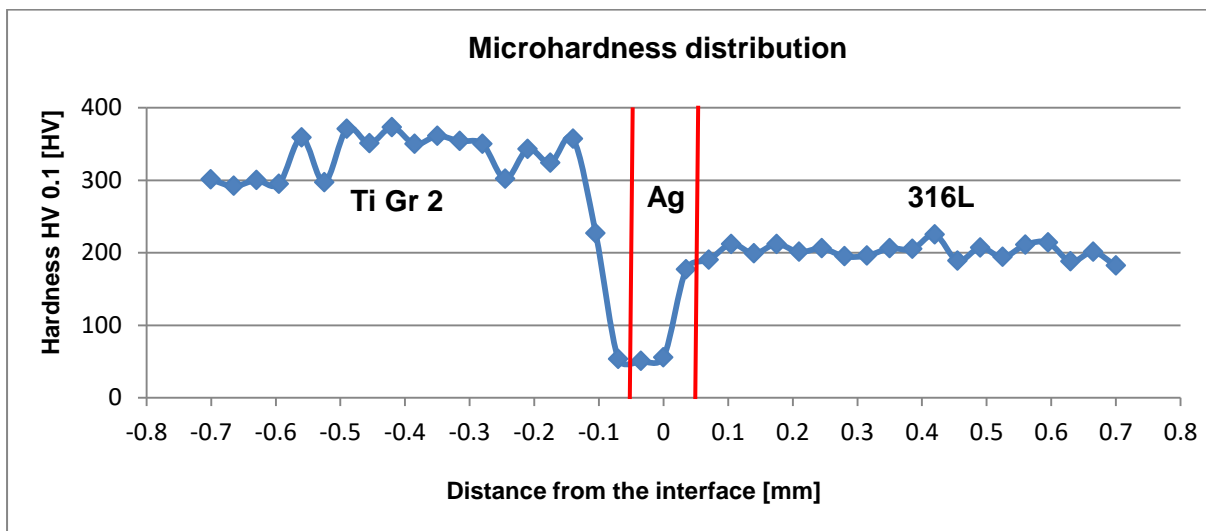


Figure 10 Micro-hardness HV 0.1 distribution over the diffusion welded joint of sample no.4 (850 °C for 10 hours) in furnace with Ag interlayer

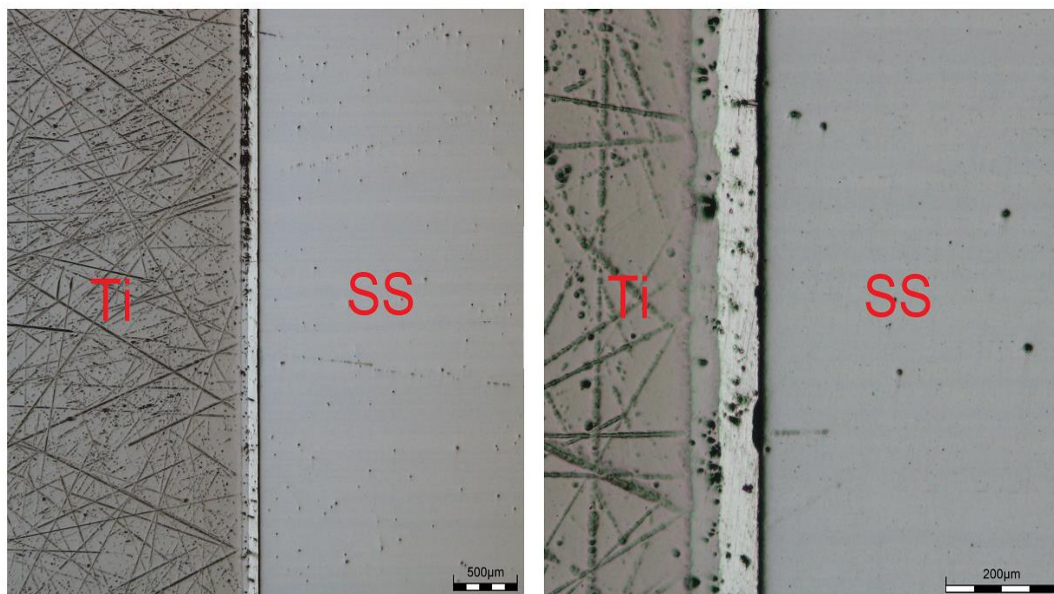


Figure 11 Metallography of sample no. 6 welded in furnace (at 850 °C for 5 hours) with Ag interlayer

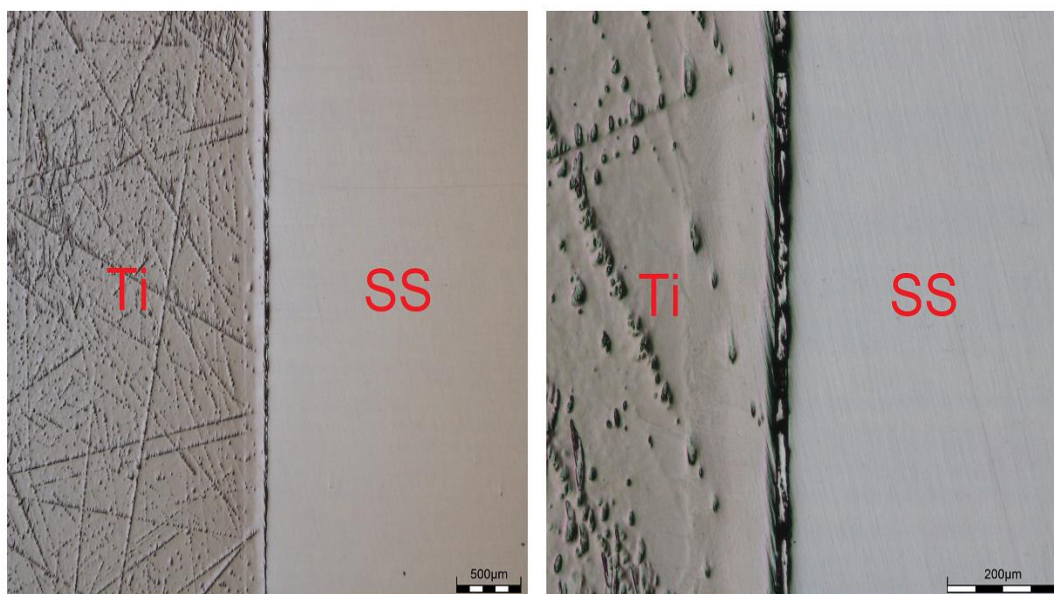


Figure 12 Metallography of sample no. 4 welded in furnace (at 850 °C for 10 hours) with Cu interlayer

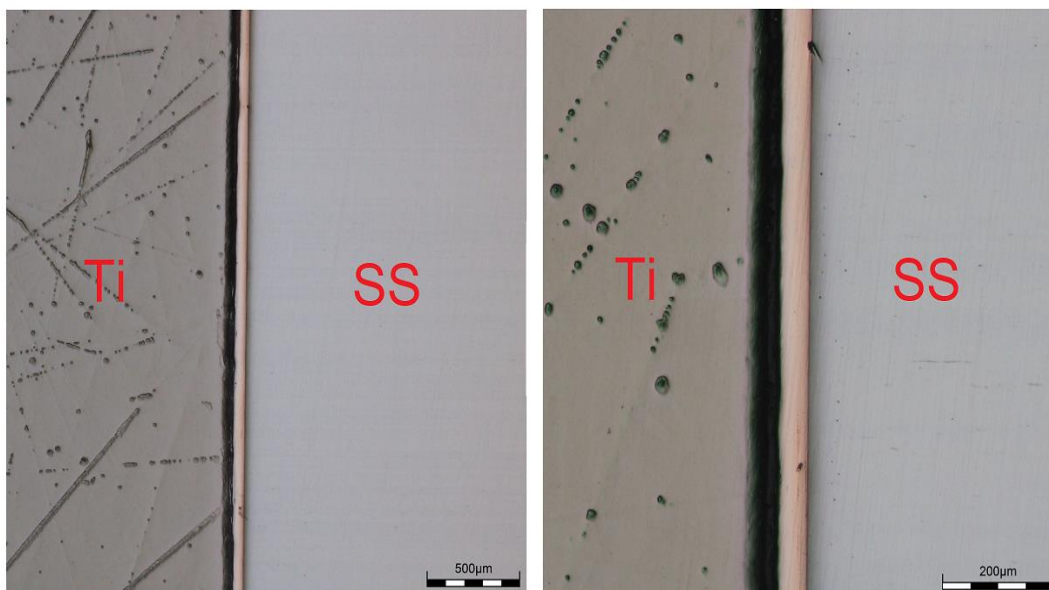


Figure 13 Metallography of sample no. 1 (T820_F0.7_t60) with Ag-Cu multi-interlayers

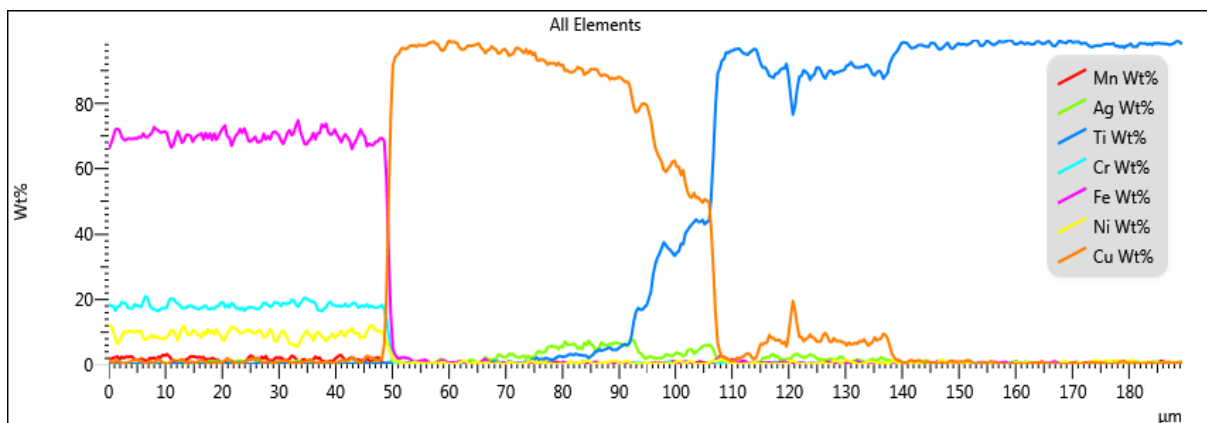
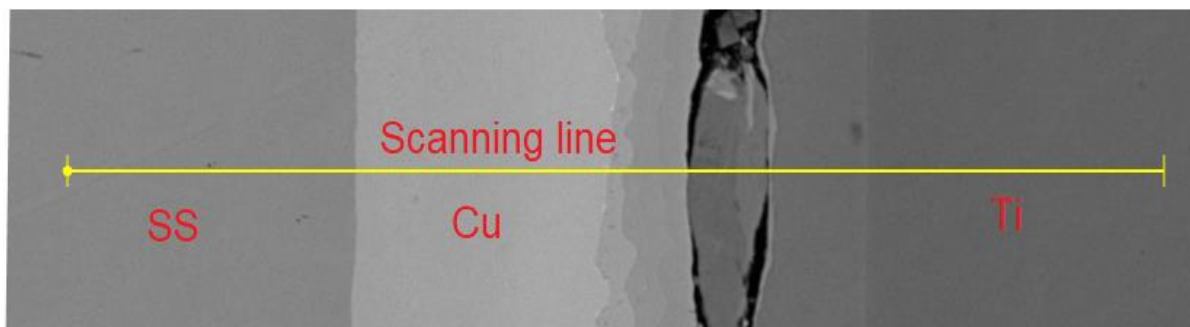


Figure 14 SEM image and corresponding EDS line scanning results of the bonded joint of sample no. 2 (T820_F0.7_t30) with Ag-Cu multi-interlayers

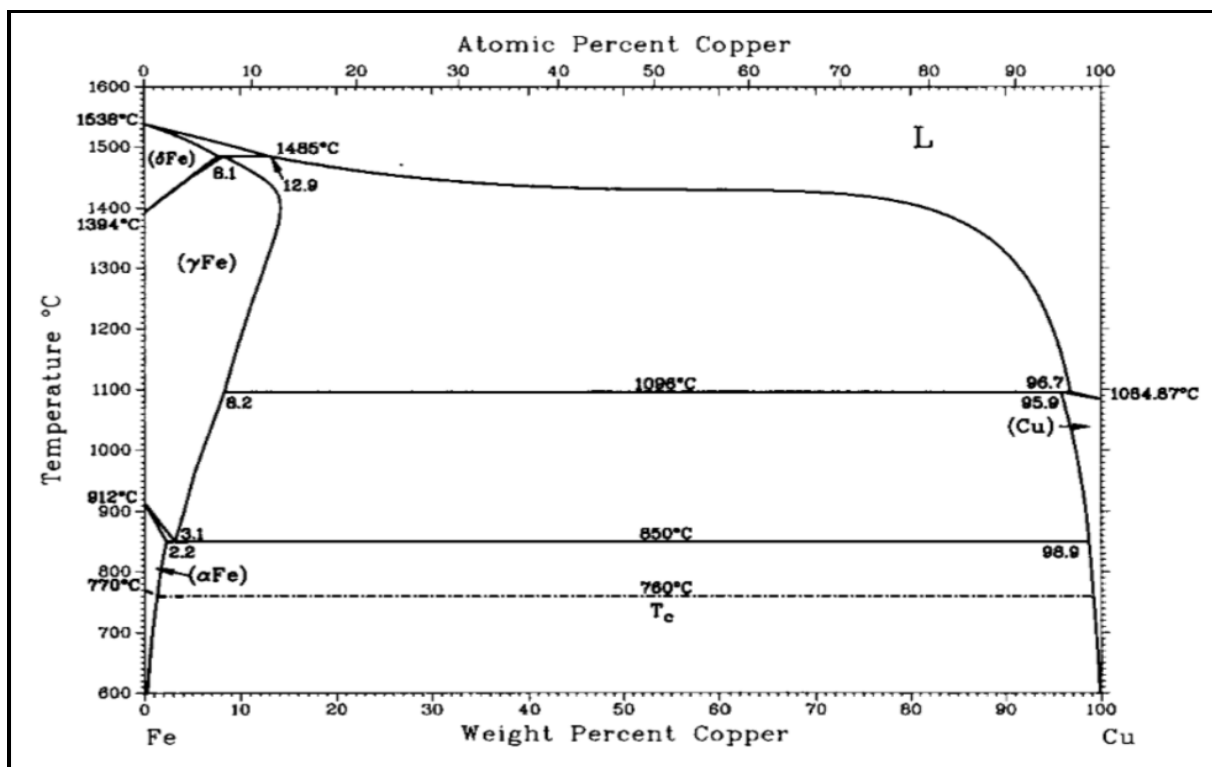


Figure 15 Fe-Cu binary phase diagrams [45]

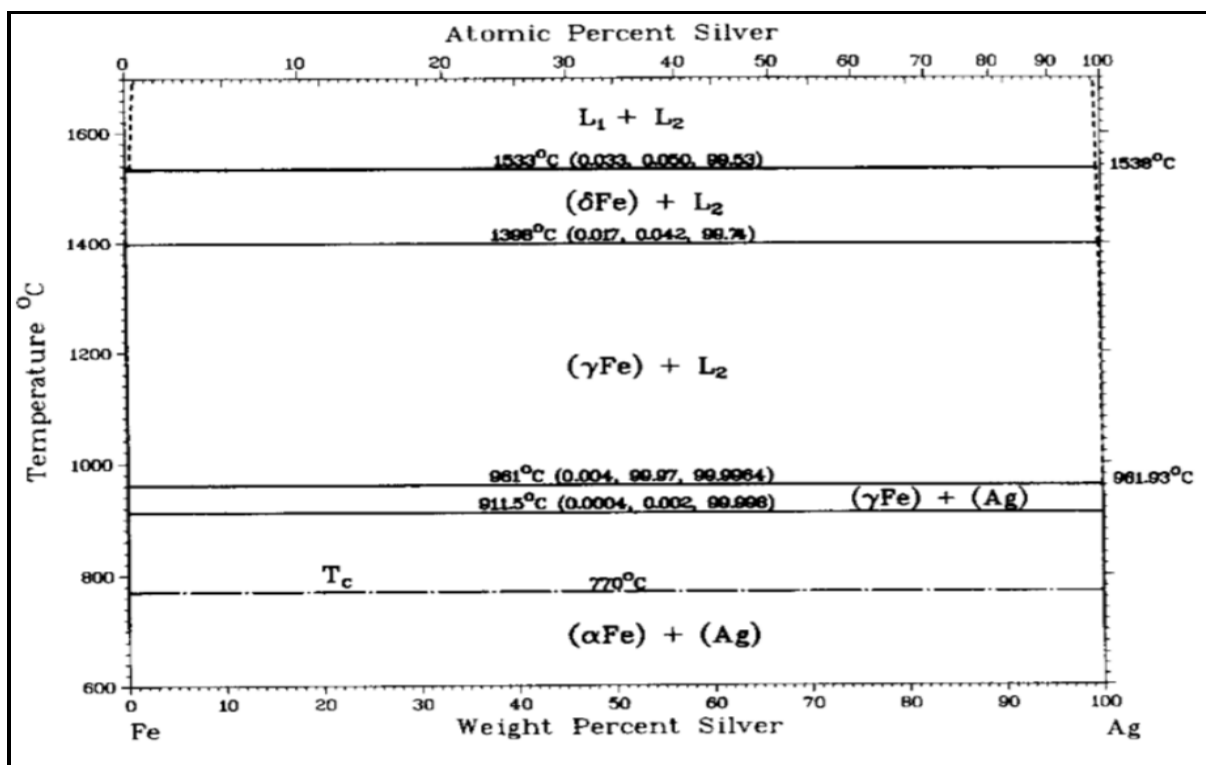


Figure 16 Fe-Ag binary phase diagrams [45]